

**Systemic Administration of Epothilone B**  
**Promotes Axon Regeneration and**  
**Functional Recovery after Spinal Cord Injury**

Dissertation

zur

Erlangung des Doktorgrades (Dr. rer. nat.)

der

Mathematisch-Naturwissenschaftlichen Fakultät

der

Rheinischen Friedrich-Wilhelms-Universität Bonn

vorgelegt von

**Jörg Ruschel**

aus

Gera

Bonn, März 2014

Angefertigt mit Genehmigung der Mathematisch-Naturwissenschaftlichen Fakultät der  
Rheinischen Friedrich-Wilhelms-Universität

**Erstgutachter:** Prof. Frank Bradke

**Zweitgutachter:** Prof. Walter Witke

**Tag der Promotion:** 17.06.2014

**Erscheinungsjahr:** 2014

## **Ehrenwörtliche Versicherung:**

Hiermit erkläre ich, dass ich die Dissertation mit dem Titel „Systemic Administration of Epothilone B Promotes Axon Regeneration and Functional Recovery After Spinal Cord Injury“ selbstständig und ohne unerlaubte Hilfe angefertigt habe. Ich habe mich dabei keiner anderen als der von mir ausdrücklich bezeichneten Hilfen und Quellen bedient.

## **Erklärung:**

Hiermit erkläre ich, dass ich mich nicht anderweitig einer Doktorprüfung ohne Erfolg unterzogen habe. Die Dissertation wurde in ihrer jetzigen oder in ähnlicher Form bei keiner anderen Hochschule eingereicht und hat noch keinen sonstigen Prüfungszwecken gedient.

Bonn, den 9. März 2014

Jörg Ruschel

Diese Doktorarbeit wurde in der Arbeitsgruppe „Axonales Wachstum und Regeneration“ von Prof. Dr. Frank Bradke am Max-Planck-Institut für Neurobiologie in Martinsried und am Deutschen Zentrum für Neurodegenerative Erkrankungen in Bonn angefertigt.

Based on my PhD studies, the following articles have been or are currently published, respectively.

**Systemic Administration of Epothilone B Promotes Axon Regeneration and Functional Recovery after Spinal Cord Injury**

**Ruschel J**, Hellal F, Flynn KC, Dupraz S, Bates M, Sliwinski C, Dobrint K, Peitz M, Brüstle O, Blesch A, Weidner N, Bunge MB, Bixby JL, Bradke F

*Science, under revision*

**Microtubule stabilization reduces scarring and causes axon regeneration after spinal cord injury.**

Hellal F, Hurtado A, **Ruschel J**, Flynn KC, Laskowski CJ, Umlauf M, Kapitein LC, Strikis D, Lemmon V, Bixby J, Hoogenraad CC, Bradke F.

*Science, 2011*

**Electrical activity suppresses axon growth through Ca(v)1.2 channels in adult primary sensory neurons.**

Enes J, Langwieser N, **Ruschel J**, Carballosa-Gonzalez MM, Klug A, Traut MH, Ylera B, Tahirovic S, Hofmann F, Stein V, Moosmang S, Hentall ID, Bradke F.

*Current Biology, 2011*

---

# Contents

<b>LIST OF FIGURES.....</b>	<b>vi</b>
<b>ABBREVIATIONS.....</b>	<b>viii</b>
<b>1. SUMMARY .....</b>	<b>1</b>
<b>2. INTRODUCTION .....</b>	<b>2</b>
<b>2.1. Spinal cord injuries have devastating and debilitating consequences .....</b>	<b>2</b>
<b>2.2. The regeneration failure of the adult, mammalian CNS.....</b>	<b>5</b>
<b>2.2.1. Adult CNS axons exhibit a poor intrinsic growth capacity .....</b>	<b>6</b>
<b>2.2.2. CNS lesion scar .....</b>	<b>8</b>
<b>2.2.3. CNS myelin and Rho signaling.....</b>	<b>12</b>
<b>2.3. The cytoskeleton .....</b>	<b>14</b>
<b>2.3.1. Actin filaments .....</b>	<b>14</b>
<b>2.3.2. Intermediate filaments .....</b>	<b>15</b>
<b>2.3.3. Microtubules .....</b>	<b>16</b>
<b>2.4. Microtubule stabilization controls axon growth.....</b>	<b>19</b>
<b>2.5. Microtubule stabilization controls cell migration.....</b>	<b>22</b>
<b>2.6. Microtubule stabilization reduces scarring and promotes axon regeneration after spinal cord injury .....</b>	<b>25</b>

---

**2.7. Research objectives: Systemic administration of epothilone B promotes axon regeneration and functional recovery after spinal cord injury.....25**

**3. RESULTS.....27**

**3.1. Local application of epothilone B promotes axon growth and reduces axon dystrophy and fibrotic scarring .....27**

**3.2. Systemic administration of epothilone B is a suitable treatment strategy to increase microtubule stabilization at the spinal cord lesion site .....30**

**3.3. Systemic and post-injury administration of epothilone B suppresses the formation of an inhibitory lesion scar after SCI .....33**

**3.4. Systemic administration of epothilone B reduces fibrotic scarring by abrogating meningeal fibroblast migration.....36**

**3.5. Microtubule stabilization through epothilone B promotes axon growth in a growth-restraining environment .....40**

**3.6. Systemic administration of epothilone B increases growth competence of injured axons in the CNS and promotes regeneration after spinal cord injury .....44**

**3.7. Systemic administration of epothilone B promotes functional recovery after clinically relevant spinal cord contusion injury .....47**

**4. DISCUSSION.....51**

**4.1. Moderate microtubule stabilization through epothilone B mimics the beneficial effects of Taxol .....53**

**4.2. Systemic administration of epothilone B is a clinically relevant treatment strategy.....54**

---

4.3. Epothilone B inhibits fibrotic scarring by abrogating cell polarity and the directed cell migration of meningeal fibroblasts .....	57
4.4. Microtubule polymerization into the growth cone propels axon growth. ....	60
4.5. Systemic administration of epothilone B reduces axon dystrophy.....	62
4.6. Systemic administration of epothilone B promotes functional raphespinal tract restoration..	64
4.7. Concluding remarks.....	69
5. MATERIAL AND METHODS .....	70
5.1 Materials.....	70
5.1.1. Chemical substance .....	70
5.1.2. Buffers and solutions .....	71
5.1.3. Commercial kits.....	73
5.1.4. Compounds, proteins and enzymes.....	74
5.1.5. Primary antibodies .....	74
5.1.6. Secondary antibodies and dyes.....	76
5.1.7. Consumables .....	77
5.1.8. Special equipment.....	78
5.2. Methods .....	80
5.2.1. Pharmacokinetic analysis of Epothilone B.....	80
5.2.2. Spinal cord injury studies .....	81

---

5.2.2.1. Spinal cord dorsal hemisection.....	81
5.2.2.2. Spinal cord contusion injury .....	81
5.2.2.3. Intracerebroventricular (i.c.v.) injections of 5,7-dihydroxytryptamine (5,7-DHT) ....	82
5.2.3. Histology .....	82
5.2.3.1. Immunohistochemistry .....	82
5.2.3.2. TUNEL staining.....	83
5.2.2.2. Giemsa staining.....	84
5.2.4. Biochemical analysis of spinal cord tissue .....	84
5.2.4.1. Western blotting .....	84
5.2.4.2. Glycosaminoglycan assay.....	85
5.2.5. Cell culture and immunocytochemistry.....	86
5.2.5.1. Culture of primary cortical neurons.....	86
5.2.5.2. Culture of primary meningeal fibroblasts.....	86
5.2.5.2. Culture of primary embryonic hippocampal neurons .....	87
5.2.6. Live imaging studies .....	88
5.2.6.1. Live cell imaging studies .....	88
5.2.6.3. <i>In vivo</i> live imaging.....	88
5.2.7. Behavioral analysis .....	89
5.2.7.1. Automated footprint analysis .....	89
5.2.7.2. Horizontal ladder test.....	90
5.2.8. Microscopy and image analysis.....	90
5.2.8.1. Confocal microscopy .....	90
5.2.9. Statistical analysis.....	91
6. REFERENCES .....	92
7. ACKNOWLEDGEMENTS .....	103



**8. CURRICULUM VITAE .....105**

**9. PUBLICATIONS.....107**

## **LIST OF FIGURES**

**Figure 2.1 Spinal cord organization and function.**

**Figure 2.2 Human spinal cord injury and its consequences.**

**Figure 2.3 Scar formation after spinal cord injury.**

**Figure 2.4 Mechanisms of myelin inhibition.**

**Figure 2.5 Structure and dynamics of actin filaments.**

**Figure 2.6 Microtubule structure and dynamics.**

**Figure 2.7 Cytoskeletal organization of the growth cone.**

**Figure 2.8 Growth cone advance is divided in three distinct steps.**

**Figure 2.9 Fibroblast migration requires extrinsic and intrinsic polarization.**

**Figure 3.1 Microtubule stabilization by epothilone B or Taxol promotes axon growth in embryonic neurons.**

**Figure 3.2 Local application of epothilone B or Taxol reduce axon dystrophy of injured spinal cord axons.**

**Figure 3.3 Local application of epothilone B or Taxol reduces fibrotic scar tissue at the spinal cord injury site.**

**Figure 3.4 Systemically administered epothilone B enters the CNS and stabilizes microtubules at the spinal cord lesion site without causing adverse side effects.**

**Figure 3.5 Systemic administration of epothilone B reduces the axon growth-inhibitory lesion scar after spinal cord injury.**

**Figure 3.6 Fibrotic scar reduction through systemic administration of epothilone B neither affects astrogliosis nor injury size after spinal cord injury.**

**Figure 3.7 Systemic administration of epothilone B neither affects cell proliferation nor cell death at the lesion site.**

**Figure 3.8 Epothilone B inhibits migration of meningeal fibroblasts by abrogating cell polarity.**

**Figure 3.9 Systemic administration of epothilone B abrogates cell polarity of meningeal fibroblasts at the spinal cord injury site.**

**Figure 3.10 Epothilone B promotes neurite growth on growth inhibitory substrates.**

**Figure 3.11 Epothilone B propels neurite growth by increasing microtubule polymerization into the growth cone.**

**Figure 3.12 Systemic administration of epothilone B reduces axon dystrophy of injured spinal cord axons.**

**Figure 3.13 Systemic administration of epothilone B promotes growth of raphespinal fibers after SCI.**

**Figure 3.14 Epothilone B decreases gait abnormalities after spinal cord contusion injury.**

**Figure 3.15 Epothilone B promotes raphespinal dependent recovery of hind limb function.**

## **ABBREVIATIONS**

<b>ADP</b>	Adenosine diphosphate
<b>ATP</b>	Adenosine triphosphate
<b>a.u.</b>	Arbitrary units
<b>BBB</b>	Blood-brain barrier
<b>BSA</b>	Bovine serum albumin
<b>BW</b>	Bodyweight
<b>C6</b>	Cervical vertebra 6
<b>cAMP</b>	Cyclic adenosine monophosphate
<b>C-domain</b>	Central domain
<b>ChAT</b>	Cholin acetyltransferase
<b>CLASPS</b>	CLIP-associated proteins
<b>CLIPS</b>	Cytoplasmatic linker proteins
<b>CRMP</b>	Collapsin response mediator protein
<b>GSK-3 beta</b>	Glycogen synthase kinase 3 beta
<b>CSPGs</b>	Chondroitin sulfate proteoglycans
<b>CNS</b>	Central nervous system
<b>Cy3</b>	Cyanine 3

<b>DAPI</b>	4',6-diamidino-2-phenylindole
<b>DetyrTub</b>	Detyrosinated tubulin
<b>5,7-DHT</b>	5,7-Deshydroxytryptamine
<b>DMSO</b>	Dimethyl sulfoxide
<b>DNA</b>	Desoxyribonucleic acid
<b>DRG</b>	Dorsal root ganglion
<b>E17</b>	Embryonic day 17
<b>EB3</b>	Plus-end binding protein 3
<b>ECM</b>	Extracellular matrix
<b>EpoB</b>	Epothilone B
<b>F-actin</b>	Filamentous actin
<b>FBS</b>	Fetal bovine serum
<b>FDA</b>	Food and drug administration
<b>Fig.</b>	Figure
<b>GAG</b>	Glycosaminoglycan
<b>GAP-43</b>	Growth associated protein 43
<b>GAPDH</b>	Glyceraldehyde 3-phosphate dehydrogenase
<b>G-actin</b>	Globular actin

<b>GDP</b>	Guanosine diphosphate
<b>GEF</b>	Guanine nucleotide exchange factor
<b>GFAP</b>	Glial fibrillary acidic protein
<b>GFP</b>	Green fluorescent protein
<b>GSK-3 <math>\beta</math></b>	Glycogen synthase kinase 3 beta
<b>GTP</b>	Guanosine triphosphate
<b>HRP</b>	Horseradish peroxidase
<b>5HT</b>	5-Hydroxytryptamine=Serotonin
<b>ICC</b>	Immunocytochemistry
<b>i.c.v.</b>	Intracerebroventricular
<b>IHC</b>	Immunohistochemistry
<b>i.p.</b>	Intraperitoneal
<b>i.v.</b>	Intravenously
<b>LIMK</b>	LIM domain kinase
<b>kdyn</b>	Kilodyne
<b>MAI</b>	Myelin-associated glycoprotein
<b>MAP</b>	Microtubule associated protein
<b>MEM</b>	Minimal essential medium

<b>MDR</b>	Multi-drug resistance
<b>mTOR</b>	Mammalian target of rapamycin
<b>MLCII</b>	Myosin 2 light chain
<b>MOPS</b>	3-morpholinopropase sulfonic acid
<b>MSAs</b>	Microtubule stabilizing agents
<b>Omgp</b>	Oligodendrocyte myelin glycoprotein
<b>P4</b>	Postnatal day 4
<b>PBS</b>	Phosphate buffered saline
<b>P-domain</b>	Peripheral domain
<b>PFA</b>	Paraformaldehyde
<b>p-gp</b>	Permeability glycoprotein
<b>P<sub>i</sub></b>	Phosphate
<b>PKA</b>	Protein kinase A
<b>PNS</b>	Peripheral nervous system
<b>PTEN</b>	Phosphatase and tensin homolog
<b>ROCK</b>	Rho kinase
<b>SCI</b>	Spinal cord injury
<b>SDS</b>	Sodium dodecyl sulfate

<b>s.e.m.</b>	Standard error of the mean
<b>Sema 3A</b>	Semaphorin 3A
<b>Syn</b>	Synaptophysin
<b>Ser</b>	Serin
<b>T8</b>	Thoracic spinal segment 8
<b>Tau</b>	Tubulin-associated unit
<b>TBS</b>	Tris-buffered saline
<b>TGF-<math>\beta</math></b>	Transforming growth factor beta
<b>Thy-1</b>	Thymus cell antigen 1
<b>+TIPs</b>	Microtubule plus-end tracking proteins
<b>TierSchG</b>	German animal protection law
<b>Tuj-1</b>	Neuronal beta-3 tubulin
<b>TUNEL</b>	Terminal deoxynucleotidyl transferase dUTP nick end labeling
<b>TyrTub</b>	Tyrosinated tubulin
<b>WB</b>	Western blot



## **1. SUMMARY**

After central nervous system (CNS) injury, such as a traumatic spinal cord injury (SCI), damaged axons fail to regenerate resulting in a permanent loss of sensorimotor functions. Regeneration is prevented by growth inhibitory factors in the lesion scar and in CNS myelin as well as by a poor axon intrinsic growth potential. Microtubule dynamics regulate key processes that are instrumental in regeneration including axon growth and scar formation. Moderate microtubule stabilization by the anti-cancer drug Taxol promotes axon integrity and axons growth and prevents the formation of the lesion scar leading to enhanced axon regeneration after SCI. However, Taxol is impractical for clinical situations. Due its poor blood-brain-barrier permeability Taxol requires CNS invasive delivery bearing the risk of additional neuronal tissue damage. Here, I report that systemic and post-injury administration of epothilone B, a microtubule stabilizing drug that crosses the blood-brain barrier, has beneficial effects after SCI. Systemic administration of epothilone B decreases fibrotic scarring in spinal cord injured rodents by disrupting cell polarity of meningeal fibroblasts, which abrogates directed cell migration. Time lapse microscopy and *in vivo* live imaging of individual axons reveal that epothilone B allows the microtubular network to protrude into the distal tip of the axon to propel axon growth through an otherwise inhibitory environment. Finally, epothilone B improves gait and coordinated walking after thoracic spinal cord contusion injury. As the epothilone B derivative ixabepilone received clinical approval, these data suggest that epothilones hold promise for clinical translation in enabling axon regeneration and functional recovery after central nervous system injury.

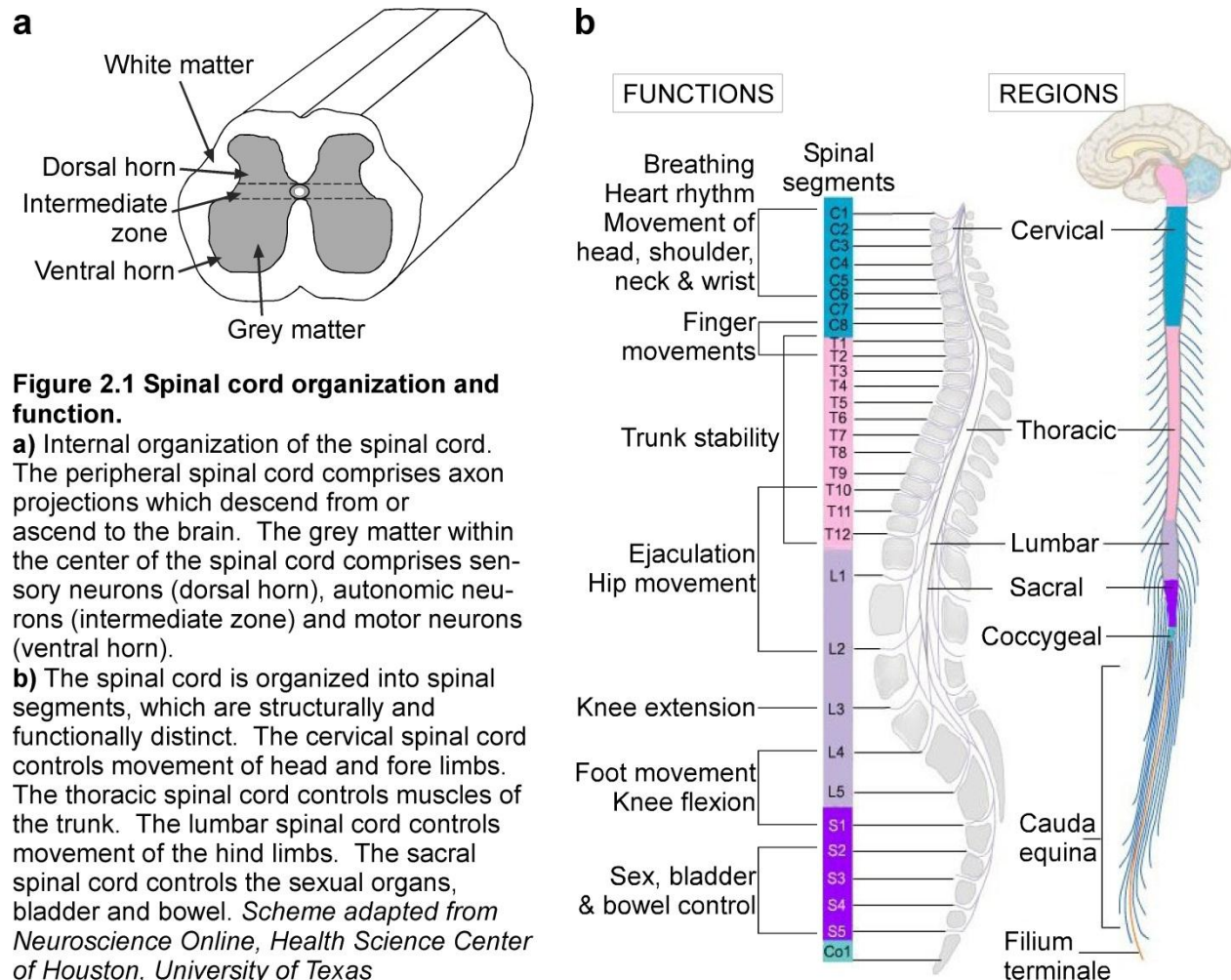
## **2. INTRODUCTION**

### **2.1. Spinal cord injuries have devastating and debilitating consequences**

The spinal cord is a cylindrical structure of nervous tissue within the vertebral column, which together with the brain, forms the central nervous system (CNS) of the body. The main function of spinal cord is mediating communication between the body and the brain and the autonomous control of organ functions. The spinal cord is composed of grey and white matter. The butterfly shaped, spinal cord grey matter resides in the central region of the spinal cord (**Fig. 2.1a**) and consists of neuronal cell bodies. The grey matter can be functionally subdivided into lateral horn, intermediate column and ventral horn. The lateral horn contains sensory neurons processing incoming somatosensory information. Neurons of the intermediate column control autonomic reflexes of the visceral and pelvic organs. The ventral horn comprises the lower motor neurons that innervate peripheral skeletal and smooth muscles, thereby produce voluntary and involuntary movement. The grey matter is surrounded by the spinal cord white matter (**Fig. 2.1a**), which is an accumulation of neuronal fibers, called axons. The white matter axons are responsible for transmitting electrical information between the brain and the body and vice versa. Supraspinal neurons within the brain descend functionally bundled axonal projections, called tracts, through the white matter and innervate and control neurons in the spinal cord grey matter. By contrast, neurons of the spinal nerves, called dorsal root ganglion (DRG) neurons, situated adjacent to the vertebral column receive sensory information from the periphery, which is transmitted by ascending axonal projections through the spinal cord to the brain.

Besides its cross-anatomical structure, the spinal cord is rostro-caudally segmented. Each spinal segment contains one pair of spinal nerves and integrates sensory-motor information of a specific part of the body (**Fig. 2.1b**). The spinal segments are integrated into four structural and functional distinct regions

dependent on their position: the cervical, thoracic, lumbar and sacral spinal cord region (**Fig. 2.1b**). The cervical segments control movement of the higher extremities, breathing and heart rhythm. The thoracic segments are involved in fore- and hindlimb movement and important for trunk stability. The major function of the lumbar spinal cord is the control of hindlimb movements e.g. walking in humans, while the sacral spinal cord regulates sex, bladder and bowel function (**Fig. 2.1b**).



Traumatic injuries to the spinal cord cause substantial damage to nervous tissue (**Fig. 2.2a**), disrupt the descending and ascending axonal tracts of spinally projecting neurons and interrupt the communication between the brain and the body. Depending on the location and severity of the damage, sensory motor

functions that are controlled by spinal segments below the injury site are permanently lost resulting in pronounced functional deficits (**Fig. 2.2b**).

Epidemiological studies reveal, that the incidence of spinal cord injury (SCI) in western countries appears to be relatively low at around 10 to 40 people per million per year in the general population (Cadotte and Fehlings, 2011). However, SCI is a chronic condition with an increased occurrence in young individuals (Chen et al., 2013). Even though SCI patients have an increased risk of morbidity and mortality, many of them live with the condition for decades. As a consequence the numbers of individuals that are affected by SCI is much higher than the incidence rate would suggest (Chen et al., 2013). Thus, in addition to the disastrous physical and psychological impact of the injury for the affected individuals, SCI poses a significant economical burden to health care systems. For instance, the economic costs for patient care and rehabilitation and also for restructuring the environment in a handicapped accessible manner are estimated in the billions of dollars per year for western countries such as the United States (Cadotte and Fehlings, 2011).

Since the consequences of spinal cord injuries are so disastrous there is a crucial need for efficient and clinically practical therapeutic strategies to ameliorate the neurological deficits accompanying the condition. In the past decades a substantial amount of basic research has been conducted, which has facilitated deeper insight into the disease pathology. However, to date the only existing therapy, which is clinically approved to promote recovery of sensorimotor function in SCI patients, is rehabilitative training (Dietz and Fouad, 2013). Rehabilitative training is effective in preventing atrophy of deinnervated body parts and promotes functional recovery in individuals with incomplete SCI by stimulating neuroplasticity (Dietz and Fouad, 2013). Nevertheless, neurorehabilitation is not ideal because it ameliorates the condition symptoms rather than addressing its fundamental cause, which is the lack of functional axon regeneration after SCI.

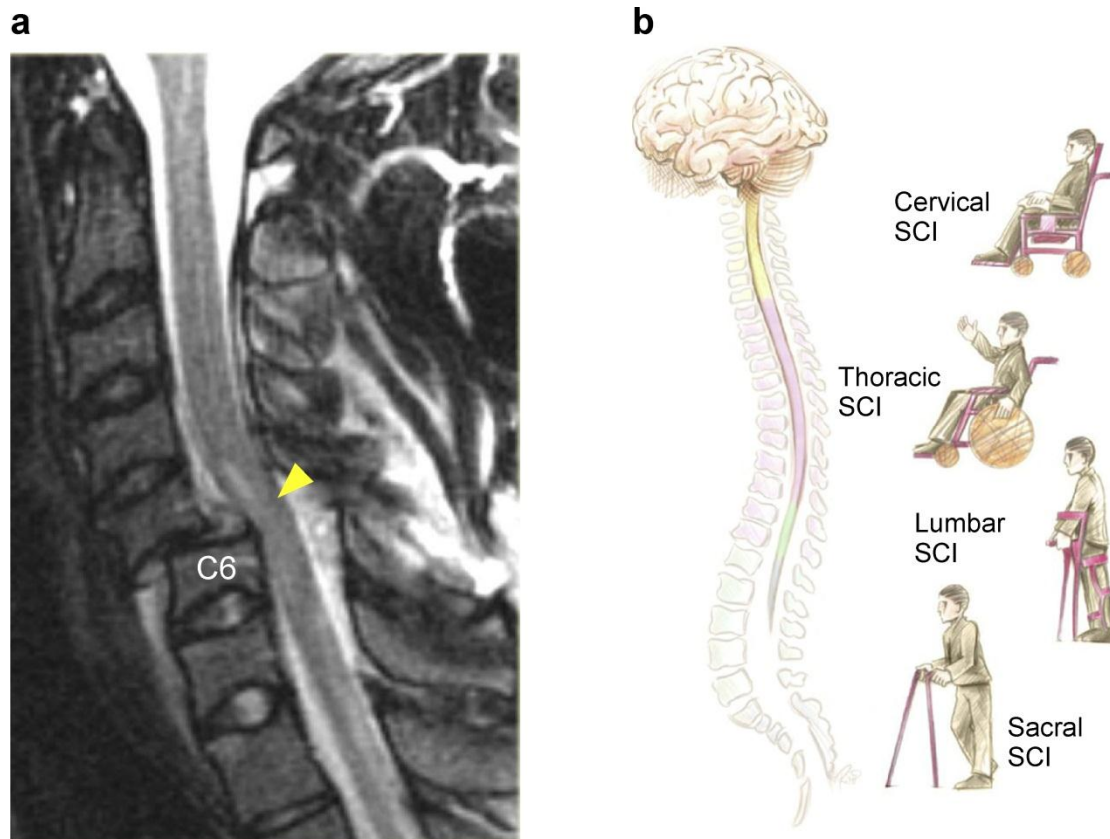


**Figure 2.2 Human spinal cord injury and its consequences.**

**a)** Magnetic resonance imaging of a cervical spinal cord injury (yellow arrowhead) which results from a compression through the cervical vertebra 6 (C6). *Picture adapted from A.Flanders, Department of Radiology and Regional Spinal Cord Injury Center of the Delaware Valley, Thomas Jefferson University Hospital, Philadelphia*

**b)** The level of a spinal cord injury (SCI) determines the functional limitations. *Drawing from "Wings of life" Foundation.*

## 2.2. The regeneration failure of the adult, mammalian CNS

Damaged axons in the adult peripheral nervous system (PNS) and in the CNS of lower vertebrate species such as fishes and amphibians are able to mount a substantial regenerative response (Ferretti et al., 2003).

Upon injury, these axons form a new growth cone at their proximal tip which grows and navigates towards its former target structure, resulting in reestablishment of functional circuits. By contrast, in the CNS of higher species, such as mammals, damaged axons do not form new growth cones, but develop dystrophic

end bulbs at their proximal tips that show only poor regenerative attempts (Bradke et al., 2012). It has been hypothesized that this inability of mammalian CNS axons to regenerate is to control plasticity of an increasingly complex nervous system (Harel and Strittmatter, 2006). This hypothesis is supported by two important observations. On the one hand, embryonic CNS axons are able to regenerate while adult CNS axons lose their intrinsic regenerative capacity (Tom et al., 2004). On the other hand, the injured, adult mammalian CNS expresses growth inhibitory molecules, which are important for consolidating plasticity after development, but counteract axon regeneration (Harel and Strittmatter, 2006). These two features, a poor neuron-intrinsic growth capacity and neuron-extrinsic inhibitory factors in the CNS environment, are the major contributors to regeneration failure in the adult CNS.

### **2.2.1. Adult CNS axons exhibit a poor intrinsic growth capacity**

Cell-autonomous mechanisms limit axon regeneration, which are developmentally regulated. Embryonic neurons that are transplanted into the adult CNS show functional axon regeneration but this regenerative ability declines with neuronal age (Brundin et al., 1988; Hankin and Lund, 1990). Similarly, cultured postnatal neurons show reduced axon growth in comparison to their embryonic counterparts (Wigley and Berry, 1988; Fawcett et al., 1989). These experiments led to the conclusion that a transitional process from embryonic to adult neurons gradually represses the intrinsic neuronal growth capacity. Similarly to embryonic neurons, adult neurons of the PNS are able to mount successful axon regeneration upon injury, which leads at least in part to targeted reinnervation and functional recovery. This regenerative ability of PNS neurons is achieved by reactivation of the embryonic growth program (Smith and Skene, 1997). A fundamental cause for the regeneration failure of injured, adult CNS neurons is their inability to reactivate this growth program.

Over the past decades, a large amount of factors have emerged that regulate the growth state of embryonic and PNS neurons. Among them the growth associated protein 43 (GAP-43), phosphatase and tensin homolog (PTEN) and cyclic adenosine monophosphate (cAMP) are particularly interesting because these

factors share common features: 1) Their developmental expression patterns or intracellular concentrations, respectively, reflect their function during the axon growth program. 2) They regulate cytoskeletal dynamics or synthesis, both critical for driving the axonal growth machinery (**see chapter 2.4.1.**). For instance, GAP-43 is a positive regulator of axon regeneration, accordingly present in embryonic neurons, reduced in most neurons during adulthood and becomes activated during regeneration (Strittmatter et al., 1992; Benowitz and Routtenberg, 1997). GAP-43 regulates cytoskeletal remodeling in the neuronal growth cone, fundamental for axon elongation (Benowitz and Routtenberg, 1997) (**see chapter 2.4.1.**). By contrast, PTEN, a negative regulator of axon growth, shows increased expression during maturation of the CNS. PTEN suppresses the activity of mammalian target of rapamycin (mTOR), which is a critical regulator of protein translation and cell growth (reviewed in (Tee and Blenis, 2005). In addition, mTOR is involved in the regulation of the cytoskeleton as for instance actin and microtubule dynamics (Caccamo et al., 2013; He et al., 2013). Genetic depletion of PTEN increases the capacity of adult neurons to regenerate their axons including retinal ganglion neurons (RGCs) (Park et al., 2008) and corticospinal neurons (Liu et al., 2010). Cyclic adenosine monophosphate (cAMP) is growth-promotive for axon growth and regeneration. Accordingly, postnatal neurons have lower levels of cAMP in comparison to embryonic neurons (Shewan et al., 2002) while injured PNS neurons elevate intraneuronal cAMP levels (Filbin, 2003). Moreover, increasing endogenous cAMP levels by injecting dibutyryl cAMP, an membrane permeable cAMP analog, into the dorsal root ganglia (Neumann et al., 2002) or by systemic administration of rolipram (Pearse et al., 2004), a drug that inhibits cAMP degradation by phosphodiesterase-4, increases regeneration of injured CNS axons. cAMP signals through protein kinase A (PKA) and induces transcriptional changes leading to increased amount of polyamine synthesis by arginase-1 (reviewed in (Filbin, 2003). Polyamines regulate the expression of various cytoskeletal proteins (Kaminska et al., 1992) and are required for microtubule formation (Banan et al., 1998).

Besides GAP-43, PTEN, and cAMP a variety of cell intrinsic factors regulate the axon growth program that is active during embryonic development and PNS regeneration but quiescent in injured axons of

mature CNS neurons (Harel and Strittmatter, 2006). Interestingly, central axons of adult DRG neurons are able to adopt an increased growth state after an experimental procedure termed “conditioning”. DRG neurons have a mixed identity because they exhibit a peripheral and a CNS axonal branch (**see chapter 2.1.**). When the peripheral branch is injured, DRG neurons are able to trigger the axon growth program by activating GAP-43, mTOR, cAMP and other growth-associated factors (reviewed in (Yang and Yang, 2012) and regenerate their peripheral axons. Remarkably, these growth competent DRG neurons have the ability to regenerate even their central axons after CNS injury, a phenomenon called the “conditioning effect” (Richardson and Issa, 1984). However, the “conditioning effect” fails to promote axon regeneration in the CNS if the peripheral nerve injury is not performed prior to CNS injury. In a recent study DRG neurons were “conditioned” 3 days after injury of their central branch. Even though the DRG neurons obtained growth competence, the damaged central axon failed to regenerate through the lesion site (Ylera et al., 2009). These findings suggest that increasing the intrinsic growth capacity of an injured CNS neuron alone is not sufficient to mount successful axon regeneration. The reason for this is the additional, neuron extrinsic barrier for axon regeneration, which is the injured CNS environment.

### **2.2.2. CNS lesion scar**

Besides a cell-autonomous loss of axonal growth capacity, extrinsic barriers to regeneration contribute to the regeneration failure in the adult mammalian CNS. The most important extrinsic obstacle is the lesion scar which forms at the lesion site after CNS injury (Silver and Miller, 2004). A traumatic insult to the CNS induces a disruption of blood vessels which opens the CNS blood-brain-barrier (BBB). Thereby, various types of blood-derived immune cells enter into the CNS parenchyma and induce an inflammatory wound healing response. However, in contrast to most peripheral tissues, wound healing in the CNS is aberrant and therefore results in excessive scar formation at the injury site. The scar tissue that forms at the CNS lesion site is not homogenous and according to its cellular composition the scar can be divided in two major types.



The glial scar forms at the lesion borders and is mainly constituted by reactive astrocytes, often referred as to astrogliosis (**Fig 2.3a**), some activated microglia, oligodendrocytes and their precursors. These cells express and release various factors that regulate fundamental processes for CNS tissue repair including inflammation, BBB consolidation and neuroprotection. Reactive astrocytes are characterized by distinct anatomical changes that appear early after injury. Resident astrocytes become hypertrophic, extend thick processes and show enhanced glial-fibrillary acidic protein (GFAP) immunofluorescence (**Fig 2.3b**). During the first days after injury, these reactive astrocytes increase in numbers, accumulate at the lesion borders and thereby enclose the lesion site (Mathewson and Berry, 1985). The closure of the CNS through the astroglial scar is crucial for recovering CNS tissue homeostasis. Genetic ablation of reactive astrocytes leads to failure in BBB repair, prolonged bleeding, secondary damage and lesion enlargement which consequently promotes neuronal death (Faulkner et al., 2004; Sabelstrom et al., 2013). However, the role of the glial scar after CNS injury is diverse. While the glial scar prevents further CNS tissue damage, it also contributes to the inhibition of axon regeneration. Reactive astrocytes produce extracellular matrix (ECM) components and axon growth inhibitory molecules including chondroitin sulfate proteoglycans (CSPGs), semaphorins and ephrins (Silver and Miller, 2004).

The second type of scar tissue at the lesion site is the fibrotic scar. After SCI, adjacent meningeal and perivascular fibroblasts invade the lesion site, proliferate and deposit a dense connective tissue containing ECM molecules such as laminin, fibronectin, collagen and CSPGs. Primarily, the fibrotic scar has been suggested to be important for the sealing of the injury site by entrapping blood-derived leukocytes (Berry et al., 1983). However, more recent studies suggest that BBB consolidation and astrocyte reactivity is normal when fibrotic scarring is inhibited, (Yoshioka et al., 2010; Hellal et al., 2011) indicating that the fibrotic scar is not instrumental for CNS repair.

The fibrotic scar is also a major impediment for regenerating axons. Injured CNS axons stall regeneration at the border of the fibrotic scar (Stichel and Müller, 1994), which expresses growth inhibitory molecules including CSPGs (Tang et al., 2003), tenascin-C (Tang et al., 2003), semaphorins (Pasterkamp et al.,

1999) and EphB2 (Bundesen et al., 2003). Interestingly, it has been shown that the loss of the axon regeneration capacity early after birth correlates with the ability of the injured CNS to form a fibrotic scar (Kawano et al., 2005). Treatments that reduce fibrotic scarring render a CNS lesion growth permissive for regenerating axons, promoting axon regeneration and functional recovery after brain injury (Stichel et al., 1999) and SCI (Klapka et al., 2005; Hellal et al., 2011).

A major cellular source of fibrotic scar tissue are meningeal fibroblasts. In the uninjured CNS, meningeal fibroblasts are quiescent and do not abundantly express ECM. However, after CNS damage meningeal fibroblasts become migratory, invade the lesion site, proliferate and produce ECM components, ultimately leading to fibrotic scar tissue (**Fig 2.3a,b**). By contrast, in a SCI model where minimal damage is applied to the meninges, no fibrotic scar formation is observed and axons are able to regenerate through the lesion site (Seitz et al., 2002). The activation of meningeal fibroblasts after injury is induced by infiltrating blood-derived monocytes (**Fig 2.3a**) and by resident microglia that secrete different cytokines including TGF- $\beta$ 1 an important fibrogenic, anti-inflammatory factor (Komuta et al., 2010). Manipulating TGF- $\beta$ 1 signaling modulates fibrotic scar formation after CNS injury. Local administration of TGF- $\beta$ 1 increases fibrotic scarring at the lesion site (Logan et al., 1994). Accordingly, interfering with TGF- $\beta$ 1 signaling through local application of decorin or Taxol reduces fibrosis and enhances axon regeneration (Davies et al., 2004; Hellal et al., 2011).

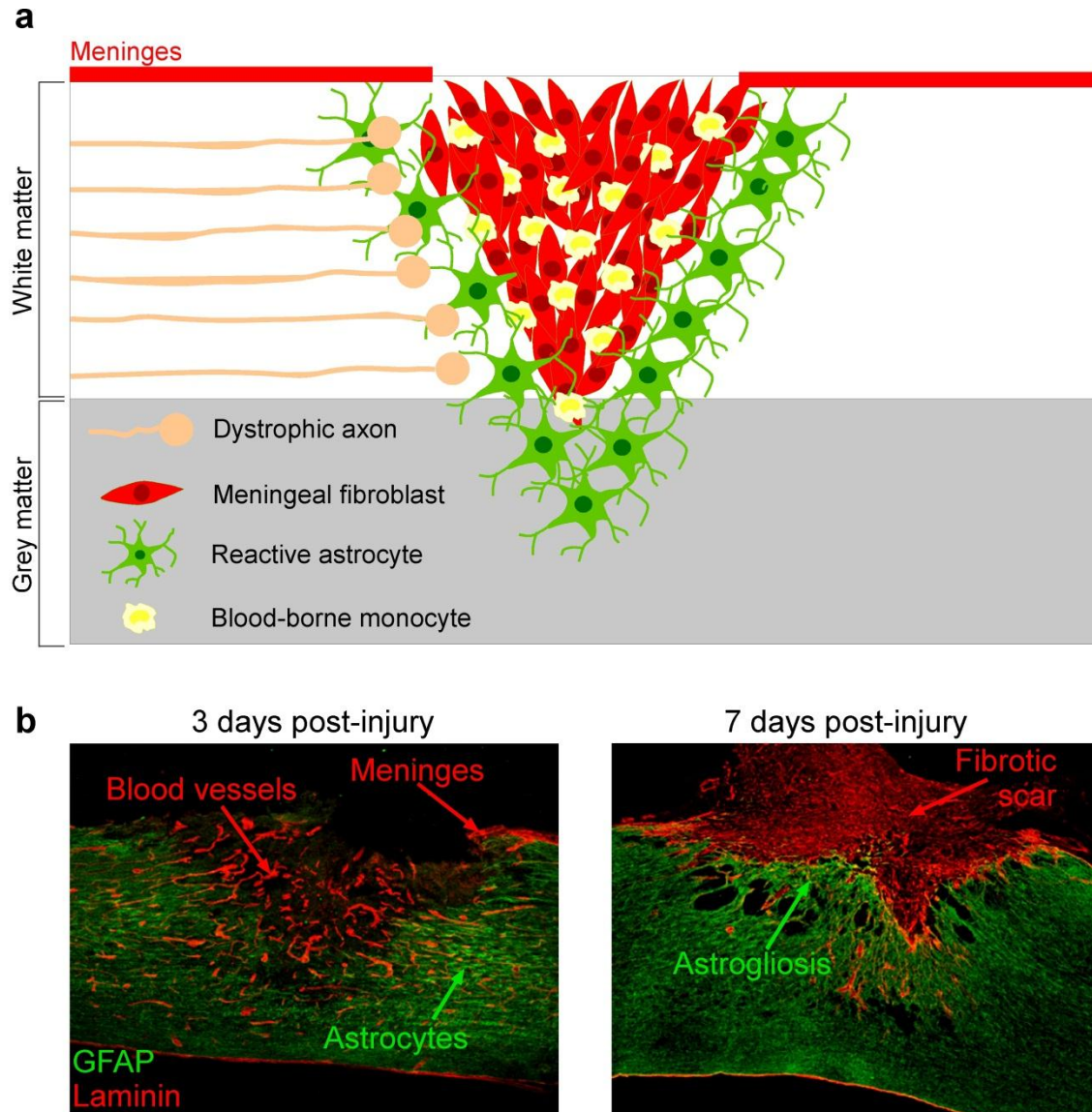


**Figure 2.3 Scar formation after spinal cord injury.**

**a)** Schematic illustration of the lesion scar that forms after spinal cord injury. Reactive astrocytes form the glial scar that secludes the lesion site and prevents the entering of blood-derived monocytes into the CNS. Meningeal fibroblasts form the fibrotic scar within the lesion epicenter. Injured CNS axons can not regenerate through the scar and become dystrophic. *Drawing adapted from Silver and Miller, Nat Rev Neurosci. 2004.*

**b)** Sagittal sections of the rat spinal cord at specific time-points after spinal cord injury stained for glial fibrillary acidic protein (GFAP) to visualize astrocytes and stained for extracellular matrix-protein laminin to visualize fibrotic scar tissue. *Pictures from F.Hellal.*

Thus, the two components of the lesion scar have different significance for the wound healing response after SCI. The astroglial scar is generally growth repelling but also neuroprotective. Therefore, interfering with astrogliosis might have detrimental effects. By contrast, the fibrotic scar is considered a strong impediment for regenerating axons and as an aberrant, but a redundant component of the lesion scar. Therefore, targeting the fibrotic scar is a promising strategy to promote axon regeneration after SCI.

### **2.2.3. CNS myelin and Rho signaling**

Besides the lesion scar, a major inhibitory factor of the CNS lesion environment is CNS myelin. CNS myelin ensheaths and insulates CNS axons, which is crucial for their function and maintenance. The myelin sheaths contain axon growth inhibitory molecules, called myelin associated inhibitors (MAIs), including Nogo-A (Prinjha et al., 2000), myelin-associated glycoprotein (MAG) (McKerracher et al., 1994) and oligodendrocyte myelin glycoprotein (Omgp) (Habib et al., 1998). A SCI disrupts the axons and their myelin sheaths, consequently resulting to a release of the MAIs at the lesion (Filbin, 2003). All MAIs bind to the NgR-P75 receptor complex (Filbin, 2003) which signals onto the small, intracellular GTPase RhoA (Dergham et al., 2002). RhoA is a central regulator of the axonal cytoskeleton and its activation induces growth cone collapse and axon growth inhibition through different mechanisms. (**Fig. 2.4**): First, RhoA induces actin contraction through its downstream effectors Rho Kinase (ROCK) and the non-muscular myosin light-chain II (MLCII) (McKerracher et al., 2012). Second, RhoA prevents actin dynamics by inactivating the actin depolymerizing and severing protein cofilin through ROCK and LIM Kinase (Hsieh et al., 2006). Third, RhoA promotes microtubule disassembly by inactivating collapsin-response mediator proteins (CRMPs) 2 and 4 (Fukata et al., 2002; Alabed et al., 2007). Besides MAIs, other important growth inhibitory molecules signal through Rho mediated pathways including CSPGs (Dickendesher et al., 2012) and semaphorins (Swiercz et al., 2002). Accordingly, when RhoA is inhibited in neurons through the bacterial enzyme C3 transferase, neuronal growth cones do not collapse upon encountering various non-permissive substrates, and neurite growth is enhanced (reviewed in (McKerracher et al., 2012).

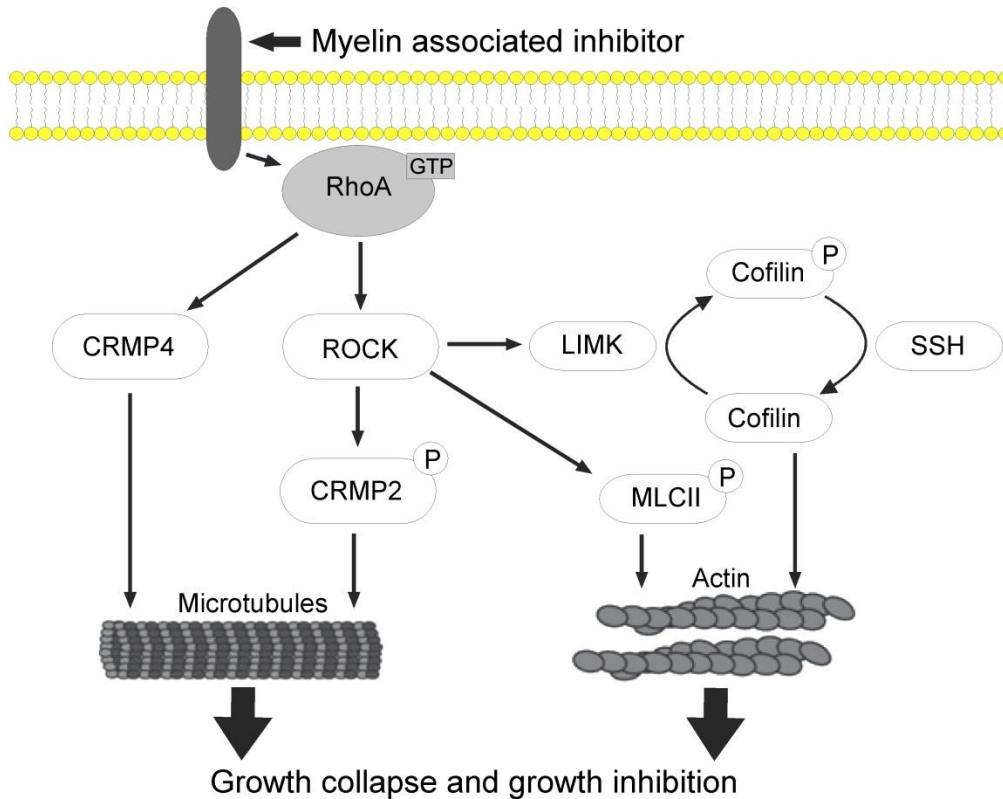


**Figure 2.4 RhoA signalling mediates myelin-associated axon growth inhibition by inducing cytoskeletal rearrangements leading to growth cone collapse.**

Various growth inhibitors activate RhoA through different cell surface receptors. RhoA and its main effector Rho Kinase (ROCK) act through collapsin response factors onto microtubules and through cofilin and myosin light chain kinase 2 (MLCII) onto actin. This leads to cytoskeletal alterations that ultimately induce growth cone collapse and axon growth inhibition. *Scheme adapted from McKerracher et al., Int Rev Neurobiol. 2012.*

Taken together, there are 3 major impediments for axon regeneration in the adult CNS. First, adult CNS neurons have a poor intrinsic ability to regrow injured axons. Second, CNS injury leads to the formation of an axon-growth inhibitory lesion scar. Third, CNS myelin components in the lesion area prevent axon regrowth by inducing growth cone collapse. Thus, the most promising strategy to promote axon regeneration are multifactorial approaches that concurrently increase the regenerative capacity of CNS neurons and combat the inhibitory action of the lesion scar and CNS myelin. Interestingly, a common regulator of these features is the cytoskeleton. It controls the axonal growth machinery, regulates migration and proliferation of scar-forming cells and is the fundamental down-stream target of inhibitory

molecules, including CNS myelin components. Thus, targeting one cellular structure, the cytoskeleton, might be sufficient to overcome both intrinsic and extrinsic obstacles to axon regeneration.

## **2.3. The cytoskeleton**

Every cell contains structured arrays of fibrous proteins that are collectively termed as the cytoskeleton. Similar to the skeleton of the human body, the cytoskeleton acts as the major scaffold of the cell. However, in contrast to the human skeleton, the cytoskeleton is a highly dynamic structure. The cytoskeleton plays an essential role in most cellular events including intracellular transport, cell division, cell migration and cell polarization. It is formed by three major components: actin filaments also termed microfilaments, intermediate filaments and microtubules.

### **2.3.1. Actin filaments**

With a diameter of approximately 7 nm actin filaments are the smallest component of the cytoskeleton. Filamentous actin, or F-actin, is a dynamic polymer that is built from globular G-actin subunits. These subunits are bound in a head-to-tail orientation, which result in two structurally distinct endings and the intrinsic polarity of the F-actin polymer. The F-actin “barbed” end preferentially binds G-actin bound to ATP (ATP-actin), which leads to polymer growth (polymerization). After incorporation into the polymer, ATP is hydrolyzed to ADP and ADP-actin dissociates from the F-actin “pointed” end. Soluble ADP-actin recycles into ATP-actin and is reincorporated into the “barbed” end (**Fig. 2.5**).

Actin filaments are organized into bundles or networks, which are structurally distinct. While actin bundles contain tightly packed actin filaments that organize in parallel arrays, actin networks contain loosely packed filaments that criss-cross at various angles. Both in bundles or networks, actin filaments are connected by actin cross linking proteins including fascin, spectrin or filamin (**Fig. 2.5**). Fascin and spectrin organize actin filaments into bundles, while filamin mediates cross-linking of actin filaments into

networks. Besides structural differences, actin bundles and networks have distinct functional differences, which are especially important for cell locomotion. A key event of cell locomotion is membrane protrusion, which is conducted by actin filaments. Actin bundles form spiky, finger-like membrane protrusions, called filopodia. By contrast, the actin network forms flattened, veil-like membrane extensions, called lamellipodia. Filopodia and lamellipodia can be observed in most migrating cells or cellular structures, reflecting their fundamental role in cellular migration.

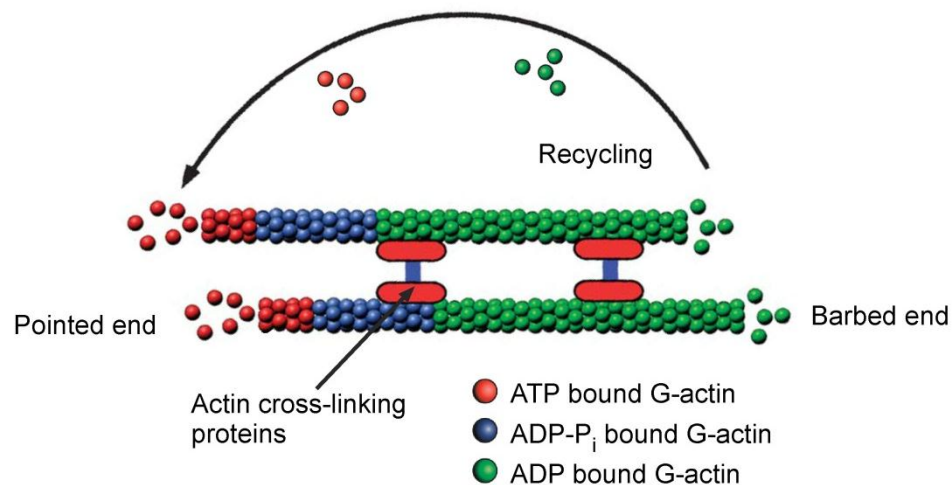


**Figure 2.5 Structure and dynamics of actin filaments.**

Actin filaments assemble G-actin bound to ATP at the barbed end and disassemble G-actin bound to ADP at the pointed end, which is then recycled for reassembly at the barbed end. Actin cross linking proteins connect individual actin filaments. *Scheme adapted from Stuessi and Bradke, Dev Neurobiol. 2011.*

### 2.3.2. Intermediate filaments

Intermediate filaments are a superfamily of  $\alpha$ -helical proteins with a diameter of about 10 nm. Unlike microfilaments or microtubules, intermediate filaments are composed of rod-shaped subunits of a widely divergent molecular origin. The subunits organize in a head-to-head orientation and therefore intermediate filaments are nonpolar. Moreover, in comparison to actin filaments and microtubules, intermediate filaments are extremely stable and show only slight dynamics. Due to this lack of intrinsic

polarity and dynamics, intermediate filaments are not fundamentally involved in cell motility. The most important function of intermediate filaments is to provide mechanical support to the plasma membrane when it contacts other cells or the ECM. However, intermediate filaments such as GFAP have also been implicated with regulatory functions such as cell-cell communication, BBB function and wound healing in the CNS (Liedtke et al., 1996).

### **2.3.3. Microtubules**

Microtubules, the largest component of the cytoskeleton, are tubular cylinders with a diameter of around 25 nm. Due to their cylindrical structure, they are stiffer than actin filaments and intermediate filaments. Similar to actin filaments, microtubules are polymers with a structural and functional polarity. The microtubule is formed by  $\alpha$ -tubulin and  $\beta$ -tubulin heterodimers, which are associated in a head-to-tail orientation, which leads to intrinsic polarity; the microtubule is said to contain a minus- and a plus-end. Both tubulin monomers bind GTP. While the binding of GTP to  $\alpha$ -tubulin is irreversible,  $\beta$ -tubulin binds and hydrolyzes GTP to GDP. GTP bound tubulin assembles at the highly dynamic plus-end of the microtubule and disassembles after GTP hydrolysis (**Fig. 2.6**). Thereby the plus-end undergoes periods of polymerization and depolymerization, which is termed dynamic instability (**Fig. 2.6**). This dynamic instability allows the microtubule to switch abruptly from growth to shrinkage, termed “catastrophe”, and from shrinkage to growth, termed “rescue”. Accordingly, microtubules can be subdivided into two populations: unstable, short-lived microtubules and stable, long-lived microtubules. Unstable microtubules are observed in cell structures that require a rapid assembly or disassembly of microtubules such as the mitotic spindle during cell mitosis. By contrast, some cell types, usually non-replicating cells, contain very stable and long-lived microtubules. An extreme example for such long-lived microtubules is the neuronal axon. Since neurons have to maintain axonal connections over long time, e.g. over decades in humans, the microtubules in these connections have to be highly stable in order to avoid the retraction of the axon and functional deinnervation.



Microtubule dynamics and stability are regulated by different factors. First, GTP-tubulin acts as a protective “GTP cap” by assembling at the plus-end of the microtubule and averting dissociation of the GDP bound tubulin (Desai and Mitchison, 1997). Second, microtubule dynamics are regulated by microtubule associated proteins (MAPs) (reviewed in (Mandelkow and Mandelkow, 1995). MAPs structurally interlink microtubules within the cytoskeleton or to the plasma membrane. In addition, MAPs, including Tau, MAP1b and 2, regulate microtubule stability (**Fig. 2.6**). For instance, dephosphorylated Tau binds predominantly to axonal microtubules and strongly stabilizes them (Mandelkow and Mandelkow, 1995). Dephosphorylated MAP2 binds specifically to microtubules in neuronal dendrites but, in contrast to Tau, preserves microtubule dynamics (Sánchez et al., 2000). A specific subclass of MAPs are plus-end binding proteins termed +TIPs, which include cytoplasmic linker proteins (CLIPs), CLIP-associated proteins (CLASPs) and end-binding proteins (EB1 and EB3). +TIPs bind specifically to the plus-end of the microtubule and regulate microtubule growth and shrinkage (**Fig. 2.6**). Moreover, +TIPs link microtubules to the actin cytoskeleton by binding to actin binding proteins (reviewed in Akhmanova and Steinmetz, 2008).

Microtubule dynamics can be also manipulated with a variety of drugs. They can be subdivided into microtubule stabilizing agents (MSAs) such as Taxol or epothilones and substances that destabilize microtubules such as nocodazole, colchicine or vinblastine. Taxol or epothilones bind to free and incorporated  $\beta$ -tubulin subunits (Bollag et al., 1995; Giannakakou et al., 2000). MSA binding to free tubulin enables polymer assembly without requiring GTP (Diaz and Andreu, 1993) and within the polymer, MSAs stabilize the lateral contacts between the individual subunits (Wade, 2009). Thereby, these drugs shift the dynamic equilibrium of polymer growth and shrinkage towards microtubule growth and furthermore protect the polymer against depolymerization similar to the microtubule stabilizing protein Tau (Kar et al., 2003). The stability of microtubules is reflected by post-translational tubulin modifications. Newly formed microtubules are mainly composed of subunits containing tyrosinated  $\alpha$ -tubulin, while in more stable and persistent microtubules,  $\alpha$ -tubulin gradually becomes detyrosinated and

acetylated (Janke and Bulinski, 2011). Accordingly, the very stable and persistent microtubules in neuronal axons show high levels of tubulin acetylation (Gomis-Ruth et al., 2008) and detyrosination (Janke and Bulinski, 2011).

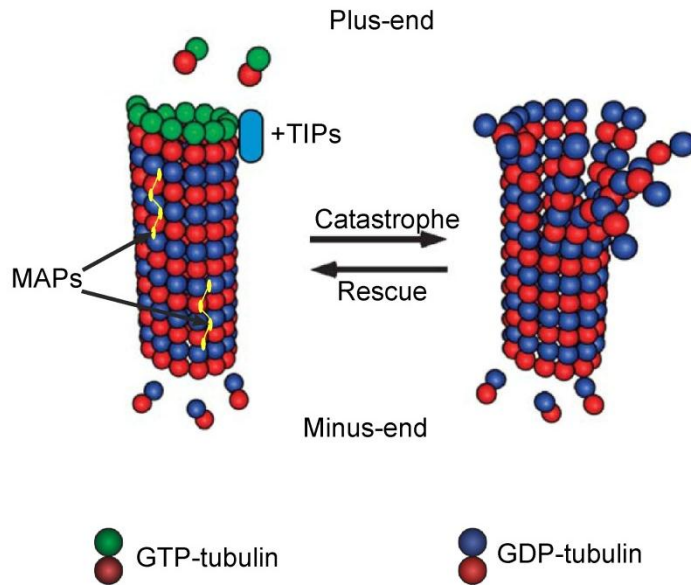


**Figure 2.6 Microtubule structure and dynamics.**

Microtubule dynamic instability. The plus-end of microtubules can switch between tubulin assembly (rescue) and tubulin disassembly (catastrophe). GTP-bound tubulin cap, microtubule associated proteins (MAPs) and plus-end binding proteins (TIPs) protect the plus-end from depolymerization (catastrophe). *Scheme adapted from Stiess and Bradke, Dev Neurobiol. 2011.*

Microtubules are involved in a wide range of cellular functions including cell proliferation, vesicular transport, cell signaling and cell motility. They underlie formation of the mitotic spindle during mitosis, control movement of cilia and flagella and act as scaffolds for vesicular transport in the cytoplasm. Microtubules also regulate every kind of cell motility including axon growth (see **chapter 2.4.**) and cell migration (see **chapter 2.5.**). Importantly, these features are critical for the regeneration failure in the adult CNS as described above. Therefore, targeting microtubules could offer a potential multifactorial approach to counteract intrinsic and extrinsic barriers in the injured CNS and to promote axon regeneration.

## **2.4. Microtubule stabilization controls axon growth**

Neurons represent extreme examples of cellular polarization. During neuronal development they compartmentalize into three main structures: 1) The neuronal soma, which contains the nucleus and the major cellular machinery. 2) The axon, a single, long process that transmits information to other neurons. 3) The dendrites, a set of typically short-growing processes that collect and integrate signals from other neurons. Before polarization into axonal and dendritic compartments, neurons form multiple short neurites, which are functionally and structurally indistinguishable. However, one of these neurites grows extensively and develops into the future axon. A critical step of this enhanced growth, is the specific stabilization of axonal microtubules (Witte et al., 2008). Accordingly, global stabilization of microtubules by low doses of Taxol (**see Chapter 2.3.3.**) leads to multiple axon formation in neurons (Witte et al., 2008). In addition, when the microtubules in one neurite are locally stabilized by photoactivatable Taxol, this neurite develops into an axon as reflected by an increased amount of axon-specific, dephosphorylated Tau and by an increased growth (Witte et al., 2008). Thus, promoting microtubule stabilization is sufficient to induce axon formation and growth. This fundamental effect of microtubules and their stability can be explained by their functional role as a part of the axonal growth machinery. During development, axons grow for long distances until they successfully innervate their target structure. Therefore, axons require a motile element that steers and navigates them to their final target, sufficient construction material to extend in length and a stable “backbone” providing sufficient structural integrity.

The motile element that drives the growing axon is the growth cone, a conical or fan-like structure at the distal axonal tip. The growth cone is a highly dynamic structure that drives elongation of the axon by migrating in response to spatial cues. The internal structure of the growth cone can be divided into three distinct domains, which are fundamental to its function (**Fig. 2.7**): The leading edge of the growth cone, called the peripheral domain (P-domain), is mainly enriched with actin filaments which form highly dynamic filopodia and lamellipodia (**see chapter 2.3.1.**). The central domain (C-domain) of the growth

cone comprises polymerizing microtubules and is the major delivery site of vesicles and organelles. The C-domain also comprises neurofilaments. The rim between the actin-rich P-domain and the microtubule rich C-domain is called transition zone and represents an interface for actin and microtubule interactions. Actin and microtubules have profound functions in axon growth and elongation. In general, actin filaments regulate growth cone shape and axon guidance, while microtubules stabilize the elongating axon shaft and steer the growth cone. Accordingly, growth cones cannot move forward when microtubules are destabilized by nocodazole (Tanaka et al., 1995), while growth cones without actin filaments can grow but in an undirected fashion (Bradke and Dotti, 1999).

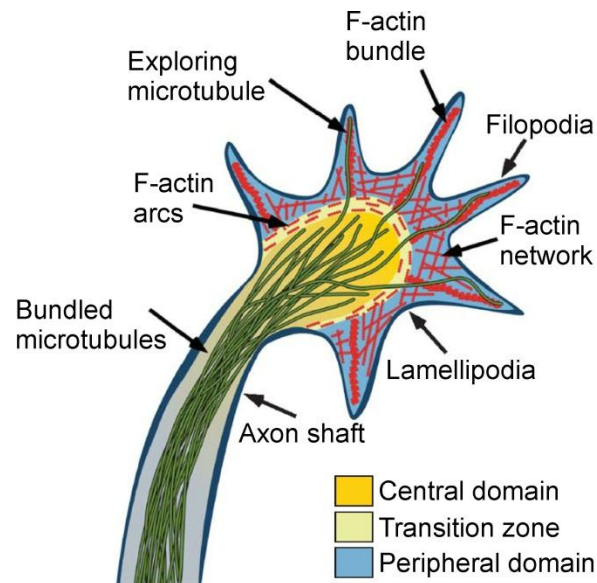


**Figure 2.7 Cytoskeletal organization of the growth cone.**

The growth cone is organized into three domains. The peripheral domain is F-actin rich and comprises membrane protrusions, such as filopodia and lamellipodia, important for growth cone guidance. The central domain is rich in microtubules, which are important for growth cone steering and advance. The transition zone is the interface between the two domains where actin and microtubules interact. *Scheme from Stuessi and Bradke, Dev Neurobiol. 2011.*

Growth cone migration and advance can be separated into three distinct stages (**Fig. 2.8**). During the first stage, called protrusion, filopodia and lamellipodia extend and elongate, which is mediated by increased F-actin polymerization. In the second stage, called engorgement, pioneer microtubules polymerize into the

area in which the peripheral actin cytoskeleton has protruded. The third and last stage is called consolidation. At this point, stable and bundled microtubules enter from the C-domain into the newly formed growth cone area, are compressed by actin filaments and then consolidated into a new part of the axon shaft. Finally, microtubules become stabilized and bundled by MAPs which are necessary for the structural integrity of the axon (Conde and Caceres, 2009). A constant repetition of these steps ultimately leads to axon elongation (reviewed in (Lowery and Van Vactor, 2009; Stiess and Bradke, 2011).

Besides their structural role in the axon shaft, stable microtubules have an instructive function for directed growth cone advance. Polymerization of microtubules into the growth cone P-domain is sufficient to steer the growth cone in a certain direction, this is supported by the observation that local stabilization of microtubules through Taxol is sufficient to steer the growth cone in the direction of the site of Taxol application (Buck and Zheng, 2002). Conversely, local destabilization of microtubules, through nocodazole treatment, induces growth cone turning away from the site of nocodazole application (Buck and Zheng, 2002). This effect is mediated by microtubule dependent remodeling of the actin cytoskeleton through Rho GTPases, and by physically fixing and supporting the direction of the growth cone (Lowery and Van Vactor, 2009). In addition, the site of microtubule stability receives an increased amount of vesicular cargo, providing the growth cone machinery with the necessary materials such as membrane vesicles and cytoskeletal elements (Zakharenko and Popov, 1998).

Finally, microtubule stabilization is instrumental for growth cone formation after axonal injury. Injured axons in the PNS normally form new growth cones and regenerate while injured CNS axons do not form growth cones but dystrophic endbulbs, termed retraction bulbs, that do not regenerate (Bradke et al., 2012). Growth cone formation in injured PNS axons requires bundling of microtubules in the distal axon (Erturk et al., 2007). By contrast, microtubules in the CNS retraction bulbs are disassembled and disorganized (Erturk et al., 2007). Moreover, when microtubules of regenerating PNS axons are destabilized by nocodazole or vincristine, growth cone formation is prevented (Pan et al., 2003; Erturk et al., 2007) and instead retraction bulbs are formed (Erturk et al., 2007). Conversely, injured axons in the

CNS that are locally treated with low doses of Taxol do not form dystrophic retraction bulbs (Erturk et al., 2007).

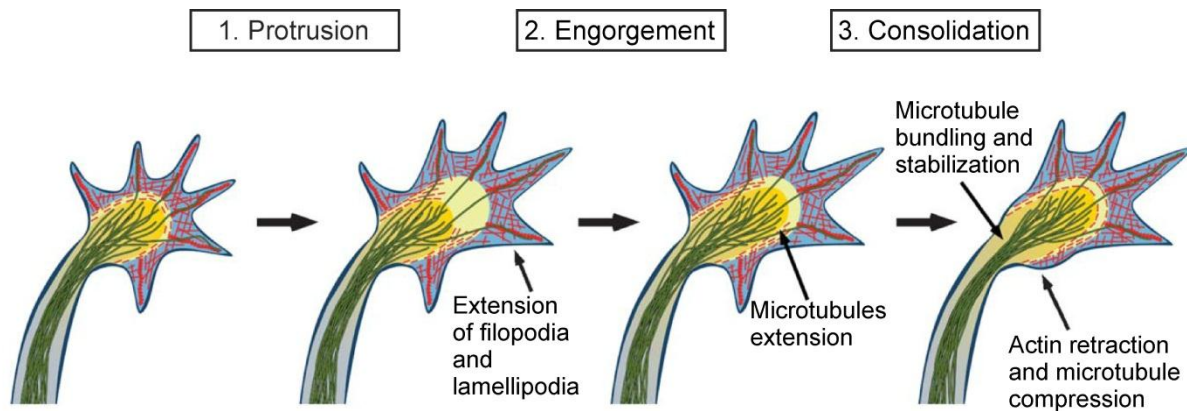


**Figure 2.8 Growth cone advance is divided in three distinct steps.**

1.) During protrusion, actin-rich filopodia and lamellipodia extend leading to extension of the central domain. 2.) During engorgement, the extended central domain is invaded by microtubules. 3.) During consolidation, microtubules in the proximal central domain are compressed by actin, bundled and stabilized. *Scheme from Stuessi and Bradke, Dev Neurobiol. 2011.*

Taken together, microtubule stabilization is critical for growth cone formation and migration. Increasing microtubule stabilization is sufficient to induce axon growth. Therefore, targeting microtubule stability in injured spinal cord axons is a conceivable strategy to stimulate their regeneration.

## 2.5. Microtubule stabilization controls cell migration

A key step of cell migration is polarization through which a migrating cell establishes a protrusive front, the leading edge, and a contractile rear, the trailing edge. To achieve polarity, a migrating cell reorganizes its microtubule array through selective formation of stable, detyrosinated microtubules near the leading

edge (**Fig. 2.9a**) (Gundersen and Bulinski, 1988). By contrast, microtubules in the rear of the cell remain dynamic, as indicated by tubulin tyrosination (Gundersen and Bulinski, 1988).

But why does a migrating cell require such a polarized microtubule array? During migration, the leading edge of a cell forms actin-dependent protrusions, called lamellipodia, which are attached to the substratum through focal adhesions in order to transmit actin protrusive forces into directional movement. By contrast, the trailing edge of the cell detaches its focal adhesions from the substrate and retracts (**Fig. 2.9b**). Microtubule stability is fundamental for both leading edge protrusion and trailing edge retraction. The stabilized microtubule array in the cell front biases the delivery of membrane vesicles to the leading edge through kinesins that preferentially bind to stable microtubules (Schmoranzer et al., 2003). In addition, stable microtubules maintain actin-dependent cell protrusions such as lamellipodia by binding and inactivating guanine exchange-factor (GEF) H1. GEF H1 negatively regulates the activity of the GTPase RhoA (Krendel et al., 2002), which inhibits lamellipodia formation (Kaibuchi et al., 1999). Destabilization of microtubules through nocodazole induces massive GEF H1 release, global activation of RhoA, which in turn prevents leading edge protrusion and cell migration (Liao et al., 1995).

In the trailing edge, however, dynamic and unstable microtubules are critical for cell locomotion. Depolymerizing microtubules release GEF H1, which induces actin contraction through RhoA (Enomoto, 1996; Ganguly et al., 2013) and ultimately to trailing edge retraction. Hence, increasing microtubule stability through Taxol leads to a concentration dependent inhibition of fibroblast migration (Liao et al., 1995).

In addition, microtubule stability regulates focal adhesions, which mediate cell attachment to the underlying substrate. *In vitro* imaging studies have demonstrated that dynamic microtubules contact focal adhesions and induce their disassembly. Accordingly, assembly and disassembly of focal adhesions correlates with the distribution of dynamic and stable microtubules in a migrating cell; focal adhesion

assembly occurs predominant at the leading edge and disassembly at the trailing edge (Kaverina et al., 1999).

Taken together, a fundamental basis for directed cell migration is polarization of the microtubule array, into stable microtubules in the cell front and dynamic microtubules in the cell rear. Consequently, manipulating the microtubule array through drugs that stabilize or destabilize microtubules is sufficient to inhibit cell migration.

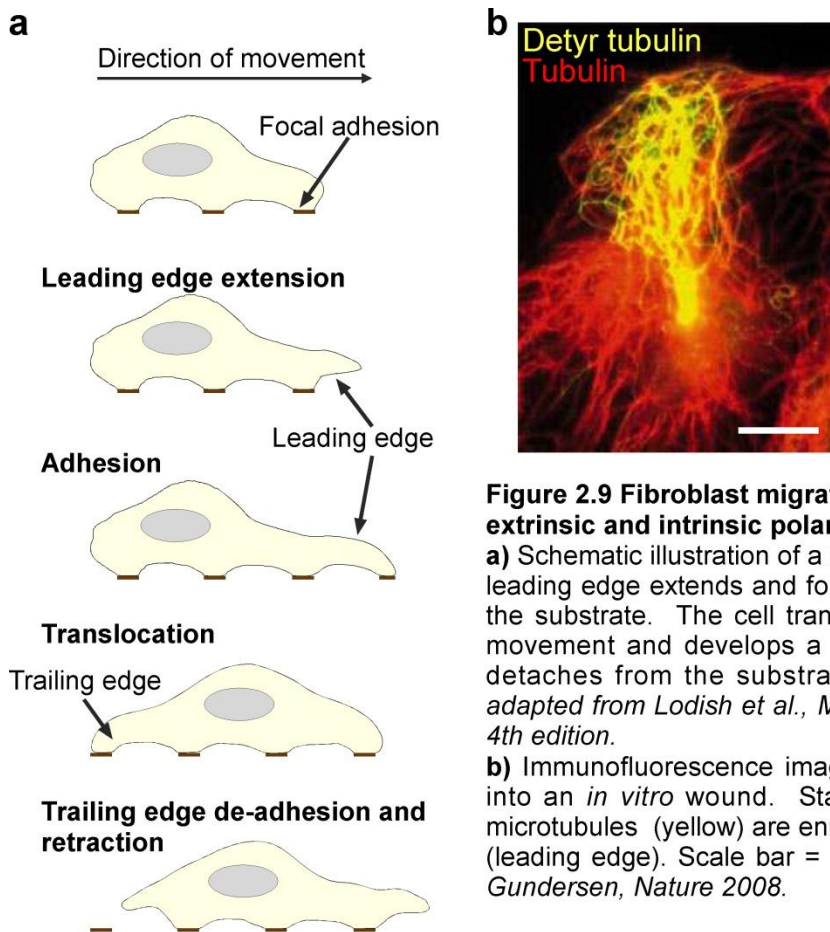


**Figure 2.9 Fibroblast migration requires extrinsic and intrinsic polarization.**  
**a)** Schematic illustration of a migrating cell. The leading edge extends and forms new focal contacts with the substrate. The cell translocates in the direction of movement and develops a trailing edge, which finally detaches from the substrate and retracts. *Drawing adapted from Lodish et al., Molecular Biology of the Cell 4th edition.*  
**b)** Immunofluorescence image of a fibroblast migrating into an *in vitro* wound. Stable, detyrosinated (detyr) microtubules (yellow) are enriched at the front of the cell (leading edge). Scale bar = 10  $\mu\text{m}$ . *Picture from Li and Gunderson, Nature 2008.*



## **2.6. Microtubule stabilization reduces scarring and promotes axon regeneration after spinal cord injury**

Microtubule stability plays a dual role during axon growth and scar formation. In axons, microtubule stability controls axon growth by regulating growth cone formation and migration (Bradke and Dotti, 1999; Buck and Zheng, 2002; Witte et al., 2008). In migrating fibroblasts, the balance between stable microtubules at the cell front and dynamic microtubules at the cell rear is critical for directed migration. Hence, perturbing this balance inhibits cell migration (Liao et al., 1995; Ganguly et al., 2013). Therefore, targeting microtubule stability could offer a multifaceted approach to promote axon regeneration after CNS injury; one side by promoting growth cone formation and axon regrowth in injured CNS axons and the other side, by interfering with lesion scar formation by inhibiting the migration of scar forming fibroblasts into the lesion site.

Indeed, a recent study showed that the microtubule stabilizing drug Taxol has promising effects on axon growth and regeneration as well as scar formation (Hellal et al., 2011). In this study, cultured, postnatal CNS neurons plated in the presence of various inhibitory factors showed enhanced axon growth when treated with low doses of Taxol. In addition, when Taxol was delivered locally to a spinal cord injury site, fibrotic scarring was strongly reduced. This dual action of Taxol increased axon regeneration and improved the functional outcome after SCI.

## **2.7. Research objectives: Systemic administration of epothilone B promotes axon regeneration and functional recovery after spinal cord injury**

Taxol would represent a promising treatment for SCI pathologies, because the drug suppresses inhibitory scarring, promotes axon regeneration and as a consequence improves functional recovery after experimental SCI (Hellal et al., 2011). However, Taxol has limited therapeutic value as a treatment for

SCI in patients, because it does not cross the blood-brain-barrier and is therefore impractical for clinical situations.

Thus, I asked whether the therapeutic strategy of pharmacological microtubule stabilization could be translated in a more clinically feasible approach. Three features are important to add clinical significance to a pharmacological treatment targeting the injured spinal cord. First, the drug should be FDA approved even if in another medical application. Second, the drug should be systemically delivered, so that the treatment is CNS non-invasive. Third, the treatment should be effective when applied delayed after injury (Kwon et al., 2002). Given these requirements, I sought a candidate drug, which stabilizes microtubules and matches the abovementioned criteria.

I identified epothilone B as such a compound. Epothilones bind and stabilize microtubules in a similar fashion to Taxol (**see chapter 2.3.3.**) (Prota et al., 2013). In contrast to Taxol however, epothilones are able to penetrate through the blood-brain-barrier (Fellner et al., 2002; Rivera et al., 2008) and therefore are able to increase microtubule stability in the CNS upon systemic administration (Brunden et al., 2010). In 2011, a derivative of the epothilone B isoform, termed ixabepilone, received clinical approval as a treatment for various types of cancer (Lechleider et al., 2008).

Given these promising features of epothilone B, I investigated whether systemic and post-injury administration of the drug has beneficial effects on SCI pathology. I propose that this treatment strategy promotes functional axon regeneration after experimental SCI by counteracting intrinsic and extrinsic barriers for regenerating axons in the injured, adult mammalian spinal cord. To test this hypothesis, I used different experimental animal models, including rats and transgenic mice with different types of spinal cord injury, to investigate axon regeneration, scar formation and functional recovery after SCI. In addition, I used cell culture models, including postnatal neuronal cultures and wound healing assays of scar-forming meningeal fibroblasts, to examine the treatment effects on the cellular level.

### 3. RESULTS

#### 3.1. Local application of epothilone B promotes axon growth and reduces axon dystrophy and fibrotic scarring

It has been shown that moderate microtubule stabilization through Taxol treatment promotes axon growth (Witte et al., 2008), counteracts dystrophy of injured CNS axons (Erturk et al., 2007), suppresses fibrotic scarring and promotes axon regeneration after SCI (Hellal et al., 2011). Epothilone B similarly stabilizes microtubules (Bollag et al., 1995) and may therefore represent a promising treatment for spinal cord repair.

To initially validate whether microtubule stabilization by epothilone B mimics the positive effects of Taxol on axon growth, dystrophy and fibrotic scar formation, I treated dissociated embryonic (E17) rat hippocampal neurons with epothilone B (3 nM) or Taxol (3 nM). A similar proportion of neurons formed multiple axons in the two drug treated conditions (**Fig. 3.1a, b**; EpoB:  $42.2\% \pm 1.6$ ,  $P=0.0003$ ; Taxol:  $39.97\% \pm 4.8$ ,  $P=0.018$ ).

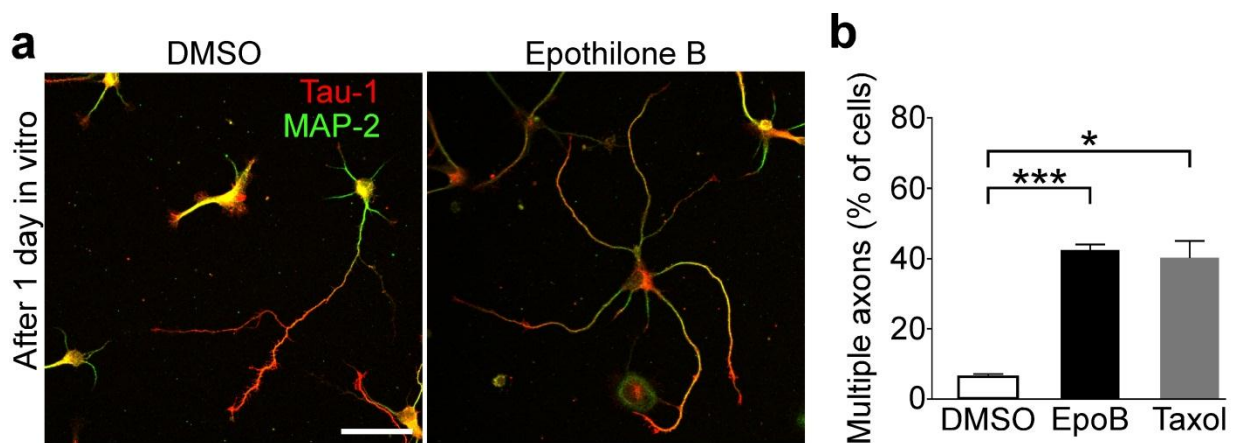


**Figure 3.1 Microtubule stabilization by epothilone B or Taxol promotes axon growth in embryonic neurons.**

(a) Rat hippocampal neurons (E17) stained for Tau-1 (axonal marker) and MAP-2 (dendritic marker). Scale bar=50  $\mu$ m.

(b) Percentage of neurons forming 2 or more axons,  $n>300$  cells/condition. Values are plotted as means+s.e.m.; \* $P<0.05$ , \*\*\* $P<0.001$ .

Next, I tested the effects of epothilone B on axon dystrophy. To this end, I transected GFP-positive sensory axons in the spinal cord of adult, transgenic Thy-1 GFP-M mice (Feng et al., 2000; Erturk et al., 2007). Then, I hourly applied either vehicle solution (5% DMSO in Saline), epothilone B (0.5 ng/ $\mu$ l) or Taxol (0.85 ng/ $\mu$ l), as a positive control, onto the injury site and repeatedly imaged the injured axons for 6 hours by using fluorescent microscopy. Almost 50% of the vehicle treated axons exhibited retraction bulbs at their proximal tip 6 hours after injury (**Fig. 3.2a, b**;  $48.8\% \pm 5.3$ ). By contrast, retraction bulb formation was significantly reduced to less than 18% when injured axons were treated with epothilone B or Taxol (**Fig. 3.2a, b**; EpoB:  $17.7\% \pm 4.4$ ,  $P=0.0001$ , Taxol:  $16.2\% \pm 7.8$ ,  $P=0.0003$ ). Importantly, epothilone B and Taxol inhibited the formation of retraction bulbs to a very similar extent.

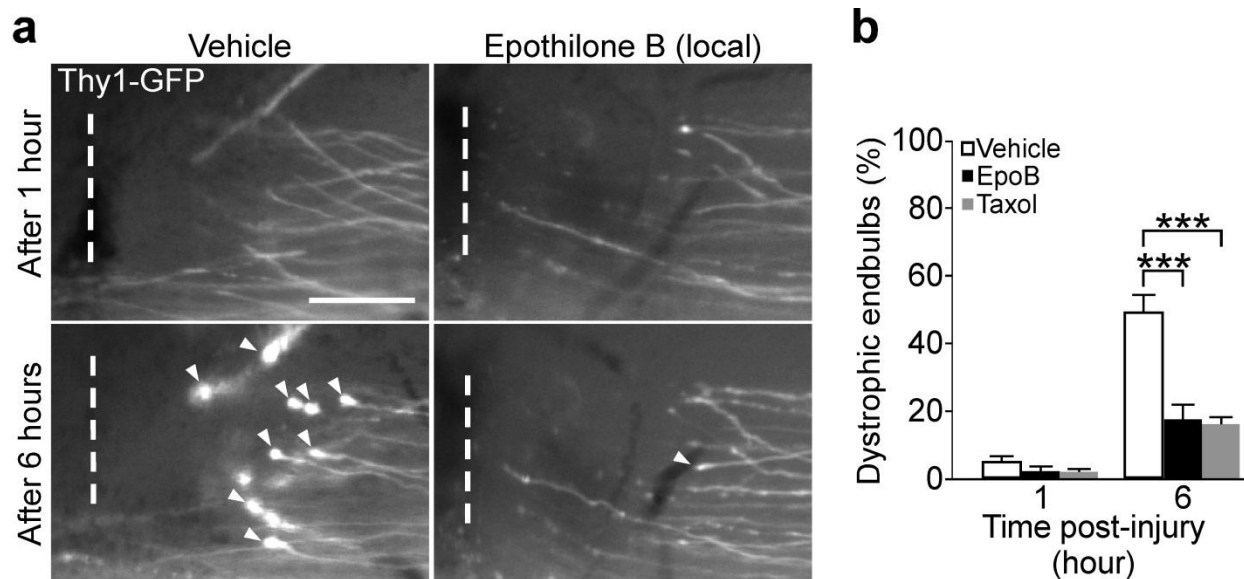
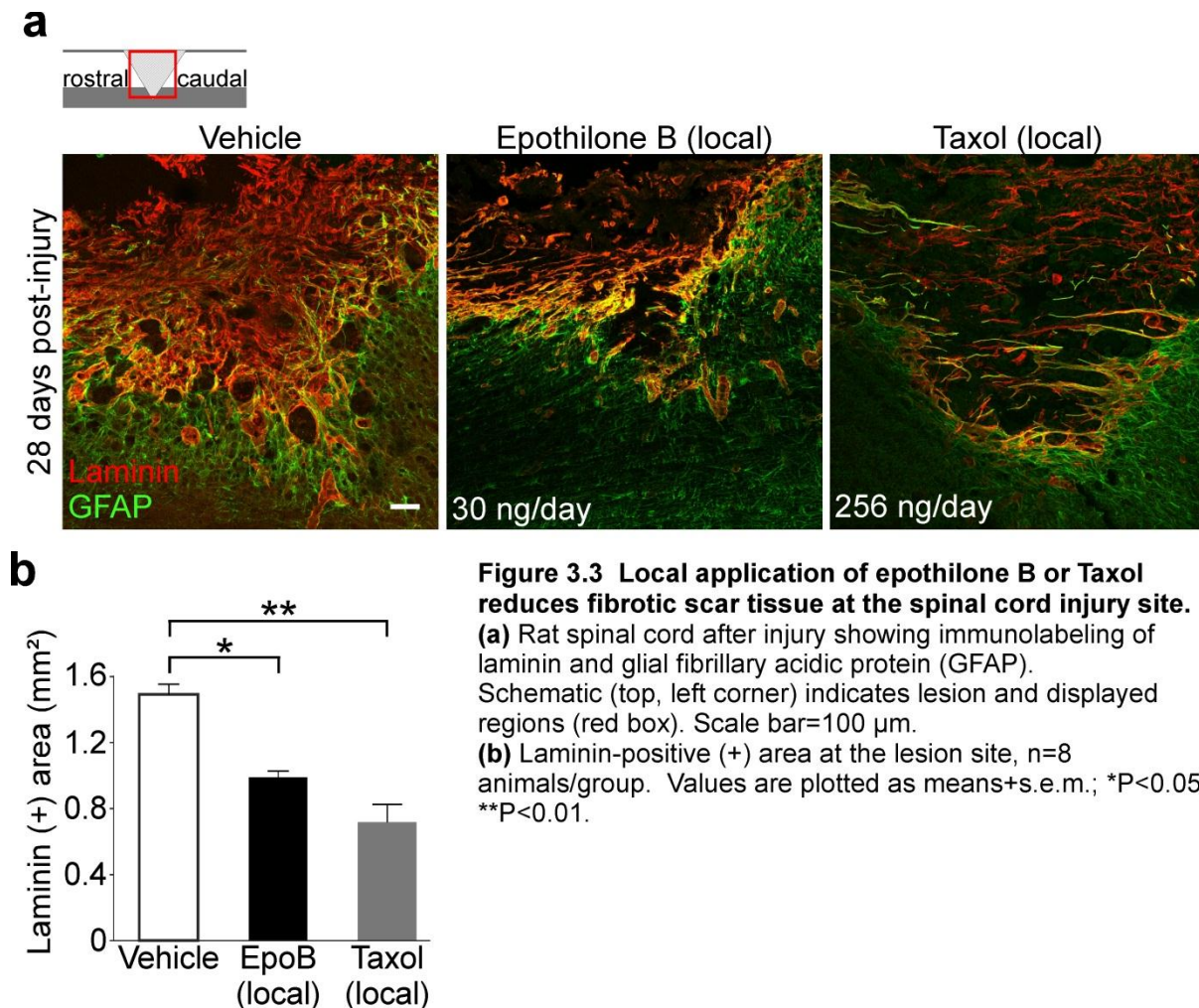


**Figure 3.2 Local application of epothilone B or Taxol reduce axon dystrophy of injured spinal cord axons.**

**(a)** Lesioned GFP-positive spinal cord axons forming retraction bulbs (white arrowheads) over time. Scale bar=100  $\mu$ m

**(b)** Percentage of injured axons forming retraction bulbs at their proximal tip at specific time-points post-injury.  $n=14$  animals/group. Values are plotted as means+s.e.m.; \*\*\* $P<0.001$ .

Finally, I compared the effects of local epothilone B and Taxol treatment on fibrotic scar formation after spinal cord injury. Adult rats underwent a spinal cord dorsal hemisection at thoracic spinal segment T8. Subsequently, epothilone B, Taxol or vehicle solution were chronically delivered to the lesion site via an intrathecal catheter connected to an osmotic pump. Vehicle treated animals showed a profound deposition of laminin-positive connective tissue at the lesion site 4 weeks post-injury (**Fig. 3.3a, b**;  $1.5 \text{ mm}^2 \pm 0.2$ ). By contrast, chronic perfusion of the injury with 30 ng/day epothilone B or 256 ng/day Taxol for 4 weeks led to comparable and significant reductions of laminin-immunopositive areas at the lesion site in comparison to injured control animals (**Fig. 3.3a, b**; EpoB:  $0.99 \text{ mm}^2 \pm 0.1$ ,  $P=0.016$ ; Taxol:  $0.7 \text{ mm}^2 \pm 0.1$ ,  $P=0.005$ ).



Collectively, these results show that moderate microtubule stabilization through epothilone B promotes axon growth in cultured CNS neurons. In addition, microtubule stabilization at the lesion site by local application of epothilone B counteracts dystrophy of injured CNS axons and suppresses fibrotic scar formation after SCI. This suggests that microtubule stabilization by epothilone B mimics the effects of Taxol treatment upon axon growth and SCI pathology.

### **3.2. Systemic administration of epothilone B is a suitable treatment strategy to increase microtubule stabilization at the spinal cord lesion site**

Epothilone B showed promising effects upon axon growth, axon dystrophy and fibrotic scar formation when given locally. However, in contrast to Taxol, epothilone B penetrates the blood-brain-barrier (BBB) and enters the CNS (Fellner et al., 2002; Rivera et al., 2008). Therefore, I asked whether systemic administration of epothilone B could be feasible to treat the injured spinal cord.

To verify whether epothilone B can indeed cross the BBB, a single dose of epothilone B (1 mg/kg bodyweight (BW)) was administered intraperitoneally (i.p.) to adult rats. Plasma and CNS concentration was then measured by mass spectrometry at specific time-points after injection. Remarkably, approximately 40 ng/g epothilone B was found in the spinal cord at 6 hours after injection (**Fig. 3.4a**, 40.7 ng/g  $\pm$  10.2) and remained at comparable levels until day 6 (**Fig. 3.4a**, 43.2 ng/g  $\pm$  13.6). Drug entrance into the brain was slower, however, after 1 day concentrations were comparable to those in the spinal cord (**Fig. 3.4a**, 44.2 ng/g  $\pm$  7.5 (day 1), 48.4 ng/g  $\pm$  3.9 (day 6)). By contrast, drug concentrations in the plasma remained below 8 ng/ml during the 6 days following injection (**Fig. 3.4a**, 3.4-7.8 ng/g). Thus, upon intraperitoneal injection, epothilone B is rapidly up-taken from the plasma into the brain and spinal cord. Furthermore, measurable CNS concentrations of epothilone B were maintained for almost one week

and exceeded plasma concentration at all times after injection, suggesting prolonged drug activity in the brain but not in the circulation.

To test the activity of the drug within the CNS, I injected adult rats intraperitoneally with 0.75 mg epothilone B per kg BW or vehicle 1 day and 15 days after a thoracic spinal cord dorsal hemisection. 4 weeks after injury, animals were sacrificed and the lesioned spinal cord was extracted from the vertebral column and processed for western blot analysis. As a baseline control, I used the thoracic spinal cord of uninjured animals, which was processed in the same way. A spinal cord dorsal hemisection decreased the levels of detyrosinated and acetylated tubulin, both markers for stable and persistent microtubules, in vehicle treated animals (see **chapter 2.3.3.**), suggesting that SCI induces microtubule disassembly (**Fig. 3.4b**). By contrast, epothilone B treated animals showed increased microtubule stability at the lesion site as reflected by increased levels of detyrosinated and acetylated tubulin that were comparable to uninjured controls (**Fig. 3.4b**). Thus, epothilone B rescues microtubule stability at the spinal cord lesion site demonstrating the microtubule stabilizing activity of the drug upon CNS entry.

Finally, I wanted to rule out severe, systemic side effects for the abovementioned treatment regimen. Rats that were i.p. injected twice with epothilone B (0.75 mg/kg BW) at 1 and 15 day(s) after SCI maintained a similar body weight to vehicle treated animals for an observed time-period of 8 weeks (**Fig. 3.4c**). In addition, the number of white blood cells was not significantly affected by systemic epothilone B administration when measured 2 weeks after the second injection (**Fig. 3.4d**, 640 cells  $\pm$  93 (vehicle) vs. 738 cells  $\pm$  196 (EpoB),  $P=0.68$ ). Both results provide evidence, that the bi-weekly intraperitoneal injections of 0.75 mg/kg epothilone B did not provoke adverse side effects in the treated animals and are therefore a well-tolerated dose regimen.

Taken together, these data provide evidence that epothilone B is pharmacological active in the CNS after systemic administration and suggest that the drug is feasible for treating SCI in rodent animal models.

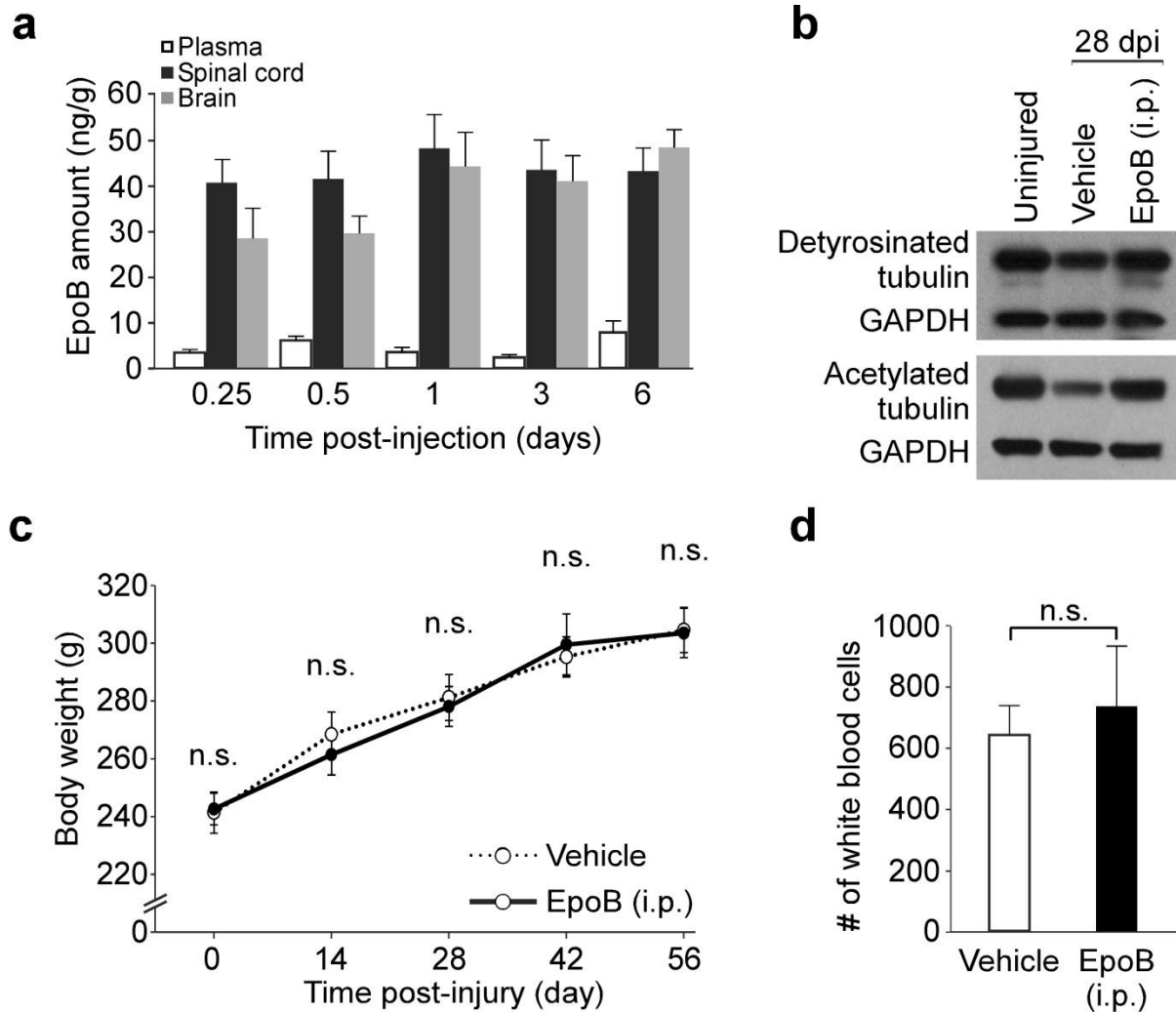


**Figure 3.4 Systemically administered epothilone B enters the CNS and stabilizes microtubules at the spinal cord lesion site without causing adverse side effects.**

**(a)** Mass spectrometric analysis of CNS tissue and blood plasma after a single i.p. injection of epothilone B, n=4 animals/time-point.

**(b)** Protein levels of indicated proteins in pooled spinal cord (lesion) extracts, n=3 animals/group.

**(c)** Time-course of animal body weight after spinal cord contusion injury, n=11-12 animals/group.

**(d)** Number of white blood cells in blood samples 4 weeks after spinal cord dorsal hemisection, n=4 animals/group.

All values are plotted as means+s.e.m.



### **3.3. Systemic and post-injury administration of epothilone B suppresses the formation of an inhibitory lesion scar after SCI**

Since systemic administration of epothilone B increased microtubule stability at the lesion site, I next asked whether this treatment strategy reduces fibrotic scar formation after SCI. Adult rats received a spinal cord dorsal hemisection and were i.p. injected with epothilone B (0.75 mg/kg BW) or vehicle at 1 day and, if applicable, at 15 days after injury. One group of animals were sacrificed 4 days after injury, a second group of animals were sacrificed 4 weeks after injury. Subsequently, the lesion site was examined by immunohistochemistry and western blotting. Fibrotic scarring at the lesion site is characterized by intense deposition of extracellular matrix (ECM) components. Immunolabeling of the ECM-protein laminin was significantly reduced upon epothilone B i.p. treatment 4 days (**Fig. 3.5a, c**;  $0.96 \text{ mm}^2 \pm 0.05$  (vehicle) vs.  $0.5 \text{ mm}^2 \pm 0.03$  (EpoB),  $P=0.000008$ ) and even 4 weeks after injury (**Fig. 3.5a, c**;  $1.2 \text{ mm}^2 \pm 0.1$  (vehicle) vs.  $0.9 \text{ mm}^2 \pm 0.1$  (EpoB),  $P=0.019$ ). Concomitantly, a second ECM protein, fibronectin, was reduced in lesion site extracts 4 weeks post-injury (**Fig. 3.5b**). The reduction of extracellular matrix (ECM) in the lesion site shows that systemic administration of epothilone B efficiently decreases fibrotic scar formation following spinal cord injury.

Besides laminin and fibronectin, the fibrotic scar comprises other molecules that are associated with the ECM including axon growth inhibitory chondroitin sulfate proteoglycans (CSPGs) (**see chapter 2.2.2.**). Therefore, I tested whether the reduction of fibrotic scar tissue upon systemic administration of epothilone B was associated with a decrease of CSPGs. Chondroitin sulfate immunostaining with the CS-56 antibody revealed a substantial reduction of CSPGs at the lesion site (**Fig. 3.5a**). By using a glycosaminoglycan assay, I found that lesion site extracts of epothilone B treated animals showed a 35% reduction of the CSPG-specific glycosaminoglycan side chains (**Fig. 3.5d**;  $5.1 \text{ mg/g} \pm 0.5$  (vehicle) vs.  $3.4 \pm 0.4 \text{ mg/g}$  (EpoB)). In addition, neurocan protein levels, an abundant CSPG at the spinal cord injury site (Asher et al., 2000), were reduced in lesion site extracts as revealed by western blotting (**Fig. 3.5b**).

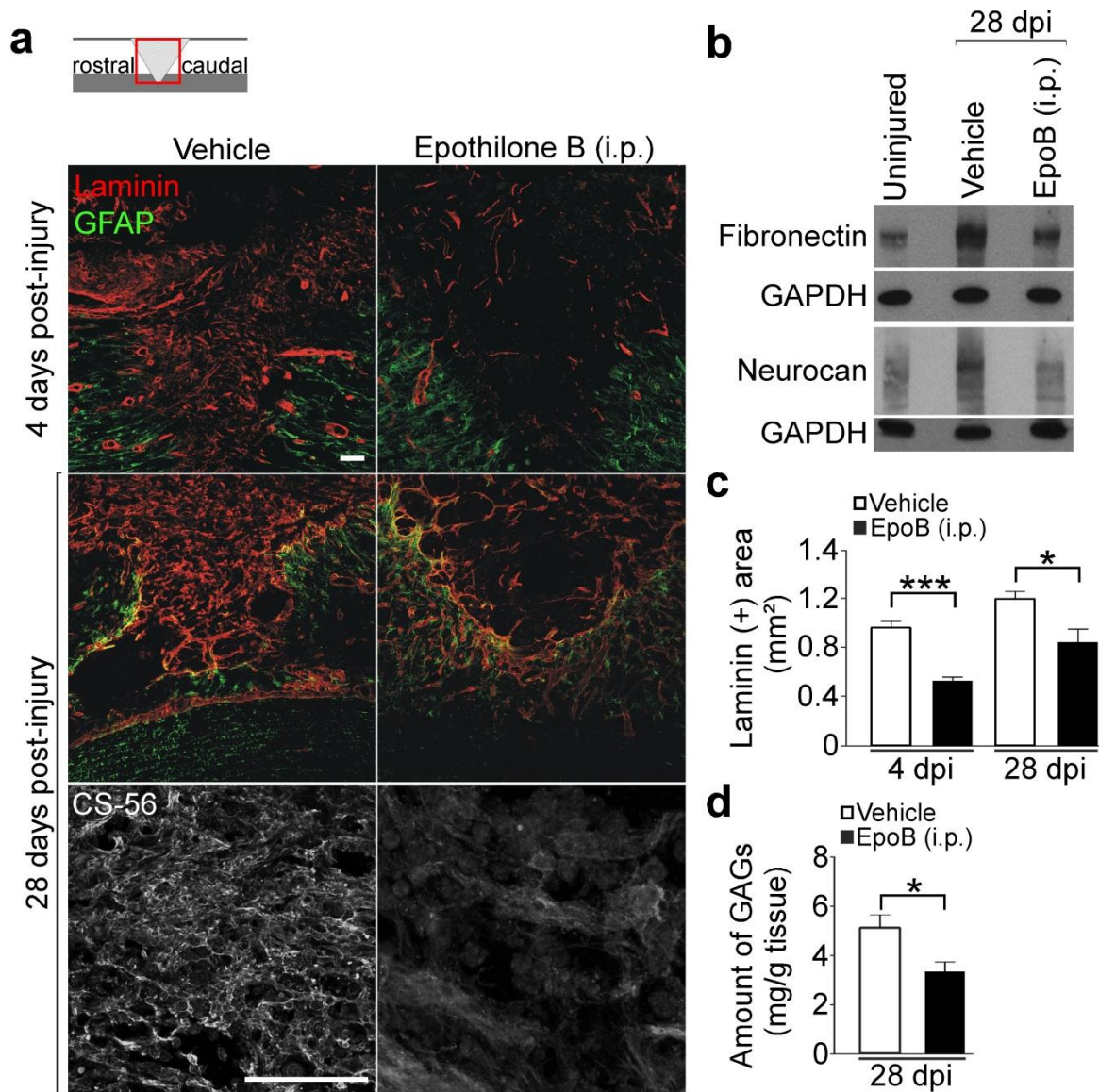


**Figure 3.5 Systemic administration of epothilone B reduces the axon growth-inhibitory lesion scar after spinal cord injury.**

(a) Rat spinal cord sagittal sections at specific time-points after dorsal hemisection showing immunolabeling of laminin, glial fibrillary acidic protein (GFAP; top and middle panel) or chondroitin sulfates (CS-56, bottom panel) at specific time-points after injury. Schematic (top, left corner) indicates lesion and displayed regions (red box). Scale bars=100  $\mu$ m.

(b) Protein levels of indicated proteins in pooled spinal cord (lesion) extracts, n=3 animals/group.

(c) Laminin-immunopositive (+) area at the lesion site, n=7-8 animals/group.

(d) Glycosaminoglycan (GAG) amounts in spinal cord lesion extracts, n=8 animals/group.

All values are plotted as means+s.e.m.; \*P<0.05, \*\*\*P<0.001. dpi=days post-injury.

Finally, I wanted to examine whether epoithilone B treatment affects astrogliosis. Astrogliosis is characterized by reactive astrocytes that overexpress glial fibrillary acidic protein (see chapter 2.2.2.). It has been shown that these reactive astrocytes are important for proper sealing of the injury site, which avoids secondary tissue damage and lesion spreading (Faulkner et al., 2004). Histological analysis of the lesion site revealed that neither GFAP immunoreactivity (Fig. 3.6a) nor injury size (Fig. 3.6b,  $1.6 \text{ mm}^2 \pm 0.2$  (vehicle) vs.  $1.6 \text{ mm}^2 \pm 0.2$  (EpoB),  $P=0.79$ ) were different between vehicle and epoithilone B treated animals, indicating a comparable astroglial response and sealing of the lesion site.

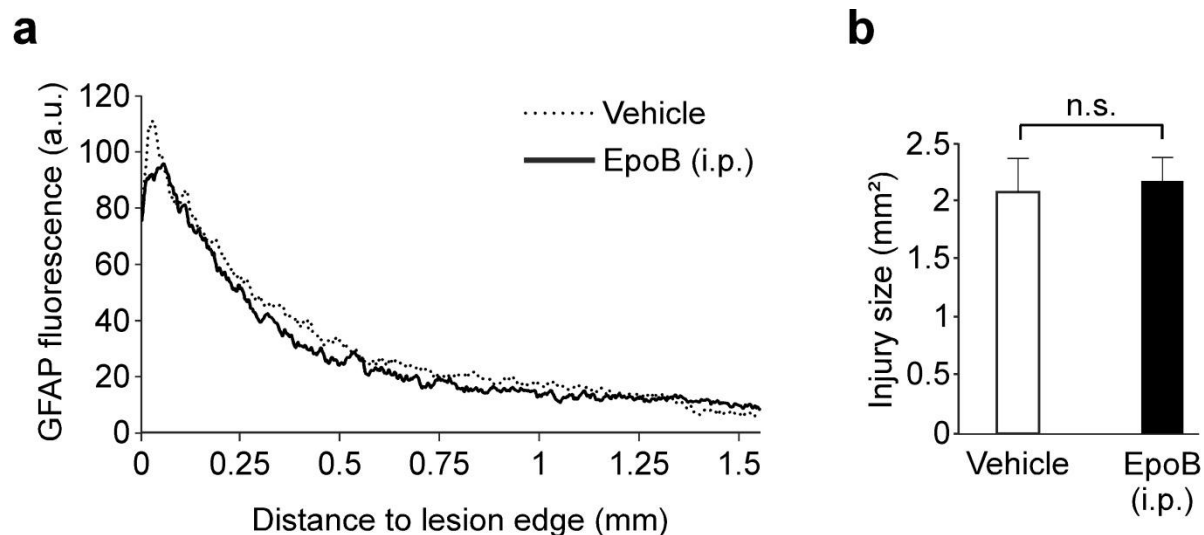


**Figure 3.6 Fibrotic scar reduction through systemic administration of epoithilone B neither affects astrogliosis nor injury size after spinal cord injury.**

(a) Glial fibrillary acidic protein (GFAP) immunofluorescence intensity at the lesion site 4 weeks after dorsal hemisection. Values are plotted as means.

(b) Lesion area 4 weeks after dorsal hemisection,  $n=7-8$  animals/group. Values are plotted as means+s.e.m.

Thus, systemic administration of epoithilone B reduces the axon growth inhibitory fibrotic scar after SCI injury without adversely affecting the regular wound closure. This suggests that systemic administration of epoithilone B renders the spinal cord lesion site more favorable for regenerating axons.

### 3.4. Systemic administration of epothilone B reduces fibrotic scarring by abrogating meningeal fibroblast migration

The fibrotic scar is mainly composed of meningeal fibroblasts that secrete ECM molecules including laminin, fibronectin and axon growth inhibitory CSPGs (Decimo et al., 2012; Kawano et al., 2012). Within the first week after SCI, meningeal fibroblasts proliferate and migrate towards the injury epicenter where they accumulate and deposit ECM components (Kawano et al., 2012). Since systemic administration of epothilone B reduces fibrotic scar tissue formation after SCI, I asked whether the treatment affects cell proliferation and/or cell migration of meningeal fibroblasts at the lesion site.

First, I examined the lesioned spinal cord immunolabeled for the cell proliferation marker phospho-histone H3 and for the apoptosis marker TUNEL. 7 days after dorsal hemisection, vehicle and epothilone B treated animals showed a similar amount of phospho-histone H3-positive cells (**Fig. 3.7a, b**; 73 cells  $\pm$  11 (vehicle) vs. 76 cells  $\pm$  15 (EpoB),  $P=0.87$ ) and of TUNEL-positive cells (**Fig. 3.7a, c**; 379 cells  $\pm$  53 (vehicle) vs. 267 cells  $\pm$  41 (EpoB),  $P=0.17$ ) at the site of the injury.

Since the treatment did not affect cell proliferation or cell apoptosis at the lesion site, I examined whether epothilone B influences cell migration. To address this, I cultured fibroblasts deriving from the meninges of postnatal rat (P4) brains and plated these cells in culture inserts of *in vitro* wound healing assays. The culture insert was removed after 1 day, thereby uncovering a defined cell-free area which simulated an *in vitro* wound. Then, cells were differentiated in a migratory stage by reducing serum content in the media to a minimal amount (Gundersen et al., 1994). DMSO treated meningeal fibroblasts migrated into the cell free area (**Fig. 3.8a**) and after 48 hours more than 80% of that area was occupied with cells (**Fig. 3.8b**, 83.3%  $\pm$  4.7). In contrast, fibroblasts treated with epothilone B (2.5 ng/ml) displayed a significantly reduced migration and covered only 38% of the *in vitro* wound after 48 hours (**Fig.3.8a, b**, 38.1%  $\pm$  16.8,  $P=0.048$ ).

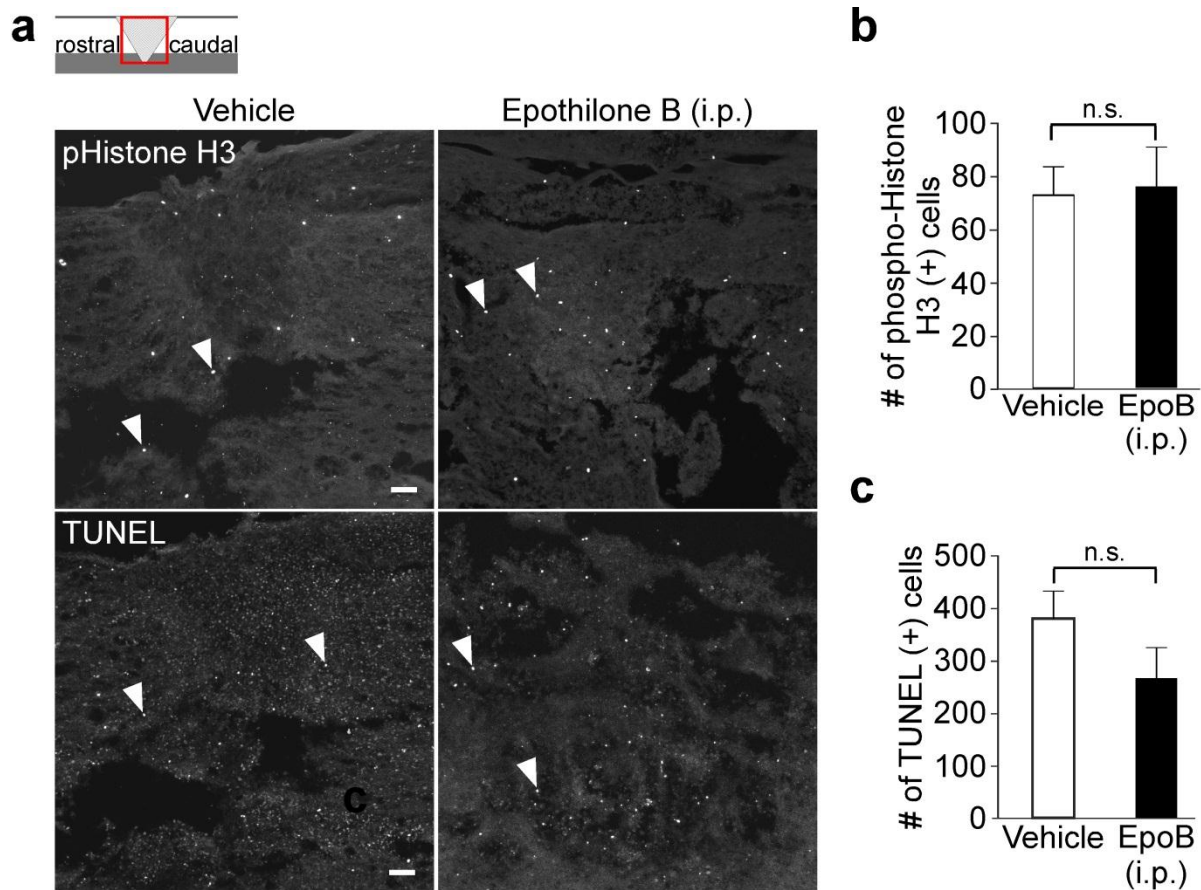


**Figure 3.7 Systemic administration of epothilone B neither affects cell proliferation nor cell death at the lesion site.**

**(a)** Rat spinal cord sagittal sections 7 days after dorsal hemisection showing cells labeled with proliferation marker phospho-Histone-H3 (top panel) or apoptosis marker TUNEL (bottom panel) as indicated by arrowheads. Schematic (top, left corner) indicates lesion and displayed regions (red box). Scale bars=100  $\mu$ m. **(b,c)** Number of phospho-Histone-H3-positive (+) cells (b) and TUNEL-positive (+) cells (c) at the lesion site, n=7-8 animals/group. All values are plotted as means+s.e.m.

Next, I sought to determine the underlying mechanism of the reduced fibroblast migration upon epothilone B treatment. It has been shown that directed cell migration requires an intrinsic polarization of the microtubule array into stable microtubules in the cell leading edge and dynamic microtubules in the cell rear (Li and Gundersen, 2008). To test whether epothilone B affects the polarization of the microtubule array, meningeal fibroblasts were immunostained for detyrosinated and tyrosinated tubulin to visualize the distribution of stable and dynamic microtubules respectively within the cells. Interestingly, epothilone B treatment induced a drastic change of the intracellular microtubular network. In control cells, the leading edge, facing the cell free area, was enriched with stable detyrosinated microtubules while the trailing edge

in the rear of the cell mainly comprised dynamic tyrosinated microtubules (**Fig. 3.8c**) as described previously (Gundersen and Bulinski, 1988). By contrast, epothilone B treated fibroblasts lost their polarity and formed neither leading nor trailing edges (**Fig. 3.8d**). Instead, epothilone B treated cells showed an increased amount of detyrosinated microtubules (**Fig. 3.8e**), which were evenly spread throughout the cell (**Fig. 3.8d**). This suggests that epothilone B abrogates the polarization of cultured meningeal fibroblasts, which prevents their directed migration.

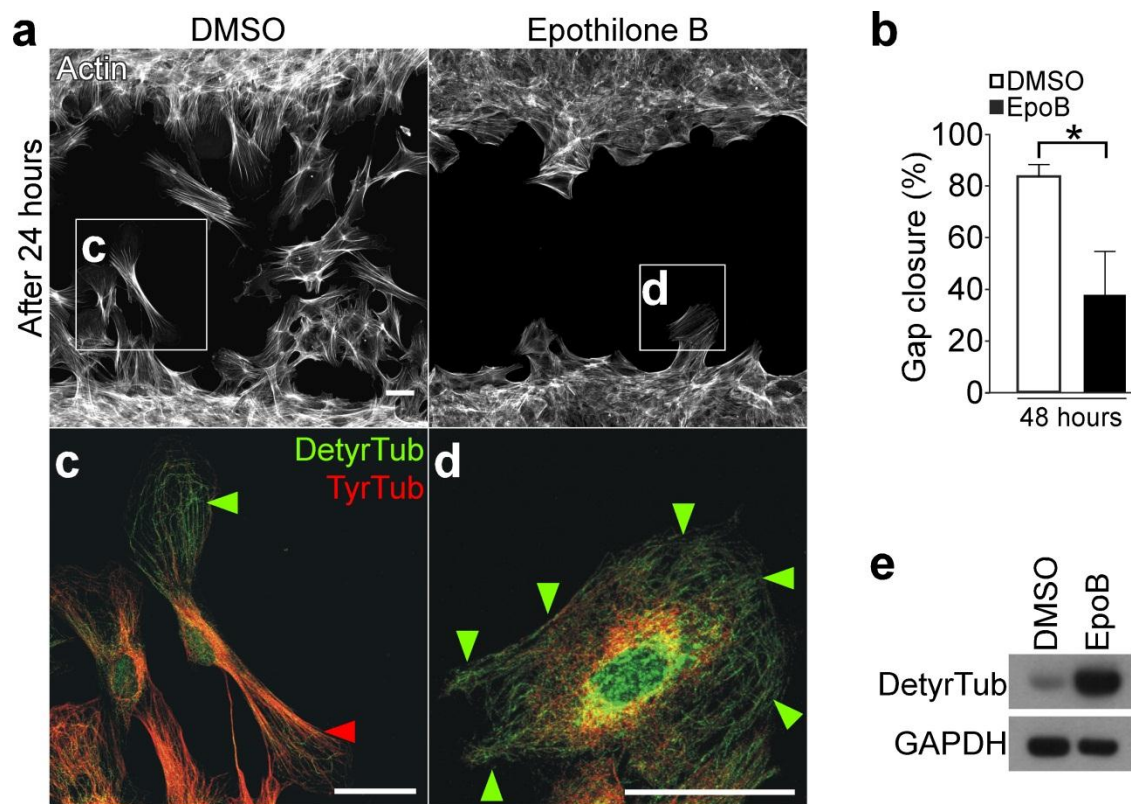


**Figure 3.8 Epothilone B inhibits migration of meningeal fibroblasts by abrogating cell polarity.**

**(a)** Cultured meningeal fibroblasts migrating into a cell free area in wound healing assays.

**(b)** Percentage of the area shown in (a) occupied with cells 48 hours after initiation of migration, n=3 experiments. Values are plotted as means+s.e.m.; \*P<0.05.

**(c,d)** High magnification pictures of the boxed areas in (a) showing tyrosinated (TyrTub, red arrowheads) and detyrosinated tubulin (DetyrTub, green arrowheads).

**(e)** Protein levels of detyrosinated tubulin and GAPDH in dissociated meningeal fibroblasts 48 hours after indicated treatment.

Finally, I wanted to verify that the abovementioned effect of epothilone B underlies the treatment-induced reduction of fibrotic scarring after SCI. I performed a co-immunostaining for fibronectin, to visualize the meninges adjacent to the spinal lesion site, and for detyrosinated and tyrosinated tubulin to visualize the microtubule array of fibroblasts within the meninges. In vehicle treated animals, meningeal fibroblasts exhibited a bipolar, migratory shape and were oriented towards the lesion epicenter. By contrast, similar to *in vitro* conditions, systemic administration of epothilone B abrogated the intrinsic polarization of meningeal fibroblasts, leading to their transformation into a round and unpolarized morphology (**Fig. 3.9**).

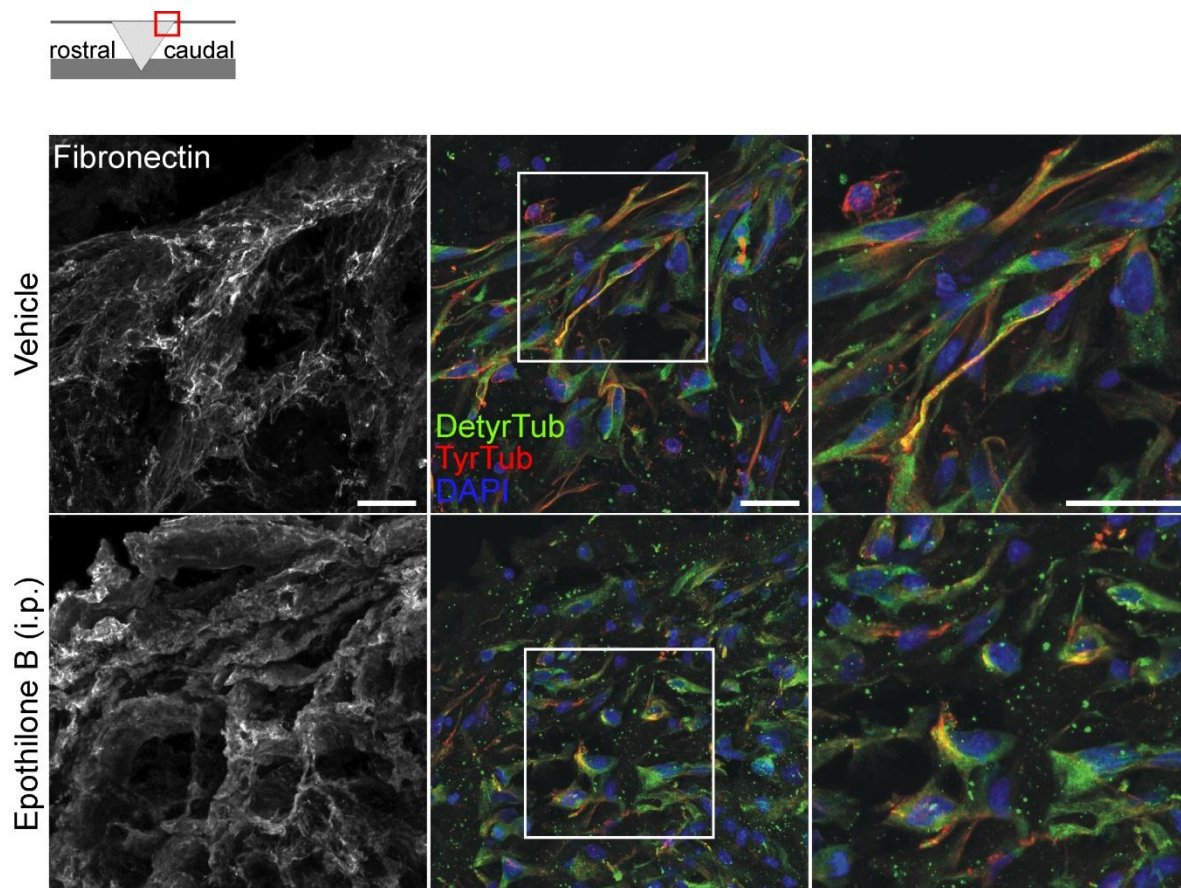


**Figure 3.9 Systemic administration of epothilone B abrogates cell polarity of meningeal fibroblasts at the spinal cord injury site.**

Rat spinal cord sagittal sections 4 days after dorsal hemisection. Shown are immunostainings for fibronectin (left panel), detyrosinated and tyrosinated tubulin (middle and right panels) in the meninges adjacent to the lesion site. Right panel shows high magnification of boxed area in the middle panel. Schematic (top, left corner) indicates lesion and displayed regions (red box). All scale bars=25  $\mu$ m.

These data provide evidence that epothilone B inhibits directed migration of meningeal fibroblasts by abrogating intrinsic cell polarity, which ultimately impedes fibrotic scar formation after spinal cord injury.

### **3.5. Microtubule stabilization through epothilone B promotes axon growth in a growth-restraining environment**

While epothilone B hindered migration of meningeal fibroblasts, the treatment induced enhanced axon growth in cultured embryonic rodent neurons as described above. Since axon growth after SCI is restrained by extrinsic factors in the CNS environment, I tested whether epothilone B also promotes axon growth of postnatal neurons that are confronted with inhibitory substrates. I dissected and dissociated postnatal rat cortical neurons (P4) and plated them in media complemented with the most common axon growth inhibitory factors, which are present at the lesion site (Fitch and Silver, 1997; Silver and Miller, 2004). Then the neurons were treated with DMSO or epothilone B and after 48 hours cells were fixed and neurite length was measured. Neurons treated with DMSO showed a profound reduction of neurite length in the presence of axon growth inhibitors Nogo-A (**Fig. 3.10a, b**;  $63.2 \mu\text{m} \pm 4.9$ ,  $P=0.009$  vs. growth-permissive condition), CSPGs (**Fig. 3.10a, b**;  $68.7 \mu\text{m} \pm 1.6$ ,  $P=0.015$  vs. growth-permissive condition) or semaphorin 3A (**Fig. 3.10a, b**;  $70.9 \mu\text{m} \pm 6.4$ ,  $P=0.01$  vs. growth-permissive condition) in comparison to neurite lengths under permissive conditions (**Fig 3.10b**,  $114.3 \mu\text{m} \pm 0.9$ ). However, when neurons were treated with epothilone B neurite growth was almost fully restored independent of the complemented growth inhibitory substrate (**Fig. 3.10a, b**;  $96 \mu\text{m} \pm 2.9$  (on Nogo-A),  $P=0.008$ ;  $96.4 \mu\text{m} \pm 5.5$  (on CSPGs),  $P=0.008$ ;  $100.4 \mu\text{m} \pm 8.3$  (on Sema 3A),  $P=0.03$ ). The used epothilone B concentration was 1 nM suggesting that moderate microtubule stabilization is sufficient to enable CNS neurons to grow neurites in an otherwise growth-restraining environment.



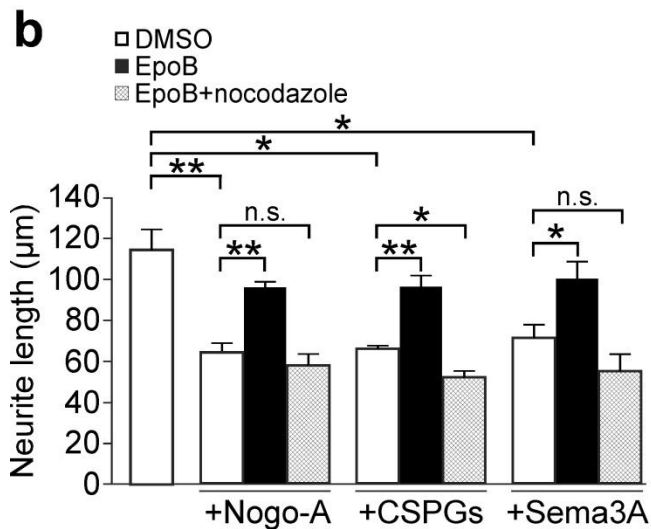
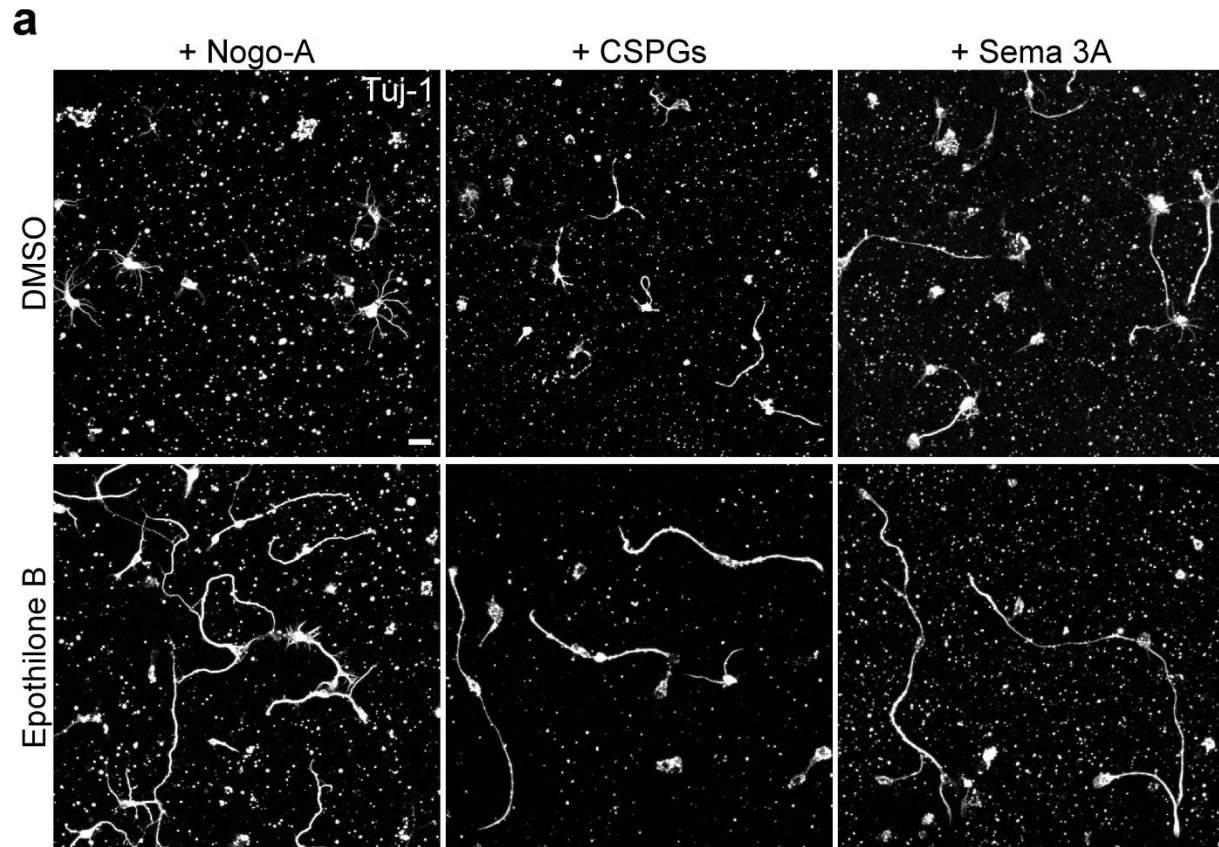


**Figure 3.10 Epothilone B promotes neurite growth on growth inhibitory substrates.**

(a) Beta-3 tubulin (Tuj-1) immunolabeling of neurons growing on inhibitory substrates (CSPGs, chondroitin sulfate proteoglycans; Sema 3A, Semaphorin 3A). Scale bar=100µm. (b) Neurite length of cortical neurons after 48 hours with indicated treatments, n=3-4 experiments. Values are plotted as means+s.e.m.; \*P<0.05, \*\*P<0.01.

Next, I sought for a mechanism underlying the increased neurite outgrowth upon epothilone B treatment. To this end, neurons were transfected with microtubule plus-end binding protein 3 (EB3) fused to green fluorescent protein (GFP), plated in Nogo-A-complemented medium and imaged, using a microscopic live cell imaging setup. EB3-GFP binds to the plus-ends of microtubules and thereby allows the visualization

of polymerizing microtubules (Flynn et al., 2012). Before epothilone B treatment, EB3 was evenly distributed throughout the neurites (**Fig. 3.11a**). However, addition of the drug led to a rapid and directed microtubule polymerization into the growth cones (**Fig. 3.11a**) indicated by increased EB3-GFP fluorescence within the neurite tip (**Fig. 3.11a, b**). Moreover, measuring neurite growth rates revealed that 2 hours after addition of epothilone B the neurite growth speed was significantly enhanced (**Fig. 3.11c**;  $1.3 \mu\text{m/h} \pm 0.4$  (EpoB) vs.  $-0.02 \mu\text{m/h} \pm 0.7$  (DMSO),  $P=0.021$ ) and increased still at 4 hours (**Fig. 3.11c**;  $1.9 \mu\text{m/h} \pm 0.8$  (EpoB) vs.  $-0.04 \mu\text{m/h} \pm 0.6$  (DMSO),  $P=0.023$ ). This suggests that microtubule polymerization into the neurite tip, induced by epothilone B treatment, promotes neurite growth in a growth inhibitory environment. To further validate this possibility, neurons were treated with low doses (10 nM) of the microtubule destabilizing drug nocodazole. In contrast to epothilone B, nocodazole treatment induced microtubule retraction from neurite growth cone as indicated by reduced EB3-GFP fluorescence towards the neurite tip (**Fig. 3.11b, d**). Strikingly, when nocodazole and epothilone B were co-administered, to the cortical neurons, they did not exhibit axon growth rescue when cultured in the presence of growth inhibitory factors. Instead, nocodazole fully abrogated the growth promoting effect of epothilone B leading to inhibition of neurite growth that was similar to or greater than that observed in control cells (**Fig. 3.10b**;  $57.6 \mu\text{m} \pm 5.6$  (on Nogo-A),  $P=0.49$ ;  $51.7 \mu\text{m} \pm 3.2$  (on CSPGs),  $P=0.03$ ;  $54.7 \mu\text{m} \pm 8.3$  (on Sema 3A),  $P=0.19$ ).

This suggests that microtubule stabilization by epothilone B promotes microtubule polymerization into the neurite growth cone, which is necessary and sufficient to propel neurite growth in a non-permissive environment.

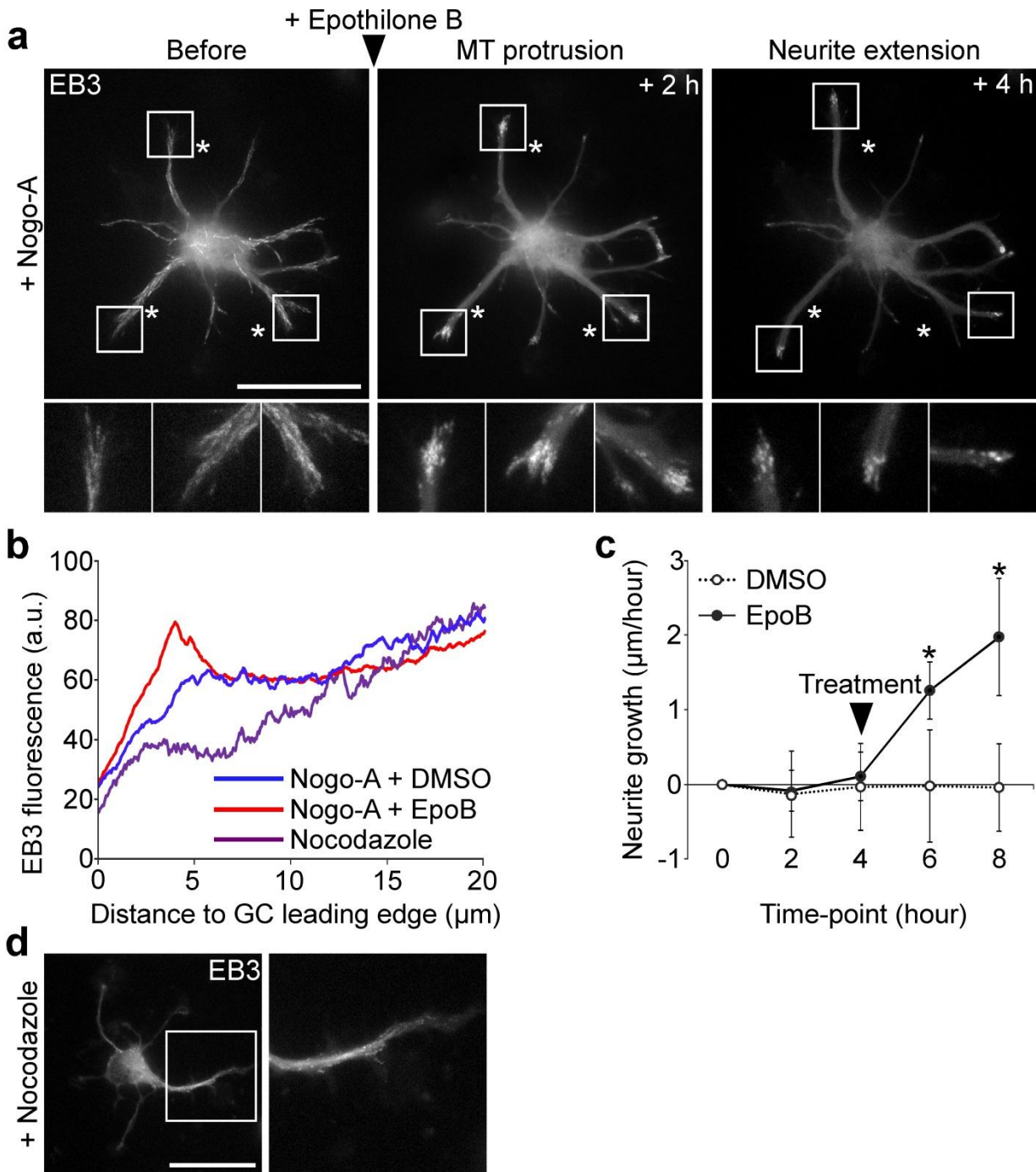


**Figure 3.11 Epothilone B propels neurite growth by increasing microtubule polymerization into the growth cone.**

(a) EB3-GFP localization in neurons cultured on Nogo-A, before and after epothilone B treatment (black arrowhead). Bottom panel, high magnification of boxed areas in top panel. Asterisks represent stable landmarks across time-points. (b) EB3-GFP fluorescence intensity in the neuritic growth cone (GC) under indicated conditions,  $n=9-16$  cells. (c) Neurite growth rates on Nogo-A before and after indicated treatment. Black arrowhead, time of treatment.  $n=12-15$  cells. (d) EB3-GFP localization in neurons treated with nocodazole. Left picture, high magnification of boxed area in right picture. All scale bars= $100\ \mu\text{m}$ . All values are plotted as means+s.e.m.; \* $P<0.05$ , \*\* $P<0.01$ .

### 3.6. Systemic administration of epothilone B increases growth competence of injured axons in the CNS and promotes regeneration after spinal cord injury

Axonal injury in the rodent CNS leads to axon degeneration which is followed by the formation of dystrophic retraction bulbs at the axon tip (Bradke et al., 2012). Retraction bulb formation is generally referred as to axon dystrophy, results from depolymerization and disorganization of microtubules (George et al., 1995; Erturk et al., 2007) and limits axon regeneration (Saxena and Caroni, 2007).

Given that local application of epothilone B prevents axon dystrophy in injured CNS neurons, I assessed the effect of the drug when given systemically. Adult transgenic mice expressing GFP in a subset of axons, were injected with epothilone B (1.5 mg/kg BW i.p.). Then, GFP labeled dorsal column axons were transected at the mid-thoracic spinal cord and imaged daily for 4 days (Erturk et al., 2007). In injured controls, more than 50% of the injured axons formed retraction bulbs 6 hours after injury (**Fig. 3.12a, b**;  $51.8\% \pm 6.2$ ). Over the course of 4 days, the amount of retraction bulbs only slightly decreased (**Fig. 3.12b**;  $46.4\% \pm 2.7$  (day 1) to  $41.8\% \pm 3.6$  (day 4)). Moreover, injured control axons frequently underwent axonal dieback and degeneration (**Fig. 3.12a**) leading to a steady increase of the distance between the axonal tip and the lesion site (**Fig. 3.12c**;  $263.7 \mu\text{m} \pm 22.2$  (day 0) to  $491.1 \mu\text{m} \pm 62.9$  (day 4)). By contrast, in epothilone B injected animals the distance between the axonal tip and the lesion site was significantly lower compared to injured control animals at days 3 and 4 (**Fig. 3.12c**;  $222.73 \mu\text{m} \pm 77.9$ ,  $P=0.03$  (day 3);  $169.6 \mu\text{m} \pm 39.1$ ,  $P=0.001$  (day 4)). Notably, in the treatment group the distance between lesioned axons and the injury site even decreased after day 2 (**Fig. 3.12c**;  $202.9 \mu\text{m} \pm 22.99$  (day 2) to  $169.6 \mu\text{m} \pm 39.1$  (day 4)) indicating axon regeneration towards the injury. Indeed, epothilone B treated animals showed significantly fewer retraction bulbs between 2 and 4 days post-injury (**Fig. 3.12a, b**;  $29.3\% \pm 2.3$ ,  $P=0.04$  (day 2),  $26.8\% \pm 3.9$ ,  $P=0.019$  (day 3);  $25.3\% \pm 3$ ,  $P=0.0032$  (day 4)), which was accompanied by regenerative sprouting from the injured axonal tip (**Fig. 3.12a**). These data suggest that

systemic administration of epothilone B reduces dystrophy of injured spinal cord axons, which is sufficient to increase their growth competence.

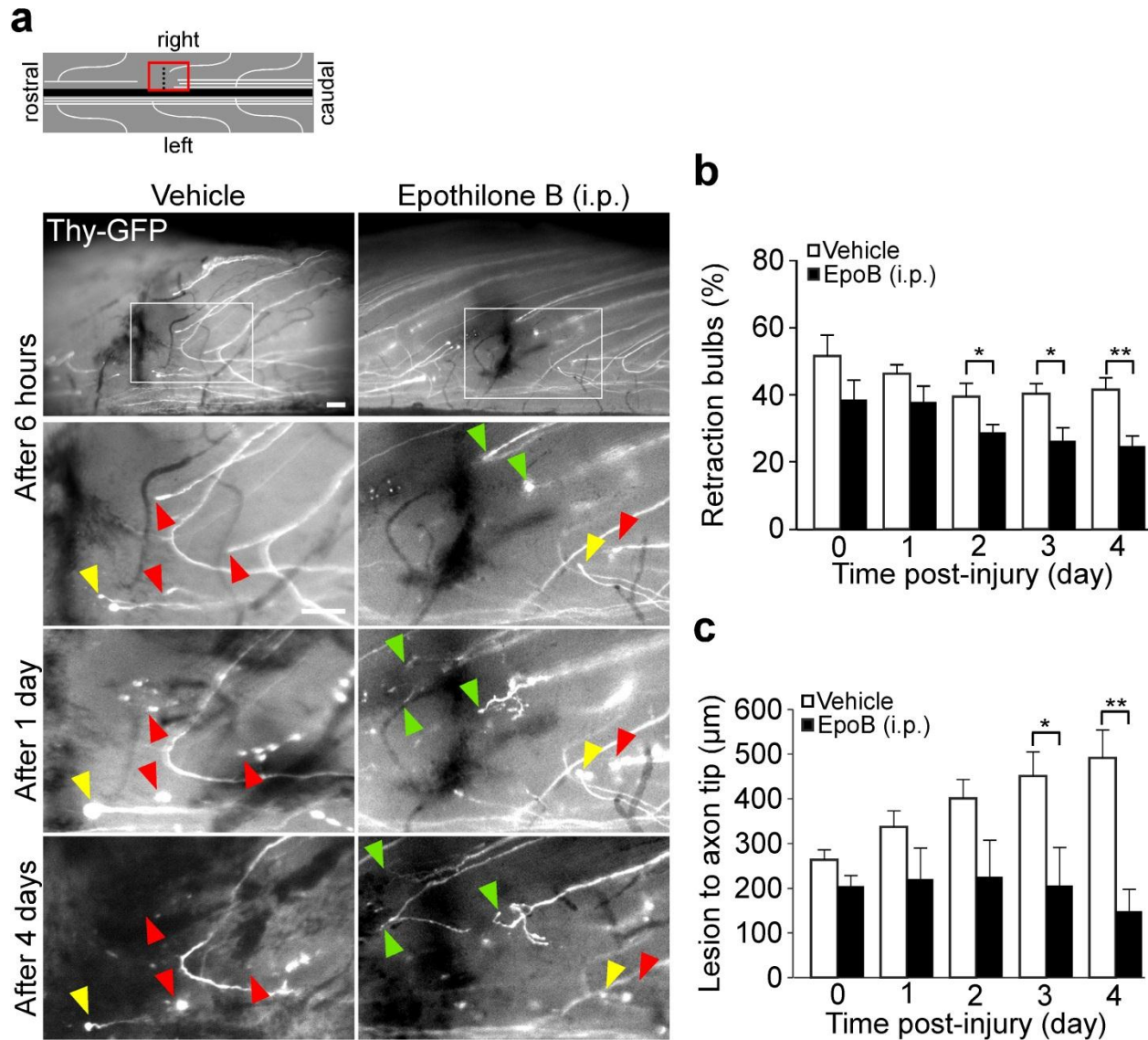


**Figure 3.12 Systemic administration of epothilone B reduces axon dystrophy of injured spinal cord axons.**

(a) Lesioned GFP-positive spinal cord axons forming retraction bulbs (yellow arrowheads), dying back (red arrowheads) or regenerating (green arrowheads) over time. Boxed area in top panel, displayed region of panels below. Schematic (top, left corner) indicates lesion and displayed region (red box). Scale bars=100 μm.

(b,c) Percentage of injured axons forming retraction bulbs (b) and distance of the lesioned proximal axon tip to the injury site (c), n=8 animals/group. All values are plotted as means+s.e.m.; \*P<0.05, \*\*P<0.01.

Since systemic administration of epothilone B increases axon growth competence and reduces the inhibitory action of the lesion scar, I next tested whether the treatment promotes axon regeneration. Adult rats received a mid-thoracic dorsal hemisection and were i.p. injected with epothilone B (0.75 mg/kg BW) at day 1 and day 15 post-injury. 4 weeks after injury, I investigated axon regeneration of fibers constituting the raphespinal tract. The raphespinal tract is the only source for serotonin (5HT) in the spinal cord and therefore can be visualized by fluorescent antibodies against 5HT. The raphespinal tract descends two main projections to the spinal cord, one in the ventral and one in the dorsal spinal cord. Since the dorsal projection is interrupted by the dorsal hemisection, every 5HT-positive fiber caudal to the injury site can be considered as a regenerated fiber from the dorsal projection or a collateral sprout arising from the intact ventral projection. Epothilone B treated animals showed an approximately 3-fold increase in serotonergic fibers caudal from the lesion site (**Fig. 3.13a, b**; 208.6 fibers  $\pm$  43.1 (EpoB) vs. 73.8 fibers  $\pm$  20.9 (vehicle),  $P=0.029$ ) indicating that the treatment promoted growth of raphespinal fibers.

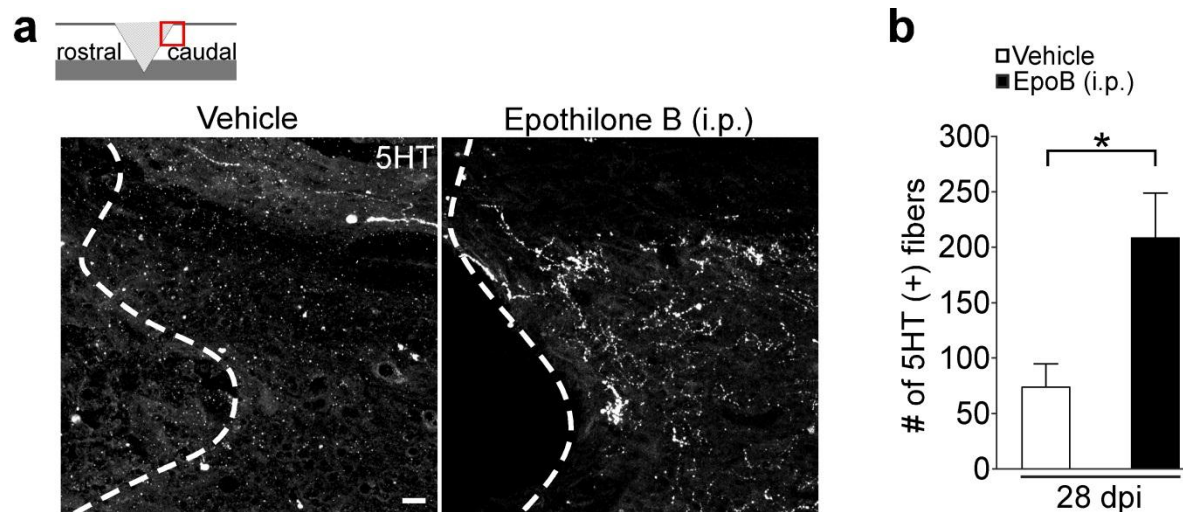


**Figure 3.13 Systemic administration of epothilone B promotes growth of raphespinal fibers after SCI.** (a) Rat spinal cord sagittal sections 4 weeks after dorsal hemisection showing serotonin (5HT) immunolabeling caudal to the lesion site (dashed line, lesion border). Schematic (top, left corner) indicates lesion and displayed regions (red box). (b) Number of 5HT-immunopositive (+) fibers caudal to the injury site,  $n=7-8$  animals/group. Values are plotted as means+s.e.m.; \* $P<0.05$ .

The perpendicular orientation of most fibers in epothilone B treated animals (**Fig. 3.13a**) suggest that these fibers are collateral sprouts from the spared, ventral raphespinal projection or distal sprouts from the dorsal projection that grew around the lesion site. Taken together, systemic administration of epothilone B prevents axon dystrophy and instead increases growth of injured spinal cord axons after SCI.

### **3.7. Systemic administration of epothilone B promotes functional recovery after clinically relevant spinal cord contusion injury**

The raphespinal tract innervates motor neurons in the spinal cord and thereby controls walking and fine-tuned locomotion (Jordan et al., 2008). Increased raphespinal innervation strongly correlates with improved functional recovery of hind limb locomotion after thoracic SCI (Kim et al., 2004; Kaneko et al., 2006).

Therefore, I examined whether systemic administration of epothilone B promotes functional recovery in a SCI model that closely mimics the human pathology (Onifer et al., 2007). To this end, adult rats received a moderate mid-thoracic spinal cord contusion of 150 kdyn, which disrupts descending motor projections and provokes deficits of hindlimbs function (Scheff et al., 2003). 1 day and 15 days after injury, the animals were i.p. injected with epothilone B (0.75 mg/kg BW i.p.).

As a first behavioral examination, animals were tested on the so-called catwalk. This device is used to visualize and record footprints of rats, walking on a plane surface. Analysis of the recorded footprints can be used for quantitative assessment of gait abnormalities resulting from the contusion injury (Pearse et al., 2004). In comparison to injured controls, epothilone B treated animals exhibited a more stable gait as reflected by increased stride length (**Fig. 3.14a**;  $16.1 \text{ mm} \pm 0.4$  (EpoB) vs.  $14.4 \text{ mm} \pm 0.7$  (vehicle),  $P=0.039$ ) and a reduced foot exorotation (**Fig. 3.14b**;  $18.1^\circ \pm 1.9$  (EpoB) vs.  $25.5^\circ \pm 2.5$  (vehicle),  $P=0.031$ ) 8 weeks after contusion injury. Moreover, epothilone B treated rats showed an increased fore-

and hindlimb coordination during walking, as indicated by increased gait regularity (**Fig. 3.14c**;  $95.9\% \pm 1.3$  (EpoB) vs.  $88.3\% \pm 1.3$  (vehicle),  $P=0.0006$ ).

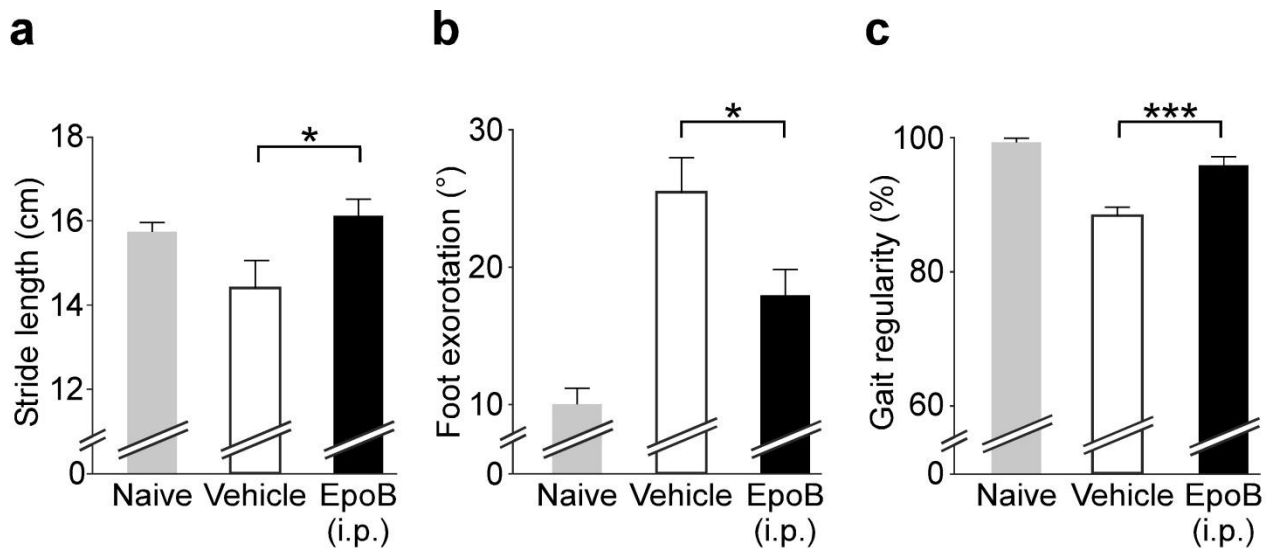


**Figure 3.14 Epothilone B decreases gait abnormalities after spinal cord contusion injury.**

(a-c) Gait analysis of spinal cord injured rats 8 weeks after contusion injury. Plotted are stride length of the hindlimbs (a), angle of foot exorotation of the hindpaws (b) and percentage of gait regularity (c),  $n=11-12$  animals/group. All values are plotted as means+sem. \* $P<0.01$ , \*\*\* $P<0.001$ .

I next investigated how the treatment affects skilled walking on a more challenging surface. Animals were therefore tested on a horizontal ladder at specific time-points after spinal cord contusion. 2 and 4 weeks post-injury, vehicle and epothilone B showed treated animals both showed a comparable recovery on this behavioral assay (**Fig. 3.15c**; 7.7-6.3 errors (vehicle) vs. 6.7-4.7 errors (EpoB),  $P=0.42$  and 0.13, respectively). However, at 6 and 8 weeks post-injury, functional recovery was significantly enhanced in epothilone B treated animals as indicated by a 50% reduction of foot misplacements in comparison to vehicle treated controls (**Fig. 3.15c**, 3.95 errors  $\pm 0.5$  to 2.3 errors  $\pm 0.5$  (EpoB) vs. 5.6 errors  $\pm 0.6$  to 4.05 errors  $\pm$  (vehicle),  $P=0.047$  and 0.015, respectively).

Together, these data demonstrate that systemic and post-injury administration of epothilone B improves the functional outcome after clinically relevant spinal cord contusion injury.



Next I sought an anatomical explanation for the aforementioned functional improvements. As epothilone B increased raphespinal regeneration after SCI (**Fig. 3.13a, b**), I examined raphespinal innervation of the lumbar spinal cord ventral horn which comprises motor neuron pools controlling the hindlimbs. Remarkably, in epothilone B treated animals the 5HT-positive area in the ventral horn was more than 50% increased at 8 weeks after contusion injury (**Fig. 3.15a,b**;  $6356.6 \mu\text{m}^2 \pm 619.7$  (EpoB) vs.  $4114.5 \mu\text{m}^2 \pm 726.3$  (vehicle),  $P=0.032$ ), suggesting that the treatment increased raphespinal innervation of lumbar motor pools (**Fig. 3.15a**).

Finally, I asked whether increased raphespinal innervation upon treatment caused the improved functional recovery. 8 weeks after contusion injury, I chemically ablated raphespinal neurons in vehicle and epothilone B injected animals by intracerebroventricular (i.c.v.) injections of 5,7-Dihydroxytryptamine (Carta et al., 2007). Injections of 5,7-DHT ablated the majority of serotonergic fibers in the lumbar spinal cord, which lead to a similar amount of raphespinal innervation in both, epothilone B and vehicle treated animals (**Fig. 3.15b**;  $1893.1 \mu\text{m}^2 \pm 257.4$  (vehicle) vs.  $1755.9 \mu\text{m}^2 \pm 192.3$  (EpoB),  $P=0.61$ ). Strikingly, this procedure abrogated the functional improvements on the horizontal ladder of epothilone B treated animals, which performed indistinguishably from injured controls (**Fig. 3.15c**;  $3.9 \text{ errors} \pm 0.6$  (epoB) vs.  $4.2 \text{ errors} \pm 0.5$  (vehicle),  $P=0.69$ ).

Thus, epothilone B treatment improved functional recovery of hindlimb locomotion after contusion injury by increasing serotonergic innervation of the lumbar spinal cord.

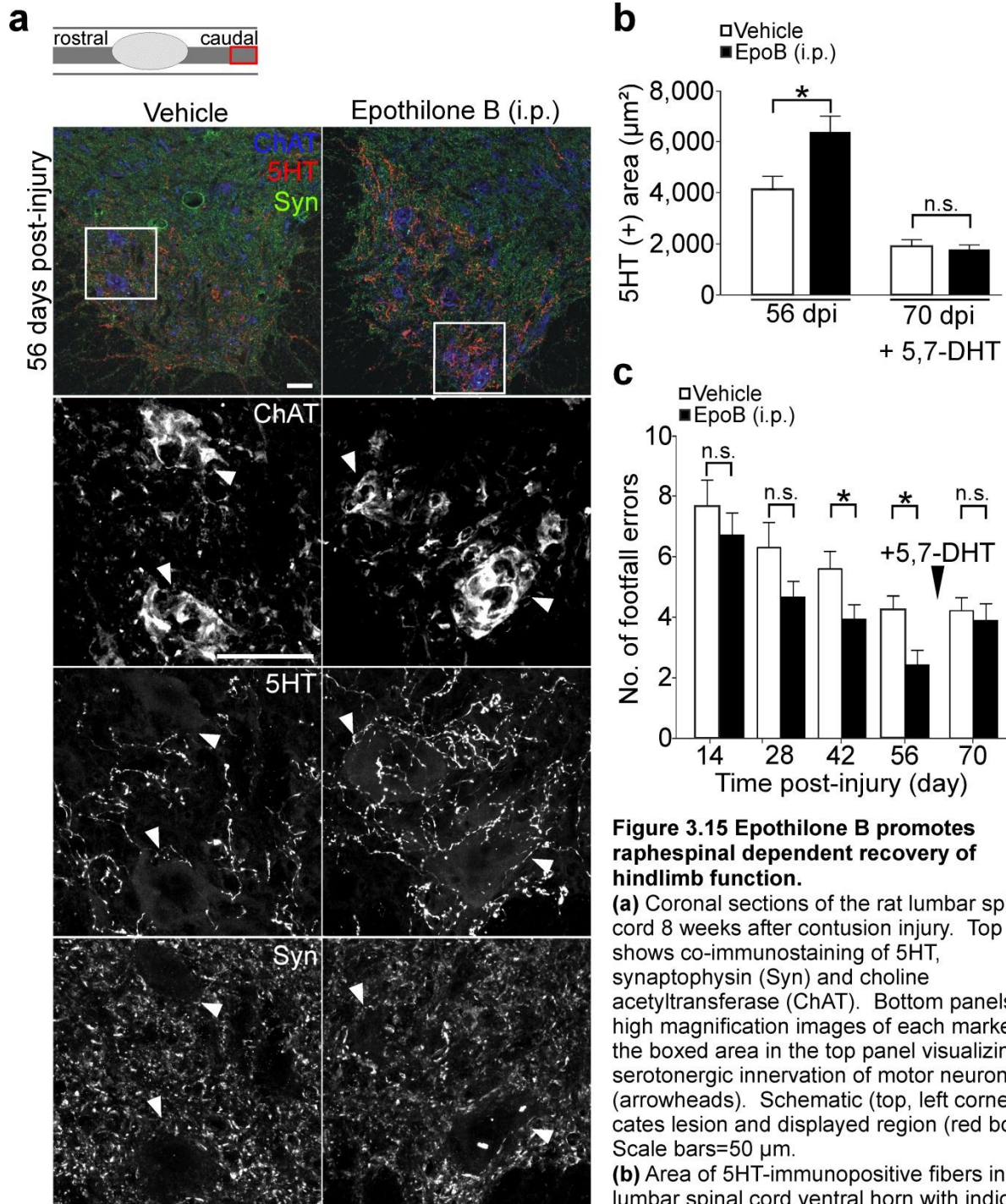


**Figure 3.15 Epothilone B promotes raphespinal dependent recovery of hindlimb function.**

(a) Coronal sections of the rat lumbar spinal cord 8 weeks after contusion injury. Top panel shows co-immunostaining of 5HT, synaptophysin (Syn) and choline acetyltransferase (ChAT). Bottom panels show high magnification images of each marker in the boxed area in the top panel visualizing serotonergic innervation of motor neurons (arrowheads). Schematic (top, left corner) indicates lesion and displayed region (red box). Scale bars=50  $\mu\text{m}$ .

(b) Area of 5HT-immunopositive fibers in the lumbar spinal cord ventral horn with indicated treatments (5,7-DHT = 5,7-Dihydroxytryptamine, n=10-12 animals/group.

(c) Number of footfalls on the horizontal ladder, n=10-11 animals/group. All values are plotted as means+s.e.m., \*P<0.05.

## **4. DISCUSSION**

Damaged axons regenerate poorly after SCI, due to a low intrinsic axon growth potential and neuron extrinsic inhibitory barriers at the lesion site, including CNS myelin and the lesion scar. Therefore, an ideal treatment to induce axon regeneration after SCI should have at least three features. It should reduce scarring (Klapka et al., 2005) and growth inhibitory factors at the lesion site (Schnell and Schwab, 1990; Bradbury et al., 2002; GrandPre et al., 2002), reactivate the intrinsic axon growth potential (Neumann et al., 2002; Qiu et al., 2002; Liu et al., 2010) and be administrable as a medication after injury. Recently, a number of combinatorial approaches have led to significant axon regeneration (Pearse et al., 2004; Alilain et al., 2011; Lu et al., 2012). These approaches, however, involve multiple drugs, enzymes and interventions, rendering clinical translation difficult. In contrast, a single drug, Taxol, acts on multiple cellular targets to promote axon regeneration through moderate microtubule stabilization (Hellal et al., 2011). Thus, microtubule stabilization is a promising therapeutic target to promote axon regeneration after CNS injury. Since Taxol is a FDA approved drug, could it be used to treat SCI in human patients?

Taxol poorly penetrates the blood-brain-barrier, which restricts the entrance of substances into the CNS (Fellner et al., 2002). Therefore, Taxol must be delivered locally to the spinal cord injury site for instance through intrathecal catheters or injections. Such CNS invasive approaches, however, pose a substantial risk of causing additional CNS damage, unreasonable danger for patients. In addition, the Taxol treatment must be conducted immediately after SCI in order to efficiently inhibit fibrotic scarring (Hellal et al., 2011). This is impossible to achieve in clinical situations, because SCI is often caused by severe accidents and stabilization of the patient's vital functions is necessary before a treatment can be initiated (Kwon et al., 2002). The requirement for immediate and local delivery to the spinal cord injury site renders Taxol impractical for clinical translation and limits its therapeutic value.

Although Taxol is not suitable for treatment of human SCI the fundamental strategy of targeting microtubule stability to induce axon regeneration in the injured CNS remains promising. Thus, I sought

for a microtubule stabilizing compound that is able to mimic the positive effects of Taxol, has the ability to cross through the blood-brain-barrier and is efficient when given at clinically relevant post-injury time-points. A variety of compounds exist which bind and stabilize microtubules (reviewed in Ballatore et al., 2012). Among them, the family of epothilones is the most promising candidate to fulfill the abovementioned criteria. Epothilones bind and stabilize microtubules very similar to Taxol (Bollag et al., 1995). However, in contrast to Taxol, epothilones are blood-brain-barrier permeable and therefore are able to stabilize microtubules in the CNS upon systemic administration (Rivera et al., 2008; Brunden et al., 2010). In addition, the isoform epothilone B and its synthetic analog ixabepilone underwent human clinical trials and even received approval by the FDA, respectively (Lechleider et al., 2008; Rivera et al., 2008).

In my thesis, I provide the first evidence that systemic and post-injury administration of the microtubule stabilizing drug epothilone B has beneficial effects on anatomical and functional outcomes after SCI. This treatment regime increases microtubule stabilization at the spinal cord injury site which hinders directed cell migration of scar forming fibroblasts and thereby reduces fibrotic scar formation. Moreover, my work demonstrates that microtubule stabilization through epothilone B promotes microtubule polymerization into the axon tip, which decreases axon dystrophy and increases axon growth under growth restraining conditions. Finally, I show that systemic and post-injury administration of epothilone B promotes functional recovery after clinically relevant spinal cord contusion injury by restoring raphespinal innervation to the spinal cord.

#### **4.1. Moderate microtubule stabilization through epothilone B mimics the beneficial effects of Taxol**

It has been shown that moderate microtubule stabilization through the drug Taxol induces axon growth in embryonic neurons (Witte et al., 2008). Furthermore, local application of Taxol reduces dystrophy of injured CNS axons (Erturk et al., 2007) and reduces fibrotic scar formation after SCI (Hellal et al., 2011). Originally, Taxol was identified as a potent anti-cancer treatment due to its ability to suppress mitotic spindle formation in rapidly dividing cancer cells. In 1995 Bollag and colleagues identified the epothilone family as microtubule stabilizing agents with a Taxol-like mechanism of action (Bollag et al., 1995). Both, Taxol and epothilones, compete for the same binding site at the beta-tubulin subunit (Kowalski et al., 1997). Binding stabilizes the lateral and longitudinal contacts between the tubulin-heterodimers and -protofilaments, respectively, thereby increasing the stability and polymerization of the microtubule (reviewed in (Goodin et al., 2004).

That Taxol and epothilones stabilize microtubules in a similar fashion is further supported by my data as epothilone B and Taxol produce comparable effects on axon growth, axon dystrophy and fibrotic scarring. In addition, these findings clearly demonstrate that these biological effects are a primary result of the microtubule stabilizing action of both drugs. In this regard, epothilone B seems to be the more potent drug since its effective dose is lower compared to Taxol. For instance, 256 ng/day of Taxol are required to inhibit fibrotic scar formation for 4 weeks after dorsal hemisection. In comparison, only 30 ng/day of epothilone B are necessary to obtain a similar result. The reason for this higher potency of epothilone B could be that both drugs, epothilone B and Taxol, are metabolized differently within cells or tissue. Moreover, it is possible that epothilone B binds more efficiently to microtubules than Taxol. This is supported by the study of Kowalski and colleagues, who showed that epothilone B exhibits a higher affinity for beta-tubulin than Taxol (Kowalski et al., 1997). In fact, the dissociation constant ( $K_d$ ) of

epothilone B and tubulin is approximately 36 nM while the  $K_d$  for Taxol is between 60 and 100 nM (Raccor, 2008).

However, besides the different potencies, locally applied epothilone B mimics several effects of Taxol that are beneficial for spinal cord repair. This suggests that epothilone B is a valid treatment alternative to Taxol for promoting axon regeneration after SCI.

#### **4.2. Systemic administration of epothilone B is a clinically relevant treatment strategy**

A therapeutic strategy for human SCI is clinically relevant when it fulfills the following criteria (Kwon et al., 2002):

- 1) The treatment must be currently available in a form that could be given to humans and must be approved as a clinical therapeutic or at least have been tested already in human clinical trials for some other related or unrelated conditions.
- 2) The treatment must be neurologically efficient when delivered systemically.
- 3) To be compatible with the complications that accompany human SCI, the treatment must be efficient when given at post-injury time-points.

From the second consideration another important feature naturally emerges.

- 4) The systemic application of the treatment must not cause adverse off-target effects on other organs.

The microtubule stabilizing drug epothilone B matches all four criteria. First, the epothilone B analog ixabepilone received clinical approval as a treatment for breast cancer in 2008 (Lechleider et al., 2008). In addition, epothilone B was tested in clinical trials as a treatment for various types of cancer and was

considered as generally safe (Rivera et al., 2008). These clinical trials revealed that peripheral neuropathy was not a primary side effect of epothilone B (Rivera et al., 2008). Notably, peripheral neuropathy is one of the most severe side effects after systemic Taxol administration in cancer treatment (Chaudhry et al., 1994).

Second, epothilone B is neurological active when administered systemically. My data show, that intraperitoneally injected epothilone B enters the CNS and increases microtubule stability as indicated by increased tubulin detyrosination and acetylation. Penetrating the blood-brain-barrier is a general feature of the epothilone family. In fact, the epothilones were developed because of their efficacy in Taxol-resistant cancer cells that overexpress the multi-drug-resistance (MDR) channel p-glycoprotein (p-gp) (Kowalski et al., 1997). P-gp is a drug efflux pump that is highly expressed in brain capillary endothelial cells, which form the blood-brain-barrier, separating blood from the CNS (Beaulieu et al., 1997). Taxol is a substrate of these efflux pumps and has therefore limited ability to penetrate the blood-brain barrier and to enter the CNS (Fellner et al., 2002). By contrast, epothilones are not a substrate of p-gp and therefore can enter the CNS even after systemic administration (reviewed in Ballatore et al., 2012). In addition, the CNS-activity of systemically delivered epothilone B is demonstrated by the fact that either local or systemic drug administration prevents axon dystrophy and scar formation. Furthermore, this suggests that epothilone B mediates these effects by acting directly at the spinal cord injury site, independent of its route of entry. Notably, local administration leads to a more pronounced reduction of dystrophic axons and scar tissue, which may be a result of higher relative drug concentrations at the lesion site in comparison to systemic treatment.

Third, my data show that delayed administration of epothilone B, at day 1 and day 15 post-injury, improves the outcomes following experimental SCI. The efficacy of delayed epothilone B delivery may be a result of its pharmacokinetic properties. The entry of epothilone B is rapid and measurable drug concentrations were present in the spinal cord after 6 hours, peaking after 1 day. Notably, epothilone B was cleared only slowly from the CNS but rapidly from the blood plasma. It is known that the drug is

rapidly metabolized and inactivated in the blood by carboxyesterases (Goodin et al., 2004). Similar enzymes may not be present in the CNS, which could explain the reduced metabolism of the drug. As a consequence, epothilone B concentrations remained at similar levels for at least 6 days. Notably, within the first 7 days after SCI the fibrotic scar forms (Hellal et al., 2011). My data suggest that due to the rapid CNS entry and slow clearance of epothilone B, a single, post-injury dosage of the drug is sufficient to reduce acute fibrotic scarring after SCI. It is possible, that initial prevention of the scarring process is sufficient for prolonged inhibition of scar tissue formation after SCI. However, when drug concentrations drop below a critical level the scarring process is presumably reinitiated. Therefore, I applied a second dose of epothilone B at 15 days after injury. Consequently, the amount of fibrotic scar tissue was still reduced 4 weeks after SCI (dorsal hemisection). It is speculative whether a third shot of epothilone B at later post-injury time-points is necessary for sustaining fibrotic scar inhibition but this requires further elucidation.

Fourth, my study provides evidence that systemic administration of epothilone B is safe under the tested parameters. Due to their antiproliferative effects, microtubule stabilizing drugs, including epothilones, are used in clinics for treating various kinds of cancer (Rivera et al., 2008). However, chemotherapeutic dosage regimens are not desirable for SCI treatment, because they cause a variety of terrible side effects. Therefore, I first sought a dosage that produces the desired effects without causing adverse events. I tested different dosing regimens ranging from 0.5 to 1.5 mg/kg BW and their effects on fibrotic scar formation after SCI and systemic toxicity, determined by body weight measurements and blood analysis (data not shown). I found that intraperitoneal administration of 0.75 mg epothilone B per kg bodyweight in adult rats, given at 1 and 15 days after SCI improved the anatomical and functional outcome of SCI without affecting bodyweight or white blood cell concentration of the experimental animals. Notably, one of the most common side effects of epothilone B in cancer treatment is neutropenia, a pathological reduction of white blood cells (Rivera et al., 2008). This suggests that the effective drug concentrations for treating SCI are lower than those used for treating cancer. In fact, two injections of 0.75 mg/kg of epothilone B is



a cumulative dose that is significantly lower than what is used for treating different kinds of experimental tumor models. For instance, in tumor-bearing nude mice a potent anti-tumor activity of the drug was observed when intravenously (i.v.) administered at a single dose of 4-6 mg/kg BW or after 2-3 i.v. injections of 3-4 mg/kg BW (Altmann et al., 2000).

Thus, my findings imply two important conclusions. First, they provide proof-of-principle evidence that systemic administration of epothilone B is a clinically practical treatment strategy to treat the injured spinal cord. Second, the reduction of the fibrotic scar is most likely not a result of an antiproliferative drug effect of the drug on either the scar forming cells in the injured spinal cord or on other cell types that contribute to the wound healing response after injury including white blood cells (reviewed in Kawano et al., 2012). The latter conclusion is further supported by the fact that the amount of proliferating or apoptotic cells at the lesion site was not altered by epothilone B treatment.

#### **4.3. Epothilone B inhibits fibrotic scarring by abrogating cell polarity and the directed cell migration of meningeal fibroblasts**

As described in the introduction, the fibrotic scar is formed by meningeal fibroblasts. After spinal cord injury, these cells proliferate, migrate into the lesion site and form the fibrotic scar (reviewed in Kawano et al., 2012). My data suggest that the treatment does not affect proliferation or apoptosis of meningeal fibroblasts. In this context, neither lesion size nor glial scarring were changed in epothilone B treated animals, two features that would be fundamentally affected by an altered cell proliferation (Goritz et al., 2011). Thus, fibrotic scar reduction after systemic epothilone B treatment is probably a result of an impaired migration of scar forming cells into the lesion site. Indeed, my data demonstrate that meningeal fibroblasts treated with epothilone B are unable to migrate in wound healing assays *in vitro*. Furthermore, I show that epothilone B disrupts the polarization of the cell's microtubule array, which prevents

polarization of the cell to form a leading and a trailing edge both *in vitro* and *in vivo*. The inability of the epothilone B treated cells to polarize most likely underlies their migration failure. It has been shown that polarization of the microtubule cytoskeleton is fundamental for cell migration and its disruption hinders directed cell migration (reviewed in Li and Gundersen, 2008). Interestingly, a recent study showed that even at low concentrations microtubule stabilizing drugs are able to inhibit migration of vascular endothelial cells at low, nanomolar concentrations (0.5 nM for Taxol) by interfering with trailing edge retraction (Ganguly et al., 2013). It is possible that due to their increased stability, microtubules are unable to depolymerize and thereby act as steric “struts” that prevent trailing edge withdrawal (Ganguly et al., 2013). In addition, epothilone B induced microtubule stabilization may interfere with the regulatory function of microtubules during trailing edge retraction. A recent publication suggests that microtubule destabilization and depolymerization is necessary for releasing focal contacts factor (Kamath et al., 2013). The authors suggest that an increased amount of stable microtubules bind GEF H1 and impede its regulatory action on RhoA and focal attachments. Consequently, the migration failure of epothilone B treated fibroblasts could result from the inability to disengage from the underlying substrate.

Another possible mechanism that underlies epothilone B induced fibrotic scar inhibition could be TGF- $\beta$ 1 signaling. TGF- $\beta$ 1 is one of the most abundant fibrogenic factors at the lesion site (Komuta et al., 2010). It was shown that the Taxol treatment *in vitro* and *in vivo* dampens TGF- $\beta$ 1 signaling by preventing microtubule dependent nuclear translocation of the TGF- $\beta$ 1 receptor target Smad2/3 (Batut et al., 2007; Hellal et al., 2011). Hellal and colleagues demonstrated that local Taxol application to the lesion site inhibits cellular Smad2/3 nuclear translocation at the lesion site, which contributed to the reduction of fibrotic scar tissue. Systemic administration of epothilone B did not induce obvious changes of Smad2/3 nuclear translocation at the lesion site (data not shown). It is possible that the critical concentration, which is necessary for inhibiting microtubule dependent signaling, was not achieved with the used epothilone B dosage. Consistently, local application of Taxol to the lesion site more efficiently reduces fibrotic scarring than systemic administration of epothilone B.

Finally, the treatment could potentially reduce the amount of pro-inflammatory, fibrogenic factors at the lesion site by interfering with cell secretion. Yet, protein levels of TGF- $\beta$ 1 were comparable between epothilone B treated animals and injured controls (data not shown). Since TGF- $\beta$ 1 is the most potent fibrogenic factor at the lesion site (Komuta et al., 2010) it is unlikely that scar reduction after systemic epothilone B delivery is a result of perturbed cell secretion.

This suggests that epothilone B reduces fibrotic scar formation primarily by perturbing the distribution of stable and dynamic microtubules in scar forming meningeal fibroblasts. This disrupts cell polarization and in turn prevents directed meningeal fibroblast migration into the spinal cord lesion.

As described previously, the fibrotic scar poses a major barrier for axon regeneration at the lesion site by expressing axon growth inhibitory molecules including CSPGs (Hellal et al., 2011; Kawano et al., 2012). Systemic administration of epothilone B reduces fibrotic scarring, which is accompanied by a significant CSPG reduction at the lesion site including neurocan one of the most abundant CSPG isoforms at the lesion site (Asher et al., 2000; Jones et al., 2003). Therefore, my study provides further evidence that the fibrotic scar is a major source of axon growth inhibitory CSPGs in the lesion scar. This is noteworthy, because cells of the glial scar were considered as the major contributors of CSPG expression after SCI (Jones et al., 2003; Silver and Miller, 2004). It is yet possible that epothilone B treatment also interferes with CSPG production by astrocytes. In fact, Taxol treated cultured astrocytes show a reduced expression of CSPGs (Hellal et al., 2011). However, the pattern of CS-56 immunofluorescence in the lesion site, which specifically visualizes chondroitin sulfates, suggests that the CSPGs reduction is primarily caused by a lack of ECM deposition in the lesion epicenter. It has been shown that meningeal fibroblasts express ECM molecules including laminin, fibronectin and also CSPGs (Decimo et al., 2012). Since meningeal fibroblasts are incapable of migrating into the lesion epicenter upon epothilone B treatment, the cellular source for ECM expression is absent. In addition, since CSPGs require the ECM as a binding-substrate, CSPGs secreted from glial cells may not disperse into the lesion site, leading to a further reduction.

---

Thus, my data provide evidence that systemically administered epothilone B suppresses CSPG deposition at the lesion site by preventing fibroblast infiltration and the concomitant ECM production.

#### **4.4. Microtubule polymerization into the growth cone propels axon growth**

It has been shown in previous studies that moderate microtubule stabilization by Taxol increases axon growth on a variety of growth inhibitory substrates (Erturk et al., 2007; Hellal et al., 2011; Sengottuvel and Fischer, 2011). My data show that epothilone B increases axon growth of postnatal neurons in the presence of growth inhibitors in a similar fashion. In addition, my study provides a cellular mechanism how a moderate increase of microtubule stabilization promotes axon growth. I show that low doses of epothilone B induce massive polymerization of microtubules closer to the growth cone tip, which precedes increased neurite outgrowth in the presence of growth-inhibitory Nogo-A. Similarly, epothilone B rescues neurite growth in the presence of inhibitory CSPGs and semaphorin 3A. This growth-promotive effect of epothilone B is compromised by the microtubule destabilizing drug nocodazole, which induces depolymerization and retraction of microtubules from the growth cone. Thus, the increased microtubule polymerization into the growth cone upon epothilone B treatment causes increased neurite growth under growth restraining conditions.

Microtubule polymerization into the peripheral growth cone is a key mechanism of axon growth. In fact, multiple axon formation by embryonic hippocampal neurons upon Taxol treatment is a direct consequence of microtubule polymerization into the distal neurite (Witte et al., 2008). Microtubules are considered to act as a “pushing force” for the elongating axon, while the actin cytoskeleton functions as a “steric hindrance” which prevents microtubules from entering the growth cone periphery (Neukirchen and Bradke, 2011). In accordance, removing the actin hindrance or promoting microtubule assembly into the P-domain is sufficient to induce axon elongation (Bradke and Dotti, 1999; Kabir et al., 2001). Massive microtubule polymerization into the growth cone by epothilone B treatment may increase the microtubule

“pushing force” against the actin hindrance leading to microtubule entrance into the growth cone periphery. In addition, the treatment could promote microtubule invasion into peripheral filopodia by stimulating the interaction between plus-tip bound EB3 and the actin-binding protein drebrin. Drebrin captures EB3-bound microtubule plus-tips and guides them to filopodial F-actin bundles (Geraldo et al., 2008). How microtubule invasion into peripheral growth cone structures promotes axon elongation is not fully understood. Microtubules may generate physical forces that are sufficient to drive the growth cone forward (Laan et al., 2008). Moreover, microtubules could maintain, stabilize and/or induce the formation of actin protrusions (Lowery and Van Vactor, 2009). Finally, microtubule-based transport provides an increased amount of cellular cargo to the site of growth, which is a rate limiting factor of axon elongation (Zakharenko and Popov, 1998).

In addition, microtubule stabilization through epothilone B may promote neurite growth by desensitizing the neurites to extracellular growth inhibitory factors. One major effector of Nogo-A, CSPGs and semaphorin 3A is the GTPase RhoA (reviewed in McKerracher et al., 2012) which regulates microtubule dynamics through its downstream target collapsin response mediator protein 2 (CRMP-2). CRMP-2 binds tubulin heterodimers and promotes increased microtubule assembly (Fukata et al., 2002). Nogo-A, CSPGs and semaphorin 3A inactivate CRMP-2 through RhoA signaling, thereby inducing microtubule disassembly and growth cone collapse (Mimura et al., 2006; McKerracher et al., 2012). Epothilone B mediated microtubule stabilization and polymerization may compensate for the loss of CRMP-2 activity; a recent publication demonstrates that CRMP-2 is replaced by epothilone B indicating a similar mode of action (Lin et al., 2011). Semaphorin 3A induces microtubule instability through an additional effector which is glycogen synthase kinase 3 beta (GSK-3 beta). GSK-3 beta phosphorylates and inactivates CRMP-2 (Yoshimura et al., 2005) and MAP 1B, a microtubule-associated protein that protects microtubules from depolymerization (Goold et al., 1999). Consistently, the semaphorin 3A-induced loss of the microtubule stabilizing function of CRMP-2 and MAP 1B may be rescued by microtubule stabilization through epothilone B.

Taken together, I hypothesize that epothilone B enables neurite outgrowth on growth inhibitory substrates by two mechanisms. On the one side, the drug promotes microtubule invasion into the growth cone P-domain which per se promotes neurite elongation. On the other side, the microtubule stabilizing action of epothilone B neutralizes growth inhibitory signaling. Further studies are required to elucidate how these mechanisms individually contribute to the growth promotive effect of microtubule stabilizing agents.

#### **4.5. Systemic administration of epothilone B reduces axon dystrophy**

Injured neurons in the PNS form new growth cones, regenerate and reinnervate, at least in part, their former target structure. By contrast, damaged axons in the CNS do not form growth cones but become dystrophic, reflected by the formation of retraction bulbs (Bradke et al., 2012).

It has been shown that axon dystrophy is caused by disorganization and disassembly of microtubules within the tip of the injured CNS axons (Erturk et al., 2007). Increasing microtubule stability by local application of Taxol or by systemic administration of epothilone D rescues axon dystrophy and axon degeneration (Erturk et al., 2007; Brunden et al., 2010).

My research demonstrates that local or systemic administration of the microtubule stabilizing drug epothilone B substantially decreases retraction bulb formation after SCI in mice. Since local application of Taxol produces a similar effect, perturbed microtubule stability within the injured axons must be a fundamental cause of axon dystrophy. There are certain lines of evidence that support this statement. Injured PNS axons that are treated with the microtubule destabilizing drug nocodazole or vincristine, a drug that inhibits microtubule assembly, do not form new growth cones but become dystrophic and stall regeneration (Pan et al., 2003; Erturk et al., 2007). In addition, Erturk and colleagues reported that microtubules within the retraction bulbs of injured CNS neurons are unbundled and disorganized, while Taxol treatment promoted microtubule rebundling and reorganization (Erturk et al., 2007). Remarkably,

injured axons of invertebrate neurons form bulb like-endings with disorganized and disassembled microtubules. However, these neurons have the intrinsic ability to reorganize their axonal microtubules into bundles, which leads to axon regeneration (Erez et al., 2007). Erturk and colleagues reported a reduction of retraction bulbs after local application of Taxol but not the formation of new growth cones at the axonal stumps. However, this could be attributed to the short observation interval of only 6 hours. In my study, reduction of retraction bulbs upon systemic administration of epothilone B precedes increased regenerative sprouting towards the injury site within one day. This suggests that microtubule stabilization is sufficient for growth cone formation of injured CNS axons presumably by promoting functional reorganization of the distal microtubules.

In addition, my study shows that systemic administration of epothilone B decreases axon dieback from the lesion site after CNS injury. A recent study from the Yaron lab demonstrated that microtubule depolymerization precedes degeneration of axotomized DRG axons in culture (Maor-Nof et al., 2013). In addition, this study revealed, that microtubule stabilization through Taxol prevents this degenerative process (Maor-Nof et al., 2013). An important trigger of microtubule disassembly is calcium, which enters the injured axon through its disrupted cell membrane and calcium-specific ion channels (George et al., 1995; Bradke et al., 2012). Even though calcium seems to be important for the formation of a new growth cone after axotomy (Kamber et al., 2009), it also induces axon degeneration (George et al., 1995) by activating microtubule-degrading calpains (Spira et al., 2003) and by inducing microtubule disassembly (O'Brien et al., 1997). Interestingly, epothilone B protects microtubules from calcium-induced depolymerization (Kowalski et al., 1997) which may contribute to the reduced axonal dieback that is observed in treated animals. Alternatively, increased microtubule stabilization may counteract calpain induced microtubule degradation. This assumption is supported by the fact that, similar to epothilone B, calpain inhibition prevents axonal dieback upon CNS injury (Kerschensteiner et al., 2005). Finally, epothilone B might compensate for axotomy-associated loss of microtubule stabilizing proteins such as Tau. Axotomy induces axon degeneration which is accompanied by Tau depletion from microtubules

(Maor-Nof et al., 2013). Interestingly, microtubule stabilizing agents such as Taxol and epothilones bind to a similar binding site as Tau and might thereby compensate for its loss. Along these lines, microtubule stabilizing agents prevent axon degeneration in experimental models of tauopathy (Zhang et al., 2005; Brunden et al., 2010) indicating that these drugs indeed rescue a loss of Tau function.

Taken together, my data suggest that systemic administration of epothilone B reduces axon dystrophy of injured mammalian CNS sensory axons by protecting microtubules from disassembly and disorganization and by promoting microtubule reorganization. The contribution of both features requires detailed investigation in future studies.

#### **4.6. Systemic administration of epothilone B promotes functional raphespinal tract restoration**

Damaged axons in the spinal cord poorly regenerate, which leads to permanent functional deficits after SCI. Axon regeneration is restricted by the intrinsic inability of mature CNS neurons to regrow their injured axons (Bradke et al., 2012), by the inhibitory lesion scar and by CNS myelin (Fitch and Silver, 2008; Kawano et al., 2012).

In my study I show that systemic administration of epothilone B promotes the growth capacity of injured CNS axons and reduces the inhibitory spinal cord lesion environment. Consequently, this leads to an increased amount of raphespinal axons caudal to the lesion site, which correlates with increased recovery of hindlimb function after spinal cord contusion injury in rats.

This latter observation is especially notable, because the rat spinal cord contusion injury model is considered as clinically relevant. The vast majority of human injuries are contusion injuries that e.g. result from spinal cord compression through delocalized vertebrae (Norenberg et al., 2004). Depending on the severity these injuries are accompanied by lesion cavitation or extensive fibrous scarring (Norenberg et al.,



2004). To test potential therapeutics for clinical translation, researchers have developed devices that produce experimental spinal cord injuries that mimic the pathophysiological aspects of human SCI (reviewed in Onifer et al., 2007). For my research, I used one of these devices, which is the “Infinite Horizon” (IH) impactor (Scheff et al., 2003). The IH impactor allows precise control over the kinetic forces applied to the spinal cord, which produces highly standardized contusion injuries (Scheff et al., 2003). For my studies, I used an impact force of 150 kdyn to produce moderate spinal cord contusions in the mid-thoracic rat spinal cord. I chose this force, because a force of 100 kdyn produces injuries that are too mild, leading to an intense spontaneous recovery that generally renders the assessment of a therapeutic intervention difficult. By contrast, a force of 200 kdyn produces injuries that are too severe, which strongly limits functional recovery and may mask positive treatment effects. Along these lines, I showed in earlier studies that local Taxol treatment to the lesion site improves recovery of walking after 150 kdyn contusion injury (Hellal et al., 2011) but not after 200 kdyn contusion injury (data not shown). In addition, the 150 kdyn contusion model offers the advantage that the injured rats recover weight supported stepping already 2 weeks after injury. Therefore, it is possible to study the effect of a treatment on gait abnormalities and the functional recovery of walking after SCI.

To assess these, I used two behavioral assays, the catwalk and the horizontal ladder, which are specifically sensitive to even mild disturbances of hindlimb function during walking. The catwalk is used to record and analyze paw placement of animals walking on a plane surface. These analysis provide detailed information about inter limb coordination, body balance and walking stability (Metz et al., 2000). The horizontal ladder test requires forelimb-hindlimb coordination and voluntary movement control and is therefore used to reveal deficits in descending fine motor control after SCI, that are not apparent during normal walking (Metz et al., 2000).

Foot-print analysis of the catwalk system revealed that a 150 kDyn contusion injury induces substantial gait abnormalities in injured controls. 8 weeks after contusion injury, control animals show less stable and less coordinated walking when compared to uninjured animals indicating the interruption of descending

and ascending spinal cord projections that control body balance, walking stability and coordination. By contrast, systemic administration of epothilone B significantly ameliorates these functional deficits suggesting that the treatment partially restores spinal cord circuits that are necessary for normal walking.

The horizontal ladder test revealed that both, epothilone B treated animals and injured controls, showed a considerable reduction of footfall errors within the first 4 weeks after contusion injury, probably owing to spontaneous recovery of walking function. In fact, the 150 kdyn contusion injury spares a substantial amount of white matter that probably contributes to these spontaneous improvements (Scheff et al., 2003). However, systemic administration of epothilone B appears to enhance this spontaneous recovery, because 6 and 8 weeks post-injury treated animals showed significantly less footfalls than control animals. Thus, my data suggest that systemic delivery of epothilone B promotes the functional restoration of descending motor tracts that control the voluntary and precise paw placement on the ladder steps.

Besides the functional data, systemic administration of epothilone B increases the amount of descending, serotonin-positive raphespinal fibers in the lumbar spinal cord ventral horn. There, raphespinal fibers, which use serotonin (5HT) as neurotransmitter, control the activity of motor neuron pools that express 5HT-receptors (Sławińska et al., 2013). My data show that in epothilone B treated animals, an increased amount of raphespinal fibers contact choline acetyltransferase (ChAT)-positive motor neuron pools that innervate the hindlimb muscles (Gilerovich et al., 2008). When this increased innervation is destroyed by 5,7-DHT, a serotonergic neurotoxin, the functional improvements of the treated animals are fully abrogated. This suggests that systemic administration of epothilone B increases recovery of function by increasing raphespinal innervation to spinal motor neurons. In accordance, a variety of studies demonstrated that increasing raphespinal regeneration promotes recovery of hindlimb function after SCI (Kim et al., 2004; Pearse et al., 2004; Kaneko et al., 2006; Hellal et al., 2011).

The specific role of the raphespinal tract in hindlimb locomotion is controversial. Earlier studies suggested that descending raphespinal projections have a modulatory rather than a mediatory function

during walking (Jacobs and Fornal, 1997). However, recent studies indicate that intrathecal application of serotonin or serotonin agonists is sufficient to produce hind limb locomotion in rodents with a complete spinal cord transection (Jordan et al., 2008). This suggests a more crucial involvement of raphespinal projections for hindlimb movement and walking. One major function of serotonin in the spinal cord is to increase motor neuron excitability and the amplitude of the motor response (Barbeau and Rossignol, 1990; Schmidt and Jordan, 2000). The contribution of serotonergic input to motor neuron excitation may even be enhanced after SCI, since motor neurons up-regulate 5HT receptors after injury and become hypersensitive to the neurotransmitter (Husch et al., 2012). Accordingly, serotonin exhibits direct effects on walking parameters. Application of serotonin to the spinal cord increases step length (Barbeau and Rossignol, 1990) and forelimb-hind limb coordination (Slawinska et al., 2013). Notably, similar gait improvements are induced by systemic administration of epothilone B, which suggests that the drug mediates these effects by promoting raphespinal function.

This raises the question how epothilone B ameliorates raphespinal function. Potentially, the treatment promotes regeneration or regenerative sprouting of raphespinal fibers and/or protects spared raphespinal projections from injury-induced degeneration. Since the data arise from analysis of fixed tissue sections, it is difficult to judge whether the increased density of raphespinal fibers in epothilone B treated animals should be attributable to increased regeneration or to neuroprotection (Tuszynski and Steward, 2012). However, certain lines of evidence suggest that epothilone B may contribute to both. The cell culture data show that neurons treated with epothilone B exhibit enhanced growth in the presence of growth inhibitory factors including the CNS myelin component Nogo-A. Neutralizing the inhibitory action of Nogo-A is sufficient to induce regeneration of raphespinal fibers after SCI in rats (Kim et al., 2004). In addition, systemic administration of epothilone B reduces growth inhibitory CSPGs at the lesion site, which is accompanied by an increased amount 5HT-positive fibers caudal to the injury site. Comparably, digestion of CSPGs by the bacterial enzyme chondroitinase ABC promotes regeneration of raphespinal axons to the caudal injury site (Alilain et al., 2011). Hence, epothilone B may promote regeneration of raphespinal

axons by desensitizing them to extrinsic growth inhibitors and by rendering the hostile lesion environment more permissive. In addition, I show by *in vivo* live imaging that local or systemic application of epothilone B protects injured sensory axons from dieback after injury. In accordance, it has been shown that systemic delivery of epothilone D, another epothilone analog, rescues axon degeneration in different models of neurodegenerative diseases by counteracting microtubule disassembly and dysfunction (Brunden et al., 2010; Cartelli et al., 2013). This suggests that systemic administered epothilones have a neuroprotective effect and conserve CNS axons under degenerative conditions. Even though SCI is not a neurodegenerative disease, the injury triggers an inflammatory process leading to degeneration of axons that were not severed by the primary insult (Cadotte and Fehlings, 2011). Accordingly, neuroprotective treatments have positive implications on SCI pathology (reviewed in (Kwon et al., 2002).

Thus, I assume that systemic administration of epothilone B promotes regeneration and prevents degeneration of raphespinal fibers thereby improving raphespinal function and locomotor recovery after spinal cord contusion injury.

#### **4.7. Concluding remarks**

Microtubules are fundamental for numerous cellular processes, including cell migration (Gundersen and Bulinski, 1988), signal integration (Hellal et al., 2011), proliferation (Glotzer, 2009) and axon growth (Witte et al., 2008). The finding that the stabilization of microtubules disrupts mitotic spindle formation and inhibits cell division established the usage of systemic microtubule stabilizing agents as a therapeutic standard for the treatment of cancer (Dumontet and Jordan, 2010). My work shows that systemic administration of the microtubule stabilizing agent epothilone B, at doses below those currently accepted for cancer treatment (Altmann et al., 2000), promotes functional recovery after SCI. My approach focuses on a single molecular target, the microtubules, yet overcomes multiple obstacles that restrain axon regeneration after SCI. This is possible because of the dichotomy of microtubule dynamics in the polarization of different cell types. In neurons, microtubule stabilization reactivated an embryonic-like growth program by promoting microtubule protrusion into the axon tip, which induced axon regeneration under pathological, growth-restraining conditions. By contrast, in scar forming fibroblasts the stabilization of microtubules abrogated cell polarity and directed cell migration, which reduced the inhibitory fibrotic scar. This dual effect of microtubule stabilization through epothilone B promotes functional restoration of the spinal cord raphespinal tract which leads to an enhanced locomotor recovery after SCI.

My study provides evidence that microtubule stabilization through epothilone B administration represents a promising treatment strategy for CNS injuries with a strong translational perspective: 1) Epothilone B has beneficial effects for SCI recovery when given by systemic and post-injury administration. 2) Epothilone B counteracts clinically relevant impediments of SCI including axon dystrophy and fibrotic scarring. 3) Epothilones are clinically approved which enables an efficient clinical translation. Thus, future work can be valuably undertaken to study the effect of epothilones in animal models of SCI to further validate their safety, efficacy and translational value.

## 5. MATERIAL AND METHODS

### 5.1 Materials

#### 5.1.1. Chemical substance

- Ammonium chloride (NH<sub>4</sub>Cl) VWR
- β-Mercaptoethanol VWR
- Borax (Sodium borat) VWR
- Boric acid VWR
- Bovine serum albumin (BSA) Sigma
- Cremophor El Sigma
- Dimethyl sulfoxide (DMSO) Roth
- Donkey serum Invitrogen
- EDTA (ethylene diamine tetraacetic acid) VWR
- Ethanol VWR
- Fetal bovine serum (FBS) Invitrogen
- Hanks balanced salt solution (HBSS) Invitrogen
- Hepes (N-2-Hydroxyethylpiperazine-N'-2-ethane sulfonic acid) Invitrogen
- Hydrochloric acid (HCl, 1 M) VWR
- Laminin (0.5 mg/ml) Roche
- Glutamine 100x Invitrogen
- Glycine Sigma
- Goat serum Invitrogen
- Methanol VWR
- Minimal essential medium (MEM) 10x Invitrogen

- MEM essential amino acids 50x Invitrogen
- MEM non-essential amino acids 100x Invitrogen
- 3-morpholinopropase sulfonic acid VWR
- Paraformaldehyde Sigma
- Parrafin VWR
- Disodium hydrogen phosphate (Na<sub>2</sub>HPO) VWR
- Sodium chloride (NaCl) VWR
- Sodium hydroxide (NaOH) VWR
- Sodium dodecylsulfate (SDS) Sigma
- Sucrose Sigma
- Tris base Sigma
- Triton X-100 Sigma
- Tween 20 (Polyoxyethylene) Sigma

### **5.1.2. Buffers and solutions**

- 50 mM ammonium chloride (NH<sub>4</sub>Cl): 1.34 g ammonium chloride in 500 ml PBS
- Blocking solution for immunocytochemistry: 2% Fetal bovine serum, 2% BSA and 0.2% Fish gelantine in H<sub>2</sub>O
- Borate buffer: 1.24 g Boric acid and 1.90 g Borax in 400 ml H<sub>2</sub>O at pH 8.5
- Citrate buffer: Sodiumcitrate 4.4 g, NaCl 8.76 g, bring to 500 ml with H<sub>2</sub>O
- 5,7-DHT solution: 150 µg (free base) 5,7-DHT dissolved in 20 µl 0.02% ascorbate-saline
- Glycosaminoglycan extraction buffer: 3 M guanidine hydrochloride/0.05 M Tris HCL buffer (pH 7.5)
- 1 M Hepes: 28.8 g Hepes in 100 ml H<sub>2</sub>O at pH 7.25 (solution is autoclaved)

- 7 mM Hepes buffered Hanks balanced salt solution (HBSS): 3.5 ml 1 M Hepes in 500 ml HBBS (solution is sterile filtered)
- 5x Laemmli buffer: 250 mM Tris/HCl (pH 6.8), 1 M  $\beta$ -Mercaptoethanol, 10% (w/v) SDS, 30% (v/v) Glycerol and bromophenolblue in H<sub>2</sub>O
- MEM: 50 ml 10x MEM, 15 ml 20% glucose, 20 ml 5.5% NaHCO<sub>3</sub>. 10 ml MEM essential amino acids 50x, 10 ml MEM non-essential amino acids 100x, bring 1 L with H<sub>2</sub>O (pH 7.3; solution is sterile filtered)
- MEM-FBS 10%: 10 ml heat-inactivated FBS in 90 ml MEM (medium is sterile filtered).
- MEM-FBS 0.5%: 500  $\mu$ m heat-inactivated FBS in 90 ml MEM (medium is sterile filtered).
- 3-morpholinopropase sulfonic acid (MOPS) SDS buffer: 0.05 M 3-morpholinopropase sulfonic acid, 0.05 M Tris base, 0.1% SDS, 20 mM EDTA
- Complete neurobasal medium: 48 ml neurobasal A medium, 1 ml FBS, 1 ml B-27, 0.5 ml glutamine (100x), 0.5 ml penicilin/streptomycin solution
- Neuronal growth medium / N2 Medium: 50 ml 10x N2 Supplement and 100 mg ovalbumin in 450 ml N-MEM (medium is sterile filtered).
- N-MEM: 50 ml 10x MEM, 5 ml 1.1% pyruvic acid, 5 ml 200 mM glutamine, 15 ml 20% glucose, 20 ml 5.5% NaHCO<sub>3</sub>, in 405 ml H<sub>2</sub>O (medium is sterile filtered).
- 16% Paraformaldehyde stock solution (for transcardiac perfusion): 320 g paraformaldehyde, 800 ml 1 M PBS bring to 2 L with H<sub>2</sub>O, 20 NaOH pellets, pH 7.4
- 16% Paraformaldehyde stock solution (for immunocytochemistry): 160 g paraformaldehyde, 160 g sucrose, 100 ml 10x PBS, bring to 1 L with H<sub>2</sub>O, NaOH pellets, pH 7.4
- Physiological saline solution (for transcardiac perfusion): 9 g NaCl in 1 L H<sub>2</sub>O
- Phosphate buffered saline (PBS) 1x: 0.2 g KCl, 0.2 g KH<sub>2</sub>PO<sub>4</sub>, 1.15 g Na<sub>2</sub>HPO<sub>4</sub> and 8 g NaCl in 1 L H<sub>2</sub>O (pH 7.4)
- 1 M PBS: 114.9 g Na<sub>2</sub>HPO<sub>4</sub>, 26.41 g NaH<sub>2</sub>PO<sub>4</sub>, 90 g NaCl bring to 1 L H<sub>2</sub>O (pH 7.4)



- Poly-L-lysine (PLL) solution: 1 mg/ml Poly-L-lysine hydrobromide in borate buffer. Solution is sterile filtered (all glass cover slips or glass bottom dishes for neuronal cultures are incubated with PLL solution overnight and then washed three time with sterile H<sub>2</sub>O)
- Radioimmunoprecipitation buffer: Sigma
- 0.1% Triton X-100: 50 µl (v/v) Triton X-100 in 50 ml PBS
- 0.5% TBS-Triton X-100: 5 ml (v/v) Triton X-100 in 1 l TBS
- TBS-T glycine: TBS-T with 0.3 M glycine
- Trypsin solution: 1 ml 1M HEPES in 99 ml Trypsin-EDTA-solution
- Transfer Buffer for western blotting: 3.2 g TrisHCL, 14.4 g Glycine and 200 ml methanol in 800 ml H<sub>2</sub>O
- Tris-acetate buffer: 50 mM Tricine, 50 mM Tris base, 0.1% SDS, pH 8.24
- 0.05% Trypsin-EDTA solution: 0.05% Trypsin, 0.53 mM EDTA\*4Na Invitrogen
- 0.25% Trypsin-EDTA solution: 0.25% Trypsin, 0.53 mM EDTA\*4Na Invitrogen

### 5.1.3. Commercial kits

Name	Provider
Amaya Nucleofector kit	Lonza
EndoFree Plasmid Maxi Kit	Quiagen
Proteoglycan Detection kit	Astarte Biologics
Super signal West Dura Extended Duration Substrate kit	Thermo Scientific
TUNEL staining kit	Invitrogen

**5.1.4. Compounds, proteins and enzymes**

<b>Name</b>	<b>Concentration</b>	<b>Provider</b>
Chicken chondroitin sulfate proteoglycans	1 µg/ml	Milipore
5,7-Deshydroxytryptamine creatine sulfate	150µg per 20 µl	Sigma
Epothilone B (for cell culture)	1–5 nM	Sigma
Epothilone B (for in vivo studies)	0.75 mg/ml	Biozol
Horseradish peroxidase	1:10000	Acris
Nocodazole	10 nM	Sigma
Nogo-A	400 ng/ml	R&D systems
Proteinase k	40 µg/ml	Applicam
Semaphorin 3A	200 ng/ml	R&D systems
Taxol	3 nM	Sigma

**5.1.5. Primary antibodies**

<b>Antigen</b>	<b>Host, type</b>	<b>Dilution</b>	<b>Application</b>	<b>Provider</b>
Acetylated tubulin	Mouse, monoclonal	1:100000	WB	Sigma
Beta-3 tubulin antibody (Tuj-1)	Mouse, monoclonal	1:1000	ICC	Sigma

*Material and Methods*

Choline acetyltransferase (ChAT)	Goat, polyclonal	1:100	IHC	Chemicon
Chondroitin sulfate (CS-56)	Mouse, monoclonal	1:100	IHC	Sigma
Detyrosinated tubulin (DetyrTub)	Rabbit, polyclonal	1:500	IHC	Milipore
Detyrosinated tubulin (DetyrTub)	Rabbit, polyclonal	1:5000	WB	Millipore
Fibronectin	Sheep, polyclonal	1:100	IHC	Abcam
Fibronectin	Rabbit, polyclonal	1:1000	WB	Abcam
Glyceraldehyde 3-phosphate dehydrogenase (GAPDH)	Mouse, monoclonal	1:10000	WB	Abcam
Glial fibrillary acidic protein (GFAP)	Mouse, monoclonal	1:200	IHC	Sigma
Laminin	Rabbit, polyclonal	1:50	IHC	Sigma
MAP-2	Rabbit, polyclonal	1:2000	ICC	Milipore
Neurocan	Mouse, monoclonal	1:100	WB	Milipore
Phospho(Ser 19)-histone-H3	Mouse, monoclonal	1:100	IHC	Millipore
Serotonin (5HT),	Rabbit, polyclonal	1:500	IHC	Sigma
Synaptophysin (Syn)	Mouse, monoclonal	1:1000	IHC	Chemicon
Tau-1	Mouse	1:1000	ICC	Milipore
Tyrosinated tubulin (TyrTub)	Mouse, monoclonal	1:250	IHC	Sigma

**5.1.6. Secondary antibodies and dyes**

<b>Name</b>	<b>Type</b>	<b>Dilution</b>	<b>Application</b>	<b>Provider</b>
Alexa 350 anti-goat	Donkey antibody, polyclonal	1:400	IHC	Invitrogen
Alexa 488 anti-mouse	Donkey antibody, polyclonal	1:400	IHC	Invitrogen
Alexa 568 anti-rabbit	Donkey antibody, polyclonal	1:400	IHC	Invitrogen
Alexa 647 anti-sheep	Donkey antibody, polyclonal	1:400	IHC	Invitrogen
Alexa 488 anti-mouse	Goat antibody, polyclonal	1:400	IHC	Invitrogen
Alexa 568 anti-rabbit	Goat antibody, polyclonal	1:400	IHC	Invitrogen
Cy3-Streptavidin	Biotin-binding protein	1:400	Histology	Invitrogen
4',6-diamidino-2-phenylindole (DAPI)	DNA-binding fluorophore	1:10000	Histology	Invitrogen
Alexa 488 anti-mouse	Goat antibody, polyclonal	1:500	ICC	Invitrogen
Alexa 488 anti-rabbit	Goat antibody, polyclonal	1:500	ICC	Invitrogen
Alexa 568 anti-rabbit	Goat antibody, polyclonal	1:500	ICC	Invitrogen
Alexa 647 anti-mouse	Goat antibody, polyclonal	1:500	ICC	Invitrogen
Phalloidin-rhodamine	Actin-binding fluorophore	1:100	ICC	Invitrogen
Giemsa	Leukocyte staining	10%	Histology	Sigma

**5.1.7. Consumables**

<b>Name</b>	<b>Application</b>	<b>Provider</b>
Rat intrathecal catheter	Intrathecal drug delivery	Alzet
Osmotic pumps 300 µl, 0.25 µl/day delivery	Intrathecal drug delivery	Alzet
Laboratory tubes	Osmotic pump – catheter connection	Sylastic
Histoacryl tissue adhesive	Osmotic pump – catheter connection	B.Braun
Shandon M1 embedding matrix	Tissue embedding for cryosectioning	Thermo Scientific
Embedding molds 16x8 mm	Tissue embedding for cryosectioning	Polysciences Inc.
Menzel Superfrost Plus microscope slides	Tissue mounting after cryosectioning	Thermo Scientific
Fluoromount	Mounting of tissue and cultured cells	Sigma
3-8% Tris-Acetate-gels	Gelelectrophoresis of fibronectin and neurocan	Novex
Nitrocell membrane 0.45 µm	Proteintransfer for western blot	Biorad
Biomax MR photographic films	Chemiluminescence detection	Kodak
Slide-A Lyzer Dialysis Cassete	Dialysis of	Thermo Scientific
96-well black/clear imaging plate	Glycosaminoglycan assay	BD Falcon

Culture inserts	In vitro wound healing assay	Ibidi
Glass-bottom dishes	Live imaging of cultured cortical neurons	MatTek

**5.1.8. Special equipment**

<b>Name</b>	<b>Application</b>	<b>Provider</b>
Infinite Horizon impactor device	SCI studies	Precision Systems
Stereotactic device	I.c.v. injections	Kopf
Masterflex perfusion pump	Transcardiac perfusion	Cole-Parmer
Cryostat microtome	Ultrathin cryosectioning	Leica
Xcell lock electrophoresis cell	SDS-polyacrylamide gel electrophoresis	Invitrogen
Transblot transfer unit	Protein transfer	Biorad
Curix 60 Processor	Film developing	Agfa
Multiplate reader	Absorption measurements	Envision
Deltavision RT live imaging setup	Live cell imaging of cortical neurons	Applied precisions
MVX10 fluorescent microscope	In vivo live imaging	Olympus
Catwalk	Automated footprint analysis	Noldus

---

*Material and Methods*

Footmisplacement device	Horizontal ladder	Bioseb
LSM 700 confocal microscope	Confocal imaging	Zeiss
Axiovision inverted microscope	Phase-contrast and epifluorescent imaging	Zeiss

## **5.2. Methods**

### **5.2.1. Pharmacokinetic analysis of epothilone B**

Pharmacokinetic analysis was performed by Pharmacelsus GmbH (Saarbrücken, Germany). Study was conducted according to German animal protection law (TierSchG). Animals were i.p. injected with 1 mg/kg epothilone B and were euthanized at specific time-points after injection. Brain and spinal cord were extracted and homogenized in PBS (1:1, w/v). Aliquots of homogenates and plasma were mixed with 1 volume acetonitrile containing 50 ng/ml diazepam as internal standard and the mixture was centrifuged at 12,000 g. Aliquots of the resulting supernatants were diluted with deionised water (1:1, v/v) and transferred to autosampler vials for LC-MS analysis. Calibration standards in the range of 0.1-240 ng/ml and quality controls were prepared in the same way as the corresponding unknown samples. HPLC system consisted of an autosampler and a HPLC pump (Surveyor, Thermo Scientific), connected to a triple quadrupole MS (TSQ Quantum Discovery Max, Thermo Scientific) equipped with an electrospray (ESI) interface (Thermo Fisher Scientific, USA) connected to a PC running the standard software Xcalibur 2.1. The HPLC pump flow rate was set to 600 µl/min and samples were separated on a Kinetex 2.6 µm Phenyl-Hexyl 100 50x2.1 mm analytical column with a Security Guard Ultra cartridge UHPLC Phenyl for 2.1 mm ID column (Phenomenex, Germany). Gradient elution was facilitated using acetonitrile/ 0.1% formic acid as organic phase (A) and 0.1% acetic acid (B): % A =5 (0-0.1 min), 97 (0.4-1.7 min), 5 (1.8-2.5 min). Full scan mass spectra were acquired in the positive mode using syringe pump infusion to identify the protonated quasimolecular ions  $[M+H]^+$ . Auto-tuning was carried out for maximizing ion abundance followed by the identification of characteristic fragment ions using a generic parameter set. Ions with the highest S/N ratio were used to quantify the item in the selected reaction monitoring mode (SRM) and as qualifier, respectively. The limit of quantification (LOQ) was defined as the lowest standard concentration taken for the corresponding calibration curve, i.e. 0.1 ng/ml.



### **5.2.2. Spinal cord injury studies**

All animal experiments were performed in compliance with the German animal protection law (TierSchG). The animals were housed and handled in accordance with good animal practice as defined by the Federation for Laboratory Animal Science Associations (FELASA).

#### **5.2.2.1. Spinal cord dorsal hemisection**

Spinal cord dorsal hemisection was performed at thoracic spinal segment T8 as previously described (Hellal et al., 2011). Adult female Sprague-dawley rats (200-250 g) were deeply anaesthetized by continuous inhalation of isoflurane (2% isoflurane/oxygen). Laminectomy of the thoracic vertebra 8 was performed to expose the spinal cord. Then, the dorsal half of the spinal cord was cut with an iridectomy scissor (FST) by transversely transecting the spinal cord extending from the dorsal surface down to 1 mm depth. For local delivery of epothilone B (30 ng/day for 4 weeks; Sigma), Taxol (256 ng/day for 4 weeks; Sigma) or vehicle (1:1 mixture of cremophor EL (Sigma) and ethanol) to the injury site an intrathecal catheter was placed at the spinal cord lesion as previously described (Hellal et al., 2011). Continuous delivery was driven by an osmotic mini-pump (Alzet) that was connected to the catheter. For systemic administration, animals received intraperitoneal (i.p.) injections of epothilone B (Biozol, 0.75 mg/kg bodyweight (BW)) or vehicle solution (50% DMSO/sterile saline) 1 day and 15 days after injury.

#### **5.2.2.2. Spinal cord contusion injury**

A moderate spinal cord contusion injury was performed at thoracic spinal cord segment 9 using the Infinite Horizon impactor device (Precision Systems) as previously described (Scheff et al., 2003). Adult female Sprague-dawley rats (200-250 g) were deeply anaesthetized by continuous inhalation of isoflurane (2% isoflurane/oxygen). Laminectomy of the thoracic vertebra 9 was performed to expose the spinal cord. Vertebral column was stabilized with 2 forceps, which were holding the lateral processes of thoracic vertebra 8 and 10. The exposed spinal cord was placed and aligned under the impactor according to

manufactures instructions. Finally, an impact of 150 kilodyne (kdyn) was applied to the spinal cord. The impact was controlled and monitored with device-specific software. 1 day and 15 days after contusion injury, animals received a single i.p. injection of epothilone B (Biozol, 0.75 mg/kg bodyweight (BW)) or vehicle solution (50% DMSO/sterile saline). Bodyweight of injected animals was monitored biweekly.

### **5.2.2.3. Intracerebroventricular (i.c.v.) injections of 5,7-dihydroxytryptamine (5,7-DHT)**

8 weeks after contusion injury, 5,7-DHT was bilaterally injected into the lateral ventricles to disrupt raphespinal neurons as previously described (Carta et al., 2007). Rats were fixed in a stereotactic device (Kopf) and were kept anaesthetized by continuous inhalation of isoflurane (2% isoflurane/oxygen) during the whole procedure. 150 µg of 5,7-DHT (Sigma) were dissolved in 10 µl ascorbate-saline solution and 5 µl solution was infused into the lateral ventricle at the following coordinates: anterior-posterior: -0.8 mm, medio-lateral: ±1.4 mm and dorso-ventral: -4.6 mm. 5,7-DHT was injected for 1 min and the cannula was kept in place for 3 min before it was carefully withdrawn. 30 min prior to 5,7-DHT injection, the specific catecholamine re-uptake inhibitor desipramine (Enzo Life Sciences) was injected i.p. (20 mg/kg BW) to prevent damage of noradrenergic neurons.

## **5.2.3. Histology**

### **5.2.3.1. Immunohistochemistry**

Immunohistochemistry was performed as previously described (Hellal et al., 2011). For tissue fixation, animals were perfused transcardially with 4% paraformaldehyd (PFA) solution (in 0.1 M PBS). Full spinal cord and brain were extracted from the vertebral column or skull, respectively. CNS tissue was post-fixed in 4% PFA solution for 24 h and then transferred to 30% Sucrose solution for cryopreservation (48 h). Subsequently, a 1 cm piece of spinal cord containing the lesion site or a 0.5 cm piece of the lumbar spinal cord, respectively, were embedded in embedding medium (Thermo Scientific) and frozen on dry

ice. 25 µm sagittal or coronal sections, respectively, were obtained using a cryostat (Leica) and mounted on superfrost plus microscope slides (Thermo scientific). Sections were quenched with 0.3 M glycine (in TBS) for 30 min and then permeabilized with TBS-TritonX (0.5%) for 30 min at room temperature. Sections were transferred to custom made wet-chambers and blocked with 5% heat-inactivated goat or donkey serum (both Invitrogen) in TBS-TritonX (0.5%) for 1 h. After blocking, sections were incubated overnight at room temperature with different combinations of antibodies diluted in TBS-TritonX (0.5%): rabbit anti-laminin (1:50; Sigma), monoclonal mouse anti-gial fibrillary acidic protein (GFAP; 1:200; Sigma), monoclonal mouse anti-chondroitin sulfate (CS-56, 1:100; Sigma), monoclonal mouse anti-tyrosinated tubulin (1:250; Sigma), rabbit anti-detyrosinated tubulin (1:500; Millipore), sheep anti-fibronectin (1:100; Abcam), rabbit anti-serotonin (5HT, 1:500; Sigma), goat anti-choline acetyltransferase (ChAT, 1:100; Chemicon), monoclonal mouse anti-synaptophysin (Syn, 1:1000; Chemicon) and/or monoclonal mouse anti-phospho(Ser 19)-histone-H3 (1:100; Millipore). After 3 washes with TBS-TritonX (0.5%) sections were incubated with corresponding secondary antibody conjugated to fluorophores Alexa 405, 488, 555, 568 (1:400; all Invitrogen) or DAPI (1:10000; Invitrogen) for 3 h at room temperature. Finally, sections were covered with Fluoromount mounting media (Invitrogen) and 20x40 mm coverslips (Marienfeld).

#### **5.2.3.2. TUNEL staining**

TUNEL staining was performed as previously described (Hellal et al., 2003). In brief, microscope slides containing 25 µm sagittal spinal cord sections were dehydrated with increasing concentrations of ethanol (75%, 90%, 100%) and then permeabilized with proteinase k (40 µg/ml in 1xPBS) at 37 °C for 30 min. After 3 washes with TBS-TritonX (0.5%) sections were incubated with terminal deoxynucleotidyl transferase and dUTP-biotin (Invitrogen) at 4 °C overnight. After stopping the reaction by incubation with citrate buffer for 15 min at room temperature, sections were 3x rinsed with TBS-TritonX 0.5%, then blocked with 5% heat-inactivated goat-serum (in TBS-T 0.5%) and incubated with Cy3-Streptavidin

(1:400; Invitrogen) for 3 h at room temperature. Finally, sections were covered with Fluoromount mounting media and 20x40 mm coverslips (Marienfeld).

#### **5.2.2.2. Giemsa staining**

White blood cells were measured in blood samples, which were collected by intracardiac puncture from vehicle (50% DMSO/Saline) or epothilone B (2x 0.75 mg/kg i.p.) treated animals 4 weeks after dorsal hemisection. 10 µl of blood were smeared onto glass slide, fixed with methanol and stained with 10% Giemsa solution (Sigma). The amount of white blood cells was obtained by counting the total number of Giemsa positive cells per slide in triplicates.

#### **5.2.4. Biochemical analysis of spinal cord tissue**

##### **5.2.4.1. Western blotting**

Spinal cord lesion sites (T8 dorsal hemisection) of vehicle (50% DMSO/Saline) or epothilone B (2x 0.75 mg/kg i.p.) treated animals and unlesioned spinal cords of naive animals were extracted from the vertebral column. Tissue was weighed and frozen in liquid nitrogen. 10 µl of radioimmunoprecipitation buffer (RIPA, Sigma) were added per 1 mg tissue. The mix was sonicated to homogenize the tissue and then incubated for 15 min (4 °C) for protein extraction. Subsequently, samples were centrifuged (10.000 rpm at 4 °C for 20 min) and the supernatant was mixed 1:1 with 1x Laemmli buffer and boiled for 5 min (95 °C). Denatured samples were electrophoresed in reducing 10% Bis-Tris-gels (custom made, for tubulin modifications) or 3-8% Tris-Acetate-gels (Novex, for fibronectin and neurocan) polyacrylamide gels by using Xcell lock electrophoresis cell containing morpholinopropase sulfonic acid (MOPS) buffer (0.05 M 3-morpholinopropase sulfonic acid, 0.05 M Tris base, 0.1% SDS, 20 mM EDTA) or Tris-acetate buffer (50 mM Tricine, 50 mM Tris base, 0.1% SDS, pH 8.24), respectively. Gels were ran at 100-150 V for 2 h and subsequently transferred overnight (4 °C) onto 0.45 µm nitrocell membranes (Biorad) with Transblot

transfer unit (Biorad) containing transfer buffer (25 mM Tris, 192 mM glycine, 20% methanol in ddH<sub>2</sub>O). After protein transfer, the membranes were blocked with 5% BSA in TBS-Tween (0.1%) for 1 h at room temperature and then incubated with the following primary antibodies overnight (4 °C): rabbit anti-detyrosinated tubulin (1:5000; Millipore), mouse anti-acetylated tubulin (1:100000; Sigma), rabbit anti-fibronectin (1:1000; Abcam), mouse anti-neurocan (1:100; Millipore) and mouse anti-glyceraldehyde 3-phosphate dehydrogenase (GAPDH, 1:10000; Abcam). After washing 3x with TBS-Tween (0.1%), the membranes were incubated with the corresponding secondary antibodies conjugated to horseradish peroxidase (HRP, 1:10.000; Acris) for 1 h at room temperature. Immunoblots were developed by chemiluminescence (Super signal west dura, Thermo scientific) using light sensitive photographic films (Kodak).

#### **5.2.4.2. Glycosaminoglycan assay**

Biochemical quantification of sulfated glycosaminoglycans (GAGs) was performed as previously described (Hellal et al., 2011). Spinal cord lesion sites (T8 dorsal hemisection) of vehicle (50% DMSO/Saline) or epothilone B (2x 0.75 mg/kg i.p.; Sellek) treated animals were extracted from the vertebral column. Tissue was weighed and frozen in liquid nitrogen. Samples were homogenized with a pestle and incubated with 3 M guanidine hydrochloride/0.05 M Tris HCl buffer (pH 7.5) overnight (4 °C) in a ratio of 10 µl solution for 1 mg of tissue. Extracts were then dialyzed against 1x TBS overnight at room temperature. Dialyzed samples were diluted 1:3 in 1x PBS and 50 µl of diluted samples were loaded into a 96-well black/clear imaging plate (BD falcon). 50 µl of 1,9-dimethylmethylene solution (Astarte Biologics) was added to each well. Shift of the absorption spectrum ( $A_{525}$ ) was measured with an Envison Multilabel reader (Perkin Elmer) and amount of sulfated GAGs was determined by using a calibration curve in accordance to manufacturer's instructions (Astarte Biologics).

### **5.2.5. Cell culture and immunocytochemistry**

#### **5.2.5.1. Culture of primary cortical neurons**

Primary cortical neurons were obtained from postnatal day 4 (P4) rat cortices as previously described (Tahirovic et al., 2010). Cortices were trypsinized (0.25% Trypsin) at room temperature for 5 min. Trypsinization was stopped by adding MEM-FBS (10%) and cells were dissociated and collected from the medium by centrifugation (800 g for 5 minutes). After 2 h of pre-plating in 75 cm<sup>2</sup> flasks containing MEM-FBS (10%), cells were collected from the medium by centrifugation (800 g for 5 min) and plated in glass bottom dishes (MatTek) containing complete neurobasal medium. The medium was mixed with 5 µg/ml laminin (Roche) plus Nogo-A (400 ng/ml, R&D systems), Semaphorin 3A (200 ng/ml; R&D systems) or chondroitin-sulfate-proteoglycans (1 µg/ml; Millipore), respectively. 48 h after plating, cells were fixed within the dish with pre-warmed PFA solution (4%) for 15 min. After 3 washes with 1x PBS, cells were quenched with 50 mM ammoniumchloride solution for 10 min and permeabilized with PBS-Triton (0.1%) for 3 min both at room temperature. Cells were incubated with blocking solution (2% FBS, 2% BSA, 0.2% fish gelatin in 1x PBS) for 1 h at room temperature and then immunostained with primary mouse anti-beta-3 tubulin antibody (Tuj-1; 1:1000; Sigma) for 1 h at room temperature. Afterwards dishes were washed 3 times with 1xPBS and incubated with secondary anti-mouse Alexa 488 antibody (1:400, Invitrogen) for 30 min (room temperature). Finally, dishes were washed 4 times with 1x PBS and cells were covered with fluoromount (Invitrogen) and coverslips.

#### **5.2.5.2. Culture of primary meningeal fibroblasts**

Primary meningeal fibroblasts were obtained from P4 rat brains. Brains were trypsinized (0.25% Trypsin) at room temperature for 5 min. Trypsinization was stopped by adding MEM-FBS (10%) and cells were dissociated and collected from the medium by centrifugation (800 g for 5 minutes). Cells were cultured in

10 cm flasks containing MEM-FBS (10%) until reaching confluence and then extracted from the flasks by trypsinization and passaged into new 10 cm flasks. After 3 passages, cells were extracted from the flasks by trypsinization and plated in culture inserts placed on 35 mm glass-bottom dishes (Ibidi). 24 h after plating, culture inserts were removed and medium was exchanged to MEM-FBS (0.5%). After 24 h, cells were treated with vehicle (DMSO) or epothilone B (5 nM). 24 h after treatment, cells were fixed with PFA solution (4%), and immunolabeled as described above with primary monoclonal mouse anti-tyrosinated tubulin antibody (1:500; kindly provided by Dr. Michael Schleicher) and rabbit anti-detyrosinated tubulin antibody (1:1500; Millipore) for 3 hours at room temperature and afterwards with corresponding secondary antibodies conjugated to Alexa 488, 647 fluorophores (1:400) and phalloidin-rhodamine (1:100; all Invitrogen).

#### **5.2.5.2. Culture of primary embryonic hippocampal neurons**

Primary hippocampal neurons were prepared from dissected E17 rat hippocampi as previously described (Witte et al., 2008). Briefly, hippocampi of embryonic day 17 rats were dissected, and trypsinized (0.05% Trypsin). Neurons were plated on poly-L-lysine (1mg/ml) coated glass cover slips in 6 cm petridishes containing MEM FBS (10%). After 6 hours, coverslips were transferred to a 6 cm dish containing cultured astrocytes in MEM and N2 supplement. To obtain astrocytes, E17 rat hippocampi and cortex were dissected, trypsinized (0.05% Trypsin) and dissociated. Cells were pre-plated in 75 cm<sup>2</sup> cell culture flasks. After reaching 80% confluence, astrocytes were trypsinized and transferred to 6 cm dishes.

1 day after transferring coverslips to astrocyte containing dishes, cells were treated with DMSO, epothilone B (3 nM; Sigma) or Taxol (3 nM; Sigma). After 1 day *in vitro*, neurons were fixed with 4% PFA and stained as described above with the primary antibodies mouse anti-Tau-1 (1:1000, Milipore) and rabbit anti-MAP2 (1:2000, Milipore) and the corresponding secondary antibodies.

## **5.2.6. Live imaging studies**

### **5.2.6.1. Live cell imaging studies**

*Primary cortical neurons* were obtained as described above. Before plating on glass-bottom dishes (MatTek), neurons were transfected with the Amaxa Nucleofector kit using EB3-GFP DNA construct (kindly provided by Drs. Vic Small and Anna Akhmanova) according to the manufacturer's instructions. Cells were plated in Nogo-A (400 ng/ml; R&D systems) containing serum and incubated for 24 h. After 24 h, image sequences (3 min every 3 s) were obtained with the DeltaVision RT live-cell imaging setup (Applied Precision). Epothilone B (1 nM; Sigma) was added to the neuronal culture while on the microscope stage. 2-6 h following epothilone B treatment, image sequences were obtained as before. EB3 fluorescence was measured in maximum intensity projections of 10-20 images in the aforementioned image sequences using ImageJ software. The quantifications were performed on the 2-h time-point following epothilone treatment. Plot profiles of EB3-GFP fluorescence of the most distally 20  $\mu\text{m}$  of all cellular neurites were background-subtracted and plotted as arbitrary units (a.u.). For testing EB3 fluorescence upon nocodazole treatment, a single imaging sequence (3 min every 3 s) was taken after 24 h of nocodazole (10 nM; Sigma) exposure. EB3 fluorescence was measured as aforementioned. For long-term imaging experiments examining neurite growth rates, images were acquired every 5 min for 4 h before and for 4 h after epothilone B treatment.

### **5.2.6.3. *In vivo* live imaging**

*In vivo* live imaging experiments were performed in compliance with the German animal protection law (TierSchG) and animals were housed and handled in accordance with good animal practice as defined by the Federation for Laboratory Animal Science Associations (FELASA). Adult Thy1-GFP mice (2-4 months, 20-30 g (Feng et al., 2000)) were deeply anaesthetized with a 2:1 mixture of xylazine (24 mg/kg)



and ketamine (115 mg/kg) diluted in sterile saline (1:3). Spinal cord injury was performed as described previously (Erturk et al., 2007). In brief, after laminectomy of thoracic vertebra T12, small bilateral lesions were performed at the level of the spinal cord dorsal column by using iridectomy scissors (FST). Animals were kept on heating pads during imaging sessions. For local drug delivery 10 µl of epothilone B (1 µM, Sigma), Taxol (1 µM, Sigma) or vehicle solution (5 % DMSO/ saline) were hourly applied onto the exposed spinal cord for 6 h. For systemic administration animals received a single intraperitoneal (i.p.) injection of 1.5 mg/kg epothilone B (Sellek) or vehicle solution (50% DMSO/Saline) 1 day before injury. *In vivo* live imaging was performed as previously described (Erturk et al., 2007). Animals were anaesthetized by injecting (i.p.) a mixture of midazolam (Dormicum; 2 mg/kg), medetomidine (Domitor; 0.15 mg/kg), fentanyl (0.05 mg/kg) and sterile saline. For every imaging session, the site of the laminectomy was re-exposed and the animal was placed under an Olympus MVX10 fluorescent microscope. Image sequences (27 images in 5 s) were obtained by using Olympus cellSens software. After imaging, the lamina was covered with dura patch and skin flaps were stapled. To antagonize anaesthesia after the imaging sessions, animals were i.p. injected with a mixture of flumazenil (Antisedan; 0.2 mg/kg), atipamezole (Anexate; 0.75 mg/kg), naloxone (Narcanti; 0.12 mg/kg) and sterile saline. To quantify retraction bulb formation and fiber retraction image sequences were analyzed by using cellSens software (Olympus).

## **5.2.7. Behavioral analysis**

### **5.2.7.1. Automated footprint analysis**

To analyze functional recovery of walking, rats were tested 8 weeks after contusion injury on the automated gait analysis system Catwalk (Noldus). Animals crossed twice over an illuminated 1 m glass bottomed runway to visualize footprints. Footprints were recorded by a camera positioned 50 cm below the runway. Recording settings were defined as follows: maximum range = 150-180; frames before delta

= 5; intensity minimum = 40; camera gain = 30; intensity threshold = 0.1. Footprint recordings were processed semi-automatically by using device-specific software quantifying step distance of the hindlimbs (stride length), interpaw coordination (regularity index) and external rotation of the hindpaws (foot exorotation).

#### **5.2.7.2. Horizontal ladder test**

To analyze functional recovery of skilled walking, rats were tested on a foot misplacement device at 2, 4, 6 and 8 weeks after contusion injury as well as after 1 and 2 weeks after 5,7-DHT i.c.v. injections. Animals crossed over a 1 m horizontal ladder, elevated 15 cm over the ground with a ladder-step distance of approximately 2 cm. 2 passages per animal were video recorded and foot misplacements were manually quantified.

#### **5.2.8. Microscopy and image analysis**

##### **5.2.8.1. Confocal microscopy**

Confocal images of spinal cord sagittal and coronal sections were obtained with a Zeiss LSM 700 confocal system in a sequential scanning mode. In order to compare immunofluorescence, standard acquisition parameters were used for each antibody staining. Quantitative measures in sagittal sections were performed in 3 representative sections of the lateral, the medio-lateral and the medial spinal cord injury site (300  $\mu$ m interval between each section). Fibrotic scarring was quantified by pixel counts of laminin staining at the lesion site using Adobe Photoshop software as previously described (Hellal et al., 2011). GFAP immunointensity profiles were measured in 1.5 mm plot profiles covering the rostral lesion site by using Image J software. Quantitative measurements in coronal sections were performed in 8 sections of the lumbar spinal cord between 0.5 cm and 1.5 cm caudal to lesion epicenter (1.4 mm interval between each section). 5HT-immunopositive pixels were quantified upon background subtraction in the left and

right ventral horns as mentioned above. Injury size was determined as the area delineated by GFAP-immunolabeling and quantified with ImageJ software. Cell free area in the wound healing assay was quantified with ImageJ software.

#### **5.2.8.2. Fluorescence microscopy and phase contrast imaging**

Zeiss AxioServer microscope was used to acquire phase contrast images of Giemsa staining and meningeal fibroblasts. Epifluorescence was used to visualize neurites of cultured neurons after fixation and immunostaining. Images were acquired by using Zeiss Axiovision software. Length of the longest neurite in neuronal cultures and cell free area in *in vitro* wound healing assays were measured by using ImageJ software.

#### **5.2.9. Statistical analysis**

All values are expressed as means  $\pm$  s.e.m. Two group comparisons were performed by using a Student's *t* test with two-tailed distribution and unequal variances.

## 6. REFERENCES

- Akhmanova A, Steinmetz MO (2008) Tracking the ends: a dynamic protein network controls the fate of microtubule tips. *Nat Rev Mol Cell Biol* 9:309-322.
- Alabed YZ, Pool M, Ong Tone S, Fournier AE (2007) Identification of CRMP4 as a convergent regulator of axon outgrowth inhibition. *J Neurosci* 27:1702-1711.
- Alilain WJ, Horn KP, Hu H, Dick TE, Silver J (2011) Functional regeneration of respiratory pathways after spinal cord injury. *Nature* 475:196-200.
- Altmann KH, Wartmann M, O'Reilly T (2000) Epothilones and related structures--a new class of microtubule inhibitors with potent in vivo antitumor activity. *Biochimica et biophysica acta* 1470:M79-91.
- Asher RA, Morgenstern DA, Fidler PS, Adcock KH, Oohira A, Braistead JE, Levine JM, Margolis RU, Rogers JH, Fawcett JW (2000) Neurocan is upregulated in injured brain and in cytokine-treated astrocytes. *J Neurosci* 20:2427-2438.
- Ballatore C, Brunden KR, Huryn DM, Trojanowski JQ, Lee VM, Smith AB, 3rd (2012) Microtubule stabilizing agents as potential treatment for Alzheimer's disease and related neurodegenerative tauopathies. *Journal of medicinal chemistry* 55:8979-8996.
- Banan A, McCormack SA, Johnson LR (1998) Polyamines are required for microtubule formation during gastric mucosal healing. *Am J Physiol* 274:G879-885.
- Barbeau H, Rossignol S (1990) The effects of serotonergic drugs on the locomotor pattern and on cutaneous reflexes of the adult chronic spinal cat. *Brain Research* 514:55-67.
- Batut J, Howell M, Hill CS (2007) Kinesin-Mediated Transport of Smad2 Is Required for Signaling in Response to TGF- $\beta$  Ligands. *Developmental Cell* 12:261-274.
- Beaulieu E, Demeule M, Ghitescu L, Beliveau R (1997) P-glycoprotein is strongly expressed in the luminal membranes of the endothelium of blood vessels in the brain. *The Biochemical journal* 326 ( Pt 2):539-544.
- Benowitz LI, Routtenberg A (1997) GAP-43: an intrinsic determinant of neuronal development and plasticity. *Trends Neurosci* 20:84-91.
- Berry M, Maxwell WL, Logan A, Mathewson A, McConnell P, Ashhurst DE, Thomas GH (1983) Deposition of scar tissue in the central nervous system. *Acta neurochirurgica Supplementum* 32:31-53.
- Bollag DM, McQueney PA, Zhu J, Hensens O, Koupal L, Liesch J, Goetz M, Lazarides E, Woods CM (1995) Epothilones, a new class of microtubule-stabilizing agents with a taxol-like mechanism of action. *Cancer research* 55:2325-2333.
- Bradbury EJ, Moon LD, Popat RJ, King VR, Bennett GS, Patel PN, Fawcett JW, McMahon SB (2002) Chondroitinase ABC promotes functional recovery after spinal cord injury. *Nature* 416:636-640.

- Bradke F, Dotti CG (1999) The role of local actin instability in axon formation. *Science* 283:1931-1934.**
- Bradke F, Fawcett JW, Spira ME (2012) Assembly of a new growth cone after axotomy: the precursor to axon regeneration. *Nat Rev Neurosci* 13:183-193.**
- Brunden KR, Zhang B, Carroll J, Yao Y, Potuzak JS, Hogan AM, Iba M, James MJ, Xie SX, Ballatore C, Smith AB, 3rd, Lee VM, Trojanowski JQ (2010) Epothilone D improves microtubule density, axonal integrity, and cognition in a transgenic mouse model of tauopathy. *J Neurosci* 30:13861-13866.**
- Brundin P, Barbin G, Strecker RE, Isacson O, Prochiantz A, Bjorklund A (1988) Survival and function of dissociated rat dopamine neurones grafted at different developmental stages or after being cultured in vitro. *Brain Res* 467:233-243.**
- Buck KB, Zheng JQ (2002) Growth cone turning induced by direct local modification of microtubule dynamics. *J Neurosci* 22:9358-9367.**
- Bundesen LQ, Scheel TA, Bregman BS, Kromer LF (2003) Ephrin-B2 and EphB2 regulation of astrocyte-meningeal fibroblast interactions in response to spinal cord lesions in adult rats. *J Neurosci* 23:7789-7800.**
- Caccamo A, Magrì A, Medina DX, Wisely EV, López-Aranda MF, Silva AJ, Oddo S (2013) mTOR regulates tau phosphorylation and degradation: implications for Alzheimer's disease and other tauopathies. *Aging Cell* 12:370-380.**
- Cadotte DW, Fehlings MG (2011) Spinal cord injury: a systematic review of current treatment options. *Clinical orthopaedics and related research* 469:732-741.**
- Carta M, Carlsson T, Kirik D, Bjorklund A (2007) Dopamine released from 5-HT terminals is the cause of L-DOPA-induced dyskinesia in parkinsonian rats. *Brain : a journal of neurology* 130:1819-1833.**
- Cartelli D, Casagrande F, Busceti CL, Bucci D, Molinaro G, Traficante A, Passarella D, Giavini E, Pezzoli G, Battaglia G, Cappelletti G (2013) Microtubule alterations occur early in experimental parkinsonism and the microtubule stabilizer epothilone D is neuroprotective. *Scientific reports* 3:1837.**
- Chaudhry V, Rowinsky EK, Sartorius SE, Donehower RC, Cornblath DR (1994) Peripheral neuropathy from taxol and cisplatin combination chemotherapy: clinical and electrophysiological studies. *Ann Neurol* 35:304-311.**
- Chen Y, Tang Y, Vogel LC, Devivo MJ (2013) Causes of spinal cord injury. *Topics in spinal cord injury rehabilitation* 19:1-8.**
- Conde C, Caceres A (2009) Microtubule assembly, organization and dynamics in axons and dendrites. *Nat Rev Neurosci* 10:319-332.**
- Davies JE, Tang X, Denning JW, Archibald SJ, Davies SJA (2004) Decorin suppresses neurocan, brevican, phosphacan and NG2 expression and promotes axon growth across adult rat spinal cord injuries. *European Journal of Neuroscience* 19:1226-1242.**

- Decimo I, Fumagalli G, Berton V, Krampera M, Bifari F (2012) Meninges: from protective membrane to stem cell niche. *American journal of stem cells* 1:92-105.
- Dergham P, Ellezam B, Essagian C, Avedissian H, Lubell WD, McKerracher L (2002) Rho signaling pathway targeted to promote spinal cord repair. *J Neurosci* 22:6570-6577.
- Desai A, Mitchison TJ (1997) Microtubule polymerization dynamics. *Annual review of cell and developmental biology* 13:83-117.
- Diaz JF, Andreu JM (1993) Assembly of purified GDP-tubulin into microtubules induced by taxol and taxotere: reversibility, ligand stoichiometry, and competition. *Biochemistry* 32:2747-2755.
- Dickendeshler TL, Baldwin KT, Mironova YA, Koriyama Y, Raiker SJ, Askew KL, Wood A, Geoffroy CG, Zheng B, Liepmann CD, Katagiri Y, Benowitz LI, Geller HM, Giger RJ (2012) NgR1 and NgR3 are receptors for chondroitin sulfate proteoglycans. *Nat Neurosci* 15:703-712.
- Dietz V, Fouad K (2013) Restoration of sensorimotor functions after spinal cord injury. *Brain : a journal of neurology*.
- Dumontet C, Jordan MA (2010) Microtubule-binding agents: a dynamic field of cancer therapeutics. *Nature reviews Drug discovery* 9:790-803.
- Enomoto T (1996) Microtubule disruption induces the formation of actin stress fibers and focal adhesions in cultured cells: possible involvement of the rho signal cascade. *Cell structure and function* 21:317-326.
- Erez H, Malkinson G, Prager-Khoutorsky M, De Zeeuw CI, Hoogenraad CC, Spira ME (2007) Formation of microtubule-based traps controls the sorting and concentration of vesicles to restricted sites of regenerating neurons after axotomy. *J Cell Biol* 176:497-507.
- Erturk A, Hellal F, Enes J, Bradke F (2007) Disorganized microtubules underlie the formation of retraction bulbs and the failure of axonal regeneration. *J Neurosci* 27:9169-9180.
- Faulkner JR, Herrmann JE, Woo MJ, Tansey KE, Doan NB, Sofroniew MV (2004) Reactive astrocytes protect tissue and preserve function after spinal cord injury. *J Neurosci* 24:2143-2155.
- Fawcett JW, Housden E, Smith-Thomas L, Meyer RL (1989) The growth of axons in three-dimensional astrocyte cultures. *Developmental biology* 135:449-458.
- Fellner S, Bauer B, Miller DS, Schaffrik M, Fankhanel M, Spruss T, Bernhardt G, Graeff C, Farber L, Gschaidmeier H, Buschauer A, Fricker G (2002) Transport of paclitaxel (Taxol) across the blood-brain barrier in vitro and in vivo. *The Journal of clinical investigation* 110:1309-1318.
- Feng G, Mellor RH, Bernstein M, Keller-Peck C, Nguyen QT, Wallace M, Nerbonne JM, Lichtman JW, Sanes JR (2000) Imaging neuronal subsets in transgenic mice expressing multiple spectral variants of GFP. *Neuron* 28:41-51.
- Ferretti P, Zhang F, O'Neill P (2003) Changes in spinal cord regenerative ability through phylogenesis and development: Lessons to be learnt. *Developmental Dynamics* 226:245-256.

- Filbin MT (2003) Myelin-associated inhibitors of axonal regeneration in the adult mammalian CNS. *Nat Rev Neurosci* 4:703-713.
- Fitch MT, Silver J (1997) Glial cell extracellular matrix: boundaries for axon growth in development and regeneration. *Cell Tissue Res* 290:379-384.
- Fitch MT, Silver J (2008) CNS injury, glial scars, and inflammation: Inhibitory extracellular matrices and regeneration failure. *Exp Neurol* 209:294-301.
- Flynn KC, Hellal F, Neukirchen D, Jacob S, Tahirovic S, Dupraz S, Stern S, Garvalov BK, Gurniak C, Shaw AE, Meyn L, Wedlich-Soldner R, Bamburg JR, Small JV, Witke W, Bradke F (2012) ADF/cofilin-mediated actin retrograde flow directs neurite formation in the developing brain. *Neuron* 76:1091-1107.
- Fukata Y, Itoh TJ, Kimura T, Menager C, Nishimura T, Shiromizu T, Watanabe H, Inagaki N, Iwamatsu A, Hotani H, Kaibuchi K (2002) CRMP-2 binds to tubulin heterodimers to promote microtubule assembly. *Nature cell biology* 4:583-591.
- Ganguly A, Yang H, Zhang H, Cabral F, Patel KD (2013) Microtubule dynamics control tail retraction in migrating vascular endothelial cells. *Molecular cancer therapeutics* 12:2837-2846.
- George EB, Glass JD, Griffin JW (1995) Axotomy-induced axonal degeneration is mediated by calcium influx through ion-specific channels. *J Neurosci* 15:6445-6452.
- Geraldo S, Khanzada UK, Parsons M, Chilton JK, Gordon-Weeks PR (2008) Targeting of the F-actin-binding protein drebrin by the microtubule plus-tip protein EB3 is required for neurogenesis. *Nature cell biology* 10:1181-1189.
- Giannakakou P, Gussio R, Nogales E, Downing KH, Zaharevitz D, Bollbuck B, Poy G, Sackett D, Nicolaou KC, Fojo T (2000) A common pharmacophore for epothilone and taxanes: Molecular basis for drug resistance conferred by tubulin mutations in human cancer cells. *Proceedings of the National Academy of Sciences* 97:2904-2909.
- Gilerovich EG, Moshonkina TR, Fedorova EA, Shishko TT, Pavlova NV, Gerasimenko YP, Otellin VA (2008) Morphofunctional characteristics of the lumbar enlargement of the spinal cord in rats. *Neuroscience and behavioral physiology* 38:855-860.
- Glotzer M (2009) The 3Ms of central spindle assembly: microtubules, motors and MAPs. *Nat Rev Mol Cell Biol* 10:9-20.
- Gomis-Ruth S, Wierenga CJ, Bradke F (2008) Plasticity of polarization: changing dendrites into axons in neurons integrated in neuronal circuits. *Current biology* : CB 18:992-1000.
- Goodin S, Kane MP, Rubin EH (2004) Epothilones: mechanism of action and biologic activity. *Journal of clinical oncology : official journal of the American Society of Clinical Oncology* 22:2015-2025.
- Goold RG, Owen R, Gordon-Weeks PR (1999) Glycogen synthase kinase 3beta phosphorylation of microtubule-associated protein 1B regulates the stability of microtubules in growth cones. *Journal of cell science* 112:3373-3384.

- Goritz C, Dias DO, Tomilin N, Barbacid M, Shupliakov O, Frisen J (2011) A pericyte origin of spinal cord scar tissue. *Science* 333:238-242.
- GrandPre T, Li S, Strittmatter SM (2002) Nogo-66 receptor antagonist peptide promotes axonal regeneration. *Nature* 417:547-551.
- Gundersen GG, Bulinski JC (1988) Selective stabilization of microtubules oriented toward the direction of cell migration. *Proc Natl Acad Sci U S A* 85:5946-5950.
- Gundersen GG, Kim I, Chapin CJ (1994) Induction of stable microtubules in 3T3 fibroblasts by TGF-beta and serum. *Journal of cell science* 107 ( Pt 3):645-659.
- Habib AA, Marton LS, Allwardt B, Gulcher JR, Mikol DD, Hognason T, Chattopadhyay N, Stefansson K (1998) Expression of the oligodendrocyte-myelin glycoprotein by neurons in the mouse central nervous system. *J Neurochem* 70:1704-1711.
- Hankin MH, Lund RD (1990) Directed early axonal outgrowth from retinal transplants into host rat brains. *J Neurobiol* 21:1202-1218.
- Harel NY, Strittmatter SM (2006) Can regenerating axons recapitulate developmental guidance during recovery from spinal cord injury? *Nat Rev Neurosci* 7:603-616.
- He Y, Li D, Cook SL, Yoon M-S, Kapoor A, Rao CV, Kenis PJA, Chen J, Wang F (2013) Mammalian target of rapamycin and Rictor control neutrophil chemotaxis by regulating Rac/Cdc42 activity and the actin cytoskeleton. *Molecular biology of the cell* 24:3369-3380.
- Hellal F, Pruneau D, Palmier B, Faye P, Croci N, Plotkine M, Marchand-Verrecchia C (2003) Detrimental role of bradykinin B2 receptor in a murine model of diffuse brain injury. *J Neurotrauma* 20:841-851.
- Hellal F, Hurtado A, Ruschel J, Flynn KC, Laskowski CJ, Umlauf M, Kapitein LC, Strikis D, Lemmon V, Bixby J, Hoogenraad CC, Bradke F (2011) Microtubule stabilization reduces scarring and causes axon regeneration after spinal cord injury. *Science* 331:928-931.
- Hsieh SH, Ferraro GB, Fournier AE (2006) Myelin-associated inhibitors regulate cofilin phosphorylation and neuronal inhibition through LIM kinase and Slingshot phosphatase. *J Neurosci* 26:1006-1015.
- Husch A, Van Patten GN, Hong DN, Scaperotti MM, Cramer N, Harris-Warrick RM (2012) Spinal cord injury induces serotonin supersensitivity without increasing intrinsic excitability of mouse V2a interneurons. *J Neurosci* 32:13145-13154.
- Jacobs BL, Fornal CA (1997) Serotonin and motor activity. *Curr Opin Neurobiol* 7:820-825.
- Janke C, Bulinski JC (2011) Post-translational regulation of the microtubule cytoskeleton: mechanisms and functions. *Nat Rev Mol Cell Biol* 12:773-786.
- Jones LL, Margolis RU, Tuszynski MH (2003) The chondroitin sulfate proteoglycans neurocan, brevican, phosphacan, and versican are differentially regulated following spinal cord injury. *Exp Neurol* 182:399-411.
- Jordan LM, Liu J, Hedlund PB, Akay T, Pearson KG (2008) Descending command systems for the initiation of locomotion in mammals. *Brain research reviews* 57:183-191.



- Kabir N, Schaefer AW, Nakhost A, Sossin WS, Forscher P (2001) Protein kinase C activation promotes microtubule advance in neuronal growth cones by increasing average microtubule growth lifetimes. *J Cell Biol* 152:1033-1044.
- Kaibuchi K, Kuroda S, Amano M (1999) Regulation of the cytoskeleton and cell adhesion by the Rho family GTPases in mammalian cells. *Annual review of biochemistry* 68:459-486.
- Kamath K, Smiyun G, Wilson L, Jordan MA (2013) Mechanisms of inhibition of endothelial cell migration by taxanes. *Cytoskeleton*.
- Kamber D, Erez H, Spira ME (2009) Local calcium-dependent mechanisms determine whether a cut axonal end assembles a retarded endbulb or competent growth cone. *Experimental Neurology* 219:112-125.
- Kaminska B, Kaczmarek L, Grzelakowska-Sztabert B (1992) Inhibitors of polyamine biosynthesis affect the expression of genes encoding cytoskeletal proteins. *FEBS letters* 304:198-200.
- Kaneko S, Iwanami A, Nakamura M, Kishino A, Kikuchi K, Shibata S, Okano HJ, Ikegami T, Moriya A, Konishi O, Nakayama C, Kumagai K, Kimura T, Sato Y, Goshima Y, Taniguchi M, Ito M, He Z, Toyama Y, Okano H (2006) A selective Sema3A inhibitor enhances regenerative responses and functional recovery of the injured spinal cord. *Nat Med* 12:1380-1389.
- Kar S, Fan J, Smith MJ, Goedert M, Amos LA (2003) Repeat motifs of tau bind to the insides of microtubules in the absence of taxol. *The EMBO journal* 22:70-77.
- Kaverina I, Krylyshkina O, Small JV (1999) Microtubule targeting of substrate contacts promotes their relaxation and dissociation. *J Cell Biol* 146:1033-1044.
- Kawano H, Li H-P, Sango K, Kawamura K, Raisman G (2005) Inhibition of collagen synthesis overrides the age-related failure of regeneration of nigrostriatal dopaminergic axons. *Journal of Neuroscience Research* 80:191-202.
- Kawano H, Kimura-Kuroda J, Komuta Y, Yoshioka N, Li HP, Kawamura K, Li Y, Raisman G (2012) Role of the lesion scar in the response to damage and repair of the central nervous system. *Cell Tissue Res* 349:169-180.
- Kerschensteiner M, Schwab ME, Lichtman JW, Misgeld T (2005) In vivo imaging of axonal degeneration and regeneration in the injured spinal cord. *Nat Med* 11:572-577.
- Kim JE, Liu BP, Park JH, Strittmatter SM (2004) Nogo-66 receptor prevents raphespinal and rubrospinal axon regeneration and limits functional recovery from spinal cord injury. *Neuron* 44:439-451.
- Klapka N, Hermanns S, Straten G, Masannek C, Duis S, Hamers FP, Muller D, Zuschratter W, Muller HW (2005) Suppression of fibrous scarring in spinal cord injury of rat promotes long-distance regeneration of corticospinal tract axons, rescue of primary motoneurons in somatosensory cortex and significant functional recovery. *Eur J Neurosci* 22:3047-3058.
- Komuta Y, Teng X, Yanagisawa H, Sango K, Kawamura K, Kawano H (2010) Expression of transforming growth factor-beta receptors in meningeal fibroblasts of the injured mouse brain. *Cellular and molecular neurobiology* 30:101-111.

- Kowalski RJ, Giannakakou P, Hamel E (1997) Activities of the microtubule-stabilizing agents epothilones A and B with purified tubulin and in cells resistant to paclitaxel (Taxol(R)). *J Biol Chem* 272:2534-2541.
- Krendel M, Zenke FT, Bokoch GM (2002) Nucleotide exchange factor GEF-H1 mediates cross-talk between microtubules and the actin cytoskeleton. *Nature cell biology* 4:294-301.
- Kwon BK, Liu J, Messerer C, Kobayashi NR, McGraw J, Oschipok L, Tetzlaff W (2002) Survival and regeneration of rubrospinal neurons 1 year after spinal cord injury. *Proc Natl Acad Sci U S A* 99:3246-3251.
- Laan L, Husson J, Munteanu EL, Kerssemakers JW, Dogterom M (2008) Force-generation and dynamic instability of microtubule bundles. *Proc Natl Acad Sci U S A* 105:8920-8925.
- Lechleider RJ, Kaminskas E, Jiang X, Aziz R, Bullock J, Kasliwal R, Harapanhalli R, Pope S, Sridhara R, Leighton J, Booth B, Dagher R, Justice R, Pazdur R (2008) Ixabepilone in combination with capecitabine and as monotherapy for treatment of advanced breast cancer refractory to previous chemotherapies. *Clinical cancer research : an official journal of the American Association for Cancer Research* 14:4378-4384.
- Li R, Gundersen GG (2008) Beyond polymer polarity: how the cytoskeleton builds a polarized cell. *Nat Rev Mol Cell Biol* 9:860-873.
- Liao G, Nagasaki T, Gundersen GG (1995) Low concentrations of nocodazole interfere with fibroblast locomotion without significantly affecting microtubule level: implications for the role of dynamic microtubules in cell locomotion. *Journal of cell science* 108 ( Pt 11):3473-3483.
- Liedtke W, Edelmann W, Bieri PL, Chiu F-C, Cowan NJ, Kucherlapati R, Raine CS (1996) GFAP Is Necessary for the Integrity of CNS White Matter Architecture and Long-Term Maintenance of Myelination. *Neuron* 17:607-615.
- Lin PC, Chan PM, Hall C, Manser E (2011) Collapsin response mediator proteins (CRMPs) are a new class of microtubule-associated protein (MAP) that selectively interacts with assembled microtubules via a taxol-sensitive binding interaction. *J Biol Chem* 286:41466-41478.
- Liu K, Lu Y, Lee JK, Samara R, Willenberg R, Sears-Kraxberger I, Tedeschi A, Park KK, Jin D, Cai B, Xu B, Connolly L, Steward O, Zheng B, He Z (2010) PTEN deletion enhances the regenerative ability of adult corticospinal neurons. *Nat Neurosci* 13:1075-1081.
- Logan A, Berry M, Gonzalez AM, Frautschy SA, Sporn MB, Baird A (1994) Effects of Transforming Growth Factor  $\beta$ 1, on Scar Production in the Injured Central Nervous System of the Rat. *European Journal of Neuroscience* 6:355-363.
- Lowery LA, Van Vactor D (2009) The trip of the tip: understanding the growth cone machinery. *Nat Rev Mol Cell Biol* 10:332-343.
- Lu P, Wang Y, Graham L, McHale K, Gao M, Wu D, Brock J, Blesch A, Rosenzweig Ephron S, Havton Leif A, Zheng B, Conner James M, Marsala M, Tuszynski Mark H (2012) Long-Distance Growth and Connectivity of Neural Stem Cells after Severe Spinal Cord Injury. *Cell* 150:1264-1273.

- Mandelkow E, Mandelkow EM (1995) Microtubules and microtubule-associated proteins. *Current opinion in cell biology* 7:72-81.
- Maor-Nof M, Homma N, Raanan C, Nof A, Hirokawa N, Yaron A (2013) Axonal pruning is actively regulated by the microtubule-destabilizing protein kinesin superfamily protein 2A. *Cell reports* 3:971-977.
- Mathewson AJ, Berry M (1985) Observations on the astrocyte response to a cerebral stab wound in adult rats. *Brain Res* 327:61-69.
- McKerracher L, Ferraro GB, Fournier AE (2012) Rho signaling and axon regeneration. *International review of neurobiology* 105:117-140.
- McKerracher L, David S, Jackson DL, Kottis V, Dunn RJ, Braun PE (1994) Identification of myelin-associated glycoprotein as a major myelin-derived inhibitor of neurite growth. *Neuron* 13:805-811.
- Metz GA, Merkler D, Dietz V, Schwab ME, Fouad K (2000) Efficient testing of motor function in spinal cord injured rats. *Brain Res* 883:165-177.
- Mimura F, Yamagishi S, Arimura N, Fujitani M, Kubo T, Kaibuchi K, Yamashita T (2006) Myelin-associated Glycoprotein Inhibits Microtubule Assembly by a Rho-kinase-dependent Mechanism. *Journal of Biological Chemistry* 281:15970-15979.
- Neukirchen D, Bradke F (2011) Neuronal polarization and the cytoskeleton. *Seminars in cell & developmental biology* 22:825-833.
- Neumann S, Bradke F, Tessier-Lavigne M, Basbaum AI (2002) Regeneration of sensory axons within the injured spinal cord induced by intraganglionic cAMP elevation. *Neuron* 34:885-893.
- Norenberg MD, Smith J, Marcillo A (2004) The pathology of human spinal cord injury: defining the problems. *J Neurotrauma* 21:429-440.
- O'Brien ET, Salmon ED, Erickson HP (1997) How calcium causes microtubule depolymerization. *Cell motility and the cytoskeleton* 36:125-135.
- Onifer SM, Rabchevsky AG, Scheff SW (2007) Rat models of traumatic spinal cord injury to assess motor recovery. *ILAR journal / National Research Council, Institute of Laboratory Animal Resources* 48:385-395.
- Pan YA, Misgeld T, Lichtman JW, Sanes JR (2003) Effects of Neurotoxic and Neuroprotective Agents on Peripheral Nerve Regeneration Assayed by Time-Lapse Imaging In Vivo. *The Journal of Neuroscience* 23:11479-11488.
- Park KK, Liu K, Hu Y, Smith PD, Wang C, Cai B, Xu B, Connolly L, Kramvis I, Sahin M, He Z (2008) Promoting axon regeneration in the adult CNS by modulation of the PTEN/mTOR pathway. *Science* 322:963-966.
- Pasterkamp RJ, Giger RJ, Ruitenber MJ, Holtmaat AJGD, De Wit J, De Winter F, Verhaagen J (1999) Expression of the Gene Encoding the Chemorepellent Semaphorin III Is Induced in the Fibroblast Component of Neural Scar Tissue Formed Following Injuries of Adult But Not Neonatal CNS. *Molecular and Cellular Neuroscience* 13:143-166.

- Pearse DD, Pereira FC, Marcillo AE, Bates ML, Berrocal YA, Filbin MT, Bunge MB (2004) cAMP and Schwann cells promote axonal growth and functional recovery after spinal cord injury. *Nat Med* 10:610-616.
- Prinjha R, Moore SE, Vinson M, Blake S, Morrow R, Christie G, Michalovich D, Simmons DL, Walsh FS (2000) Inhibitor of neurite outgrowth in humans. *Nature* 403:383-384.
- Prota AE, Bargsten K, Zurwerra D, Field JJ, Diaz JF, Altmann KH, Steinmetz MO (2013) Molecular mechanism of action of microtubule-stabilizing anticancer agents. *Science* 339:587-590.
- Qiu J, Cai D, Dai H, McAtee M, Hoffman PN, Bregman BS, Filbin MT (2002) Spinal axon regeneration induced by elevation of cyclic AMP. *Neuron* 34:895-903.
- Raccor BS (2008) Mechanisms and Kinetics of Microtubule Perturbing Agents. In.
- Richardson PM, Issa VM (1984) Peripheral injury enhances central regeneration of primary sensory neurones. *Nature* 309:791-793.
- Rivera E, Lee J, Davies A (2008) Clinical development of ixabepilone and other epothilones in patients with advanced solid tumors. *The oncologist* 13:1207-1223.
- Sabelstrom H, Stenudd M, Reu P, Dias DO, Elfineh M, Zdunek S, Damberg P, Goritz C, Frisen J (2013) Resident neural stem cells restrict tissue damage and neuronal loss after spinal cord injury in mice. *Science* 342:637-640.
- Sánchez C, Díaz-Nido J, Avila J (2000) Phosphorylation of microtubule-associated protein 2 (MAP2) and its relevance for the regulation of the neuronal cytoskeleton function. *Progress in neurobiology* 61:133-168.
- Saxena S, Caroni P (2007) Mechanisms of axon degeneration: from development to disease. *Progress in neurobiology* 83:174-191.
- Scheff SW, Rabchevsky AG, Fugaccia I, Main JA, Lumppp JE, Jr. (2003) Experimental modeling of spinal cord injury: characterization of a force-defined injury device. *J Neurotrauma* 20:179-193.
- Schmidt BJ, Jordan LM (2000) The role of serotonin in reflex modulation and locomotor rhythm production in the mammalian spinal cord. *Brain Res Bull* 53:689-710.
- Schmoranzler J, Kreitzer G, Simon SM (2003) Migrating fibroblasts perform polarized, microtubule-dependent exocytosis towards the leading edge. *Journal of cell science* 116:4513-4519.
- Schnell L, Schwab ME (1990) Axonal regeneration in the rat spinal cord produced by an antibody against myelin-associated neurite growth inhibitors. *Nature* 343:269-272.
- Seitz A, Aglow E, Heber-Katz E (2002) Recovery from spinal cord injury: A new transection model in the C57Bl/6 mouse. *Journal of Neuroscience Research* 67:337-345.
- Sengottuvel V, Fischer D (2011) Facilitating axon regeneration in the injured CNS by microtubules stabilization. *Communicative & integrative biology* 4:391-393.

- Shewan D, Dwivedy A, Anderson R, Holt CE (2002) Age-related changes underlie switch in netrin-1 responsiveness as growth cones advance along visual pathway. *Nat Neurosci* 5:955-962.
- Silver J, Miller JH (2004) Regeneration beyond the glial scar. *Nat Rev Neurosci* 5:146-156.
- Slawinska U, Miazga K, Cabaj AM, Leszczynska AN, Majczynski H, Nagy JI, Jordan LM (2013) Grafting of fetal brainstem 5-HT neurons into the sublesional spinal cord of paraplegic rats restores coordinated hindlimb locomotion. *Exp Neurol* 247:572-581.
- Slawińska U, Miazga K, Cabaj AM, Leszczyńska AN, Majczyński H, Nagy JI, Jordan LM (2013) Grafting of fetal brainstem 5-HT neurons into the sublesional spinal cord of paraplegic rats restores coordinated hindlimb locomotion. *Experimental Neurology* 247:572-581.
- Smith DS, Skene JH (1997) A transcription-dependent switch controls competence of adult neurons for distinct modes of axon growth. *J Neurosci* 17:646-658.
- Spira ME, Oren R, Dormann A, Gitler D (2003) Critical calpain-dependent ultrastructural alterations underlie the transformation of an axonal segment into a growth cone after axotomy of cultured *Aplysia* neurons. *The Journal of comparative neurology* 457:293-312.
- Stichel CC, Müller HW (1994) Relationship between injury-induced astrogliosis, laminin expression and axonal sprouting in the adult rat brain. *Journal of neurocytology* 23:615-630.
- Stichel CC, Hermanns S, Luhmann HJ, Lausberg F, Niermann H, D'Urso D, Servos G, Hartwig H-G, Müller HW (1999) Inhibition of collagen IV deposition promotes regeneration of injured CNS axons. *European Journal of Neuroscience* 11:632-646.
- Stuess M, Bradke F (2011) Neuronal polarization: the cytoskeleton leads the way. *Developmental neurobiology* 71:430-444.
- Strittmatter SM, Vartanian T, Fishman MC (1992) GAP-43 as a plasticity protein in neuronal form and repair. *J Neurobiol* 23:507-520.
- Swiercz JM, Kuner R, Behrens J, Offermanns S (2002) Plexin-B1 directly interacts with PDZ-RhoGEF/LARG to regulate RhoA and growth cone morphology. *Neuron* 35:51-63.
- Tahirovic S, Hellal F, Neukirchen D, Hindges R, Garvalov BK, Flynn KC, Stradal TE, Chrostek-Grashoff A, Brakebusch C, Bradke F (2010) Rac1 regulates neuronal polarization through the WAVE complex. *J Neurosci* 30:6930-6943.
- Tanaka E, Ho T, Kirschner MW (1995) The role of microtubule dynamics in growth cone motility and axonal growth. *The Journal of Cell Biology* 128:139-155.
- Tang X, Davies JE, Davies SJA (2003) Changes in distribution, cell associations, and protein expression levels of NG2, neurocan, phosphacan, brevican, versican V2, and tenascin-C during acute to chronic maturation of spinal cord scar tissue. *Journal of Neuroscience Research* 71:427-444.
- Tee AR, Blenis J (2005) mTOR, translational control and human disease. *Seminars in cell & developmental biology* 16:29-37.
- Tom VJ, Steinmetz MP, Miller JH, Doller CM, Silver J (2004) Studies on the Development and Behavior of the Dystrophic Growth Cone, the Hallmark of Regeneration Failure, in an In

- 
- Vitro Model of the Glial Scar and after Spinal Cord Injury. The Journal of Neuroscience 24:6531-6539.**
- Tuszynski Mark H, Steward O (2012) Concepts and Methods for the Study of Axonal Regeneration in the CNS. Neuron 74:777-791.**
- Wade RH (2009) On and around microtubules: an overview. Molecular biotechnology 43:177-191.**
- Wigley CB, Berry M (1988) Regeneration of adult rat retinal ganglion cell processes in monolayer culture: comparisons between cultures of adult and neonatal neurons. Brain Res 470:85-98.**
- Witte H, Neukirchen D, Bradke F (2008) Microtubule stabilization specifies initial neuronal polarization. J Cell Biol 180:619-632.**
- Yang P, Yang Z (2012) Enhancing intrinsic growth capacity promotes adult CNS regeneration. J Neurol Sci 312:1-6.**
- Ylera B, Erturk A, Hellal F, Nadrigny F, Hurtado A, Tahirovic S, Oudega M, Kirchhoff F, Bradke F (2009) Chronically CNS-injured adult sensory neurons gain regenerative competence upon a lesion of their peripheral axon. Current biology : CB 19:930-936.**
- Yoshimura T, Kawano Y, Arimura N, Kawabata S, Kikuchi A, Kaibuchi K (2005) GSK-3 $\beta$  Regulates Phosphorylation of CRMP-2 and Neuronal Polarity. Cell 120:137-149.**
- Yoshioka N, Hisanaga S-I, Kawano H (2010) Suppression of fibrotic scar formation promotes axonal regeneration without disturbing blood-brain barrier repair and withdrawal of leukocytes after traumatic brain injury. The Journal of comparative neurology 518:3867-3881.**
- Zakharenko S, Popov S (1998) Dynamics of axonal microtubules regulate the topology of new membrane insertion into the growing neurites. J Cell Biol 143:1077-1086.**
- Zhang B, Maiti A, Shively S, Lakhani F, McDonald-Jones G, Bruce J, Lee EB, Xie SX, Joyce S, Li C, Toleikis PM, Lee VM-Y, Trojanowski JQ (2005) Microtubule-binding drugs offset tau sequestration by stabilizing microtubules and reversing fast axonal transport deficits in a tauopathy model. Proceedings of the National Academy of Sciences of the United States of America 102:227-231.**

## **7. ACKNOWLEDGEMENTS**

First of all, I am deeply grateful to Frank for his supervision, training for talks, poster presentation and many other things as well as for promoting me for instance by sending me to workshops and conferences. I am especially thankful, that you allowed me to go abroad for my graduate exchange program at the Miami Project. I also want to thank you for being patient with me and my sometimes chaotic way of working. Last but not least, thank you for advising me in emotionally challenging situations, I really appreciated. I am also very obliged, that you designated Farida as my trainer at the very beginning of my PhD.

Great thanks to Farida for your training, for supervising and supporting my experiments and for providing your expertise in various circumstances. It is indeed hard to phrase how much of that thesis owes to you and your training. I really appreciated and deeply miss discussing and working with you. Besides work, I am grateful for your friendship and for taking care of me during the whole time we worked together, I will never forget that.

Third, I want to thank all the other lab members. It is a big honor and pleasure to have you guys as colleagues and to more or less extend also as friends. I am very grateful for the lab atmosphere that you guys create(d) and also for your professional support and fruitful (or sometimes nonsense but funny) discussions. I am particularly thankful to Dodo, Michi, Ali, Kevin, Sebastian, Liane, Kerstin, Charlotte and David; Dodo and Michi for welcoming me so nicely in the lab, for incorporating myself into the lab and the MPI community and for becoming good friends; Ali, for teaching me the in vivo live imaging and for introducing me to the MPI football “league”; Kevin, for helping me with the cell culture experiments, teaching me the live cell imaging and for being my power work-out buddy; Sebastian, for helping me with the western blotting and meningeal fibroblast experiments, for critically reading this thesis and for cheering me up with his great way of humor. I am also much obliged for the help of our lab technicians

## Acknowledgement

Liane and Kerstin for assisting me with the cell culture and *in vivo* experiments, respectively. I am also very grateful to Charlotte and David for proof-reading this thesis and for suggesting corrections.

I am grateful to Professors John Bixby and Vance Lemmon, who gave me the opportunity to undergo a graduate exchange program in their lab. I am especially obliged to John for his hospitality and for taking care of me during my time in Miami. I am also very thankful to Dinara Strikis, who helped me organizing my experiments and my personal matters in Miami.

I am deeply grateful to the animal care takers, in particular Tanja Irl and Daniela Fleischer, for assisting me during the animal surgeries and for taking good care of the operated animals.

I also want to thank all my collaborators that contributed experiments for my paper and to everyone who helped with the manuscript writing.

Zum Schluss, mein ganz persönlicher Dank an meine Familie ins besondere an meine Eltern. Danke für eure Unterstützung, für eure Liebe, für eure Sorge um mich. Diese Doktorarbeit wäre ohne euch und eure Anstrengungen, die ihr in mich investiert habt, nicht möglich gewesen. Großes Dankeschön auch an meine Schwester, die mir oft geholfen hat auf den rechten Weg zurück zu finden, als ich dabei war abzudriften. Ich bin dankbar, dass ich mit einer Familie gesegnet bin auf die ich mich verlassen kann und die mich in schwierigen Zeiten auffängt und wieder aufbaut. An dieser Stelle möchte ich mich auch bei meiner lieben Katharina bedanken: Danke das du mir immer wieder neue Hoffnung gegeben hast in Zeiten der gefühlten Ausweglosigkeit. Danke, für dein Verständnis, wenn ich mal wieder schlecht gelaunt von der Arbeit kam. Danke, dass immer für mich da warst und bist. Es war ein Glücksfall, dass die Arbeit für diese Dissertation mich zu dir geführt hat und ich bin dankbar und glücklich, dass ich dich habe.



## **8. CURRICULUM VITAE**

### **PhD THESIS**

- Since 7/2008                                  PhD thesis with Prof. Dr. Frank Bradke at the Max-Planck Institute of Neurobiology (Martinsried, Germany) and at the Center for Neurodegenerative Diseases (Bonn, Germany)
- 4/2010-8/2010                                Graduate Exchange Program in the laboratory of Prof. Dr. John Bixby at the “Miami Project to Cure Paralysis”, Miller School of Medicine (Miami, USA)
- 7/2008-8/2008                                Spinal Cord Research Techniques Course in the laboratory of Prof. Dr. Oswald Steward at the Reeve-Irvine-Research Center, University of California, Irvine (Irvine, USA)

### **UNDERGRADUATE STUDIES**

- 6/2007-3/2008                                Diploma thesis with Drs. Thomas Fenzl and Chadi Touma at the Max-Planck-Institute of Psychiatry (Munich, Germany)
- 10/2002-3/2008                                Ludwig-Maximilian-University (Munich, Germany)
- Dipl. rer. nat. Biology*
- 6/2002-7/2002                                Internship in the department of Prof. Dr. Axel Ullrich at the Max-Planck-Institute of Biochemistry (Martinsried, Germany)

### **SCHOOL**

- 7/2001-5/2002                                Civilian service
- 8/1993-6/2001                                Georg-Christoph-Lichtenberg-Gymnasium, Gera
- Abitur*

## 9. PUBLICATIONS

### From Phd studies

#### **Systemic Administration of Epothilone B Promotes Axon Regeneration and Functional Recovery after Spinal Cord Injury**

**Ruschel J**, Hellal F, Flynn KC, Dupraz S, Bates M, Sliwinski C, Dobrint K, Peitz M, Brüstle O, Blesch A, Weidner N, Bunge MB, Bixby JL, Bradke F

*Science, Under revision*

#### **Microtubule stabilization reduces scarring and causes axon regeneration after spinal cord injury.**

Hellal F, Hurtado A, **Ruschel J**, Flynn KC, Laskowski CJ, Umlauf M, Kapitein LC, Strikis D, Lemmon V, Bixby J, Hoogenraad CC, Bradke F.

*Science. 2011*

#### **Electrical activity suppresses axon growth through Ca(v)1.2 channels in adult primary sensory neurons.**

Enes J, Langwieser N, **Ruschel J**, Carballosa-Gonzalez MM, Klug A, Traut MH, Ylera B, Tahirovic S, Hofmann F, Stein V, Moosmang S, Hentall ID, Bradke F.

*Curr Biol. 2010*

### From Diploma thesis

#### **Sleep disturbances in highly stress reactive mice: modeling endophenotypes of major depression.**

Fenzl T, Touma C, Romanowski CP, **Ruschel J**, Holsboer F, Landgraf R, Kimura M, Yassouridis A.

*BMC Neurosci. 2011*

#### **Rhythmicity in mice selected for extremes in stress reactivity: behavioural, endocrine and sleep changes resembling endophenotypes of major depression.**

Touma C, Fenzl T, **Ruschel J**, Palme R, Holsboer F, Kimura M, Landgraf R.

*PLoS One. 2009*